Section 23

Chemical Reactors

Stanley M. Walas, Ph.D., *Professor Emeritus, Department of Chemical and Petroleum Engineering, University of Kansas; Fellow, American Institute of Chemical Engineers*

MODELING CHEMICAL REACTORS

Mathematical Models 23-4
Modeling Principles 23-5
Chemical Kinetic Laws 23-5
Basic Reactor Elements 23-9
Material Balances 23-9
Heat Transfer and Mass Transfer 23-9
Case Studies 23-9
Example 1: Kinetics and Equilibria of Methanol Synthesis 23-13
Example 2: Coping with Multiple Reactants and Reactions 23-13
Example 3: Thermal Cracking of Heavy Oils (Visbreaking) 23-13
Example 4: Styrene from Ethylbenzene 23-14

RESIDENCE TIME DISTRIBUTION (RTD) AND REACTOR EFFICIENCY

Tracers 23-15
Reactor Efficiency 23-15
Tracer Response 23-16
Kinds of Inputs 23-17
Response Functions 23-17
Elementary Models 23-17
Real Behavior 23-17
Tracer Equations 23-17
Ideal CSTR 23-17
Plug Flow Reactor (PFR) 23-18
Multistage CSTR 23-19
Combined Models, Transfer Functions 23-19
Characterization of RTD Curves 23-19
Gamma or Erlang Distribution 23-19
Gaussian Distribution 23-19
Gram-Charlier Series 23-20
Empirical Equations 23-20
Chemical Conversion 23-21
Segregated Flow 23-21
Maximum Mixedness 23-21
Dispersion Model 23-23
Boundary Conditions 23-23
Comparison of Models 23-23
Multiplicity and Stability 23-23
Example (*a*) 23-23
Example (*b*) 23-23
Example (*c*) 23-23
Example (*d*) 23-25

CATALYSIS

Homogeneous Catalysis 23-26
Immobilized or Polymer Bound, or Heterogenized Catalysts 23-26
Phase-Transfer Catalysis 23-26
Effect of Concentration 23-26
Catalysis by Solids 23-26
Selection of Catalysts 23-26
Kinds of Catalysts 23-28
Kinds of Catalyzed Organic Reactions 23-28
Physical Characteristics 23-29
Rate of Reaction 23-29
Effectiveness 23-30
Example 5: Application of Effectiveness 23-30
Adiabatic Reactions 23-30
Deactivation in Process 23-30
Distribution of Catalyst in Pores 23-31
Catalytic Membrane Reactors 23-32

HOMOGENEOUS REACTIONS

Liquid Phase 23-32
Laminar Flow 23-33
Nonisothermal Operation 23-33
Gas Phase 23-33
Supercritical Conditions 23-34
Polymerization 23-35
Kinds of Polymerization Processes 23-36
Bulk Polymerization 23-36
Bead Polymerization 23-36
Emulsions 23-36
Solution Polymerization 23-36

FLUIDS AND SOLID CATALYSTS

Single Fixed Beds 23-36
Multiple Fixed Beds 23-36
Multitubular Reactors 23-37
Slurry Reactors 23-38
Transport (or Entrainment) Reactors 23-38
Fluidized Beds 23-38
Moving Beds 23-38
Thin Beds and Wire Gauzes 23-38

GAS/LIQUID REACTIONS

Mass Transfer Coefficients . . . 23-39
Countercurrent Absorption Towers . . . 23-41
First-Order or Pseudo-First-Order Reaction in a Liquid Film . . . 23-42
Second-Order Reaction in a Liquid Film . . . 23-42
Scale-Up from Laboratory Data . . . 23-43
- Hatta Number . . . 23-43
- Specific Rate k_c . . . 23-43
- Gas-Film Coefficient k_g . . . 23-43
- Liquid-Film Coefficients k_L (Physical) and Ek_L (Reactive) . . . 23-43

Industrial Gas-Liquid Reaction Processes . . . 23-44
- Removal of CO_2 and H_2S from Inert Gases, Packed and Tray Towers . . . 23-44
- Sulfur Dioxide, Spray Towers . . . 23-44
- Stirred Vessels . . . 23-44
- Hydrogenation of Oils in Stirred Tanks . . . 23-46
- Aerobic Fermentation . . . 23-49
- Bubble Reactors . . . 23-49
- Liquid Dispersion . . . 23-49
- Tubular Reactors . . . 23-49
- Reaction in a Centrifugal Pump . . . 23-50
- Falling Film Reactor . . . 23-50

LIQUID/LIQUID REACTIONS

Equipment . . . 23-50
Mechanisms . . . 23-50
Operating Data . . . 23-50
Laboratory Studies . . . 23-50
Mass-Transfer Coefficients . . . 23-52
Choice of Dispersed Phase . . . 23-52
References for Liquid/Liquid Reactors . . . 23-52

GAS/LIQUID/SOLID REACTIONS

Overall Rate Equations with Diffusional Resistances . . . 23-52
Trickle Beds . . . 23-53
- Trickle Bed Hydrodesulfurization . . . 23-53

Flooded Fixed Bed Reactors . . . 23-53
Suspended Catalyst Beds . . . 23-54
- Slurry Reactors with Mechanical Agitation . . . 23-54
- Entrained Solids Bubble Columns with the Solid Fluidized by Bubble Action . . . 23-54
- GLS Fluidized with a Stable Level of Catalyst . . . 23-54

Trickle Bed Parameters . . . 23-54
- Pressure Drop . . . 23-55
- Example 6: Conditions of a Trickle Bed . . . 23-55
- Liquid Holdup . . . 23-55
- Gas/Liquid Mass Transfer . . . 23-55
- Gas/Liquid Interfacial Area . . . 23-55
- Liquid/Solid Mass Transfer . . . 23-55
- Axial Dispersion and the Peclet Number . . . 23-55

References for Gas/Liquid/Solid Reactions . . . 23-55

REACTIONS OF SOLIDS

Thermal Decompositions . . . 23-56
- Organic Solids . . . 23-56
- Exothermic Decompositions . . . 23-56
- Endothermic Decompositions . . . 23-56

Solid Reaction Examples . . . 23-56
- Carbothermic Reactions . . . 23-58

Solids and Gases . . . 23-58
- Literature . . . 23-58

Equipment and Processes . . . 23-58
- Pyrometallurgical Processes . . . 23-60
- Desulfurization with Dry Lime . . . 23-61

References for Reactions of Solids . . . 23-61

Nomenclature and Units

Following is a listing of typical nomenclature and units expressed in SI and U.S. customary. Specific definitions and units are stated at the place of application in the section.

Symbol	Definition	SI units	U.S. customary units
A, B, C, . . .	Names of substances, or their concentrations		
A^0	Free radical, as CH_j^0		
C_a	Concentration of substance A	kg mol/m^3	lb mol/ft^3
C^0	Initial mean concentration in vessel	kg mol/m^3	lb mol/ft^3
C_p	Heat capacity	kJ/(kg·K)	Btu/(lbm·°F)
CSTR	Continuous stirred tank reactor		
D, D_e, D_x	Dispersion coefficient	m^2/s	ft^2/s
D_{eff}	Effective diffusivity	m^2/s	ft^2/s
D_K	Knudsen diffusivity	m^2/s	ft^2/s
$E(t)$	Residence time distribution		
$E(t_r)$	Normalized residence time distribution		
f_a	C_a/C_{a0} or n_a/n_{a0}, fraction of A remaining unconverted		
$F(t)$	Age function of tracer		
ΔG	Gibbs energy change	kJ	Btu
Ha	Hatta number		
ΔH_r	Heat of reaction	kJ/kg mol	Btu/lb mol
K, K_c, K_y, K_ϕ	Chemical equilibrium constant		
k, k_c, k_p	Specific rate of reaction	Variable	Variable
L	Length of path in reactor	m	ft
n	Parameter of Erlang or gamma distribution, or number of stages in a CSTR battery		
n_a	Number of mols of A present		
n_a'	Number of mols flowing per unit time, the prime (′) may be omitted when context is clear		
n_t	Total number of mols		
p_a	Partial pressure of substance A	kPa	psi
Pe	Peclet number for dispersion		
PFR	Plug flow reactor		
Q	Heat transfer	kJ	Btu
r	Radial position	m	ft
r_a	Rate of reaction of A per unit volume	Variable	Variable
R	Radius of cylindrical vessel	m	ft
Re	Reynolds number		
Sc	Schmidt number		

Symbol	Definition	SI units	U.S. customary units
t	Time	s	s
$\bar{t}$	Mean residence time	s	s
t_r	$t/\bar{t}$, reduced time		
TFR	Tubular flow reactor		
u	Linear velocity	m/s	ft/s
$u(t)$	Unit step input		
V	Volume of reactor contents	m^3	ft^3
V'	Volumetric flow rate	m^3/s	ft^3/s
V_r	Volume of reactor	m^3	ft^3
x	Axial position in a reactor	m	ft
x_a	$1 - f_a = 1 - C_a/C_{a0}$ or $1 - n_a$, n_{a0}, fraction of A converted		
z	x/L, normalized axial position		
	Greek letters		
β	r/R, normalized radial position		
$\gamma^3(t)$	Skewness of distribution		
$\delta(t)$	Unit impulse input, Dirac function		
ε	Fraction void space in a packed bed		
ϑ	$t/\bar{t}$, reduced time		
η	Effectiveness of porous catalyst		
$\Lambda(t)$	Intensity function		
μ	Viscosity	Pa·s	lbm/(ft·s)
ν	v/ρ, kinematic viscosity	m^2/s	ft^2/s
π	Total pressure	Pa	psi
ρ	Density	kg/m^3	lbm/ft^3
ρ	r/R, normalized radial position in a pore		
$\sigma^2(t)$	Variance		
$\sigma^2(t_r)$	Normalized variance		
τ	$t/\bar{t}$, reduced time		
τ	Tortuosity		
ϕ	Thiele modulus		
ϕ_m	Modified Thiele modulus		
	Subscripts		
0	Subscript designating initial or inlet conditions, as in C_{a0}, n_{a0}, V_0', . . .		

MODELING CHEMICAL REACTORS

General References: The General References listed in Sec. 7 are applicable for Sec. 23. References to specific topics are made throughout this section.

An industrial chemical reactor is a complex device in which heat transfer, mass transfer, diffusion, and friction may occur along with chemical reaction, and it must be safe and controllable. In large vessels, questions of mixing of reactants, flow distribution, residence time distribution, and efficient utilization of the surface of porous catalysts also arise. A particular process can be dominated by one of these factors or by several of them; for example, a reactor may on occasion be predominantly a heat exchanger or a mass-transfer device. A successful commercial unit is an economic balance of all these factors.

Some modes of heat transfer to stirred tank reactors are shown in Fig. 23-1 and to packed bed reactors in Fig. 23-2. Temperature and composition profiles of some processes are shown in Fig. 23-3. Operating data, catalysts, and reaction times are stated for a number of industrial reaction processes in Table 23-1.

Many successful types of reactors are illustrated throughout this section. Additional sketches may be found in other books on this topic, particularly in Walas (*Chemical Process Equipment Selection and Design,* Butterworths, 1990) and Ullmann (*Encyclopedia of Chemical Technology* (in German), vol. 3, Verlag Chemie, 1973, pp. 321–518).

The general characteristics of the main types of reactors—batch and continuous—are clear. Batch processes are suited to small production rates, to long reaction times, or to reactions where they may have superior selectivity, as in some polymerizations. They are conducted in tanks with stirring of the contents by internal impellers, gas bubbles, or pumparound. Temperature control is with internal surfaces or jackets, reflux condensers, or pumparound through an exchanger.

Large daily production rates are mostly conducted in continuous equipment, either in a series of stirred tanks or in units in which some degree of plug flow is attained. Many different equipment configurations are illustrated throughout this section for reactions of liquids, gases, and solids, singly or in combinations. By showing how something has been done previously, this picture gallery may suggest how a similar new process could be implemented.

Continuous stirred tank reactors (CSTRs) are frequently employed multiply and in series. Reactants are continuously fed to the first vessel; they overflow through the others in succession, while being thoroughly mixed in each vessel. Ideally, the composition is uniform in individual vessels, but a stepped concentration gradient exists in the system as a whole. For some cases, a series of five or six vessels approximates the performance of a plug flow reactor. Instead of being in distinct vessels, the several stages of a CSTR battery can be put in a single shell. If horizontal, the multistage reactor is compartmented by vertical weirs of different heights, over which the reacting mixture cascades. When the reactants are of limited miscibilities and have a sufficient density difference, the vertical staged reactor lends itself to countercurrent operation, a real advantage with reversible reactions. A small fluidized bed is essentially completely mixed. A large commercial fluidized bed reactor is of nearly uniform temperature, but the flow patterns consist of mixed and plug flow and in-between zones.

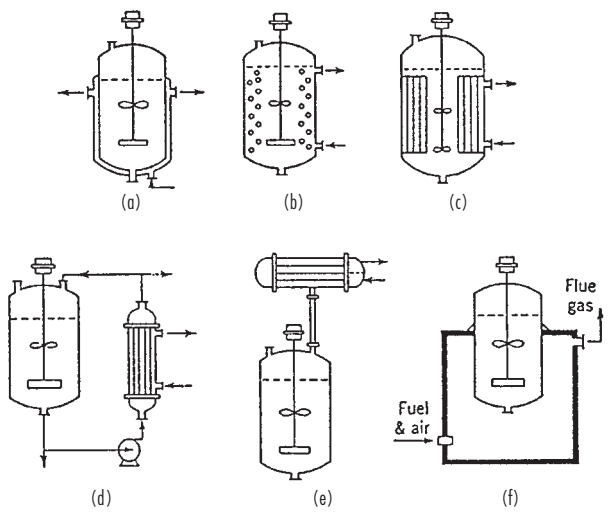

FIG. 23-1 Heat transfer to stirred tank reactors. (*a*) Jacket. (*b*) Internal coils. (*c*) Internal tubes. (*d*) External heat exchanger. (*e*) External reflux condensor. (*f*) Fired heater. (*Walas,* Reaction Kinetics for Chemical Engineers, *McGraw-Hill, 1959*).

Tubular flow reactors (TFRs) are characterized by continuous gradients of concentration in the direction of flow that approach plug flow, in contrast to the stepped gradient characteristic of the CSTR battery. They may have several pipes or tubes in parallel. The reactants are charged continuously at one end and products are removed at the other end. Normally a steady state is attained, a fact of importance for automatic control and for laboratory work. Both horizontal and vertical orientations are common. When heat transfer is needed, individual tubes are jacketed or shell-and-tube construction is used. In the latter case the reactants may be on either the shell or the tube side. The reactant side may be filled with solid particles, either catalytic (if required) or inert, to improve heat transfer by increased turbulence or to improve interphase contact in heterogeneous reactions. Large-diameter vessels with packing or trays may approach plug flow behavior and are widely employed. Some of the configurations in use are axial flow, radial flow, multiple shell, with built-in heat exchangers, horizontal, vertical and so on. *Quasi-plug flow reactors* have continuous gradients but are not quite in plug flow.

Semiflow or batch flow operations may employ a single stirred tank or a series of them. Some of the reactants are loaded into the reactors as a single charge and the remaining ones are then fed gradually. This mode of operation is especially favored when large heat effects occur and heat-transfer capability is limited, since exothermic reactions can be slowed down and endothermic rates maintained by limiting the concentrations of some of the reactants. Other situations making this sort of operation desirable occur when high concentrations may result in the formation of undesirable side products, or when one of the reactants is a gas of limited solubility so that it can be fed only at the dissolution rate.

Relative advantages and fields of application of continuous stirred and plug flow reactors may be indicated briefly. A reaction battery is a highly flexible device, although both mechanically and operationally more expensive and complex than tubular units. Relatively slow reactions are best conducted in a CSTR battery, which is usually cheaper than a single reactor for moderate production rates. The tubular reactor is especially suited to cases needing considerable heat transfer, where high pressures and very high or very low temperatures occur, and when relatively short reaction times suffice.

MATHEMATICAL MODELS

A model of a reaction process is a set of data and equations that is believed to represent the performance of a specific vessel configuration (mixed, plug flow, laminar, dispersed, and so on). The equations include the stoichiometric relations, rate equations, heat and material balances, and auxiliary relations such as those of mass transfer, pressure variation, contacting efficiency, residence time distribution, and so on. The data describe physical and thermodynamic properties and, in the ultimate analysis, economic factors.

Correlations of heat and mass-transfer rates are fairly well developed and can be incorporated in models of a reaction process, but the chemical rate data must be determined individually. The most useful rate data are at constant temperature, under conditions where external mass transfer resistance has been avoided, and with small particles

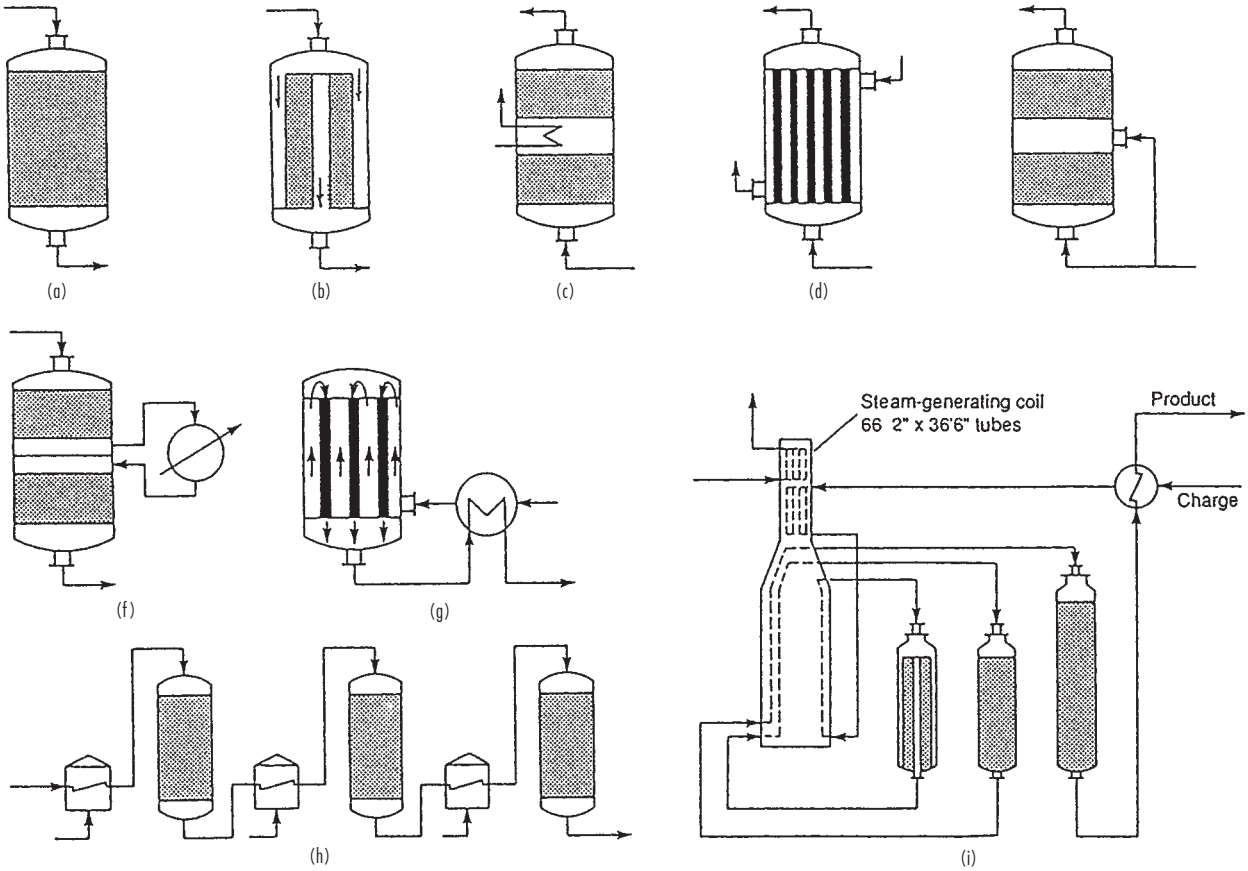

FIG. 23-2 Heat exchange in packed reactors. (*a*) Adiabatic downflow. (*b*) Adiabatic radial flow, low ΔP. (*c*) Built-in interbed exchanger. (*d*) Shell and tube. (*e*) Interbed cold-shot injection. (*f*) External interbed exchanger. (*g*) Autothermal shell, outside influent/effluent heat exchanger. (*h*) Multibed adiabatic reactors with interstage heaters. (*i*) Platinum catalyst, fixed bed reformer for 5,000 BPSD charge rate; reactors 1 and 2 are 5.5 by 9.5 ft and reactor 3 is 6.5 by 12.0 ft; temperatures 502 ⇒ 433, 502 ⇒ 471, 502 ⇒ 496°C. To convert ft to m, multiply by 0.3048; BPSD to m^3/h, multiply by 0.00662.

with complete catalyst effectiveness. Equipment for obtaining such data is now widely used, especially for reactions with solid catalysts, and it is virtually essential for serious work. Simpler equipment gives data that are more difficult to interpret but may be adequate for exploratory work.

Once fundamental data have been obtained, the goal is to develop a mathematical model of the process and to utilize it to explore such possibilities as product selectivity, start-up and shut-down behavior, vessel configuration, temperature, pressure, and conversion profiles, and so on.

How complete a model has to be is an open question. Very elaborate ones are justifiable and have been developed only for certain widely practiced and large-scale processes, or for processes where operating conditions are especially critical. The only policy to follow is to balance the cost of development of the model against any safety factors that otherwise must be applied to a final process design. Engineers constantly use heat and material balances without perhaps realizing, like Moliere's Bourgeois, that they are modeling mathematically. The simplest models may be adequate for broad discrimination between alternatives.

MODELING PRINCIPLES

How a differential equation is formulated for some kinds of ideal reactors is described briefly in Sec. 7 of this Handbook and at greater length with many examples in Walas (*Modeling with Differential Equations in Chemical Engineering,* Butterworth-Heineman, 1991). First, a mechanism is assumed: whether completely mixed, plug flow, laminar, with dispersion, with bypass or recycle or dead space, steady or unsteady, and so on. Then, for a differential element of space and/or time the elements of a conservation law,

$$\text{Inputs} + \text{Sources} = \text{Outputs} + \text{Sinks} + \text{Accumulations}$$

are formulated and put together. Any transport properties are introduced through known correlations together with the parameters of specified rate equations. The model can be used to find the performance under various conditions, or its parameters can be evaluated from experimental data. The two comprehensive examples in this section evaluate performance when all the parameters are known. There are other examples in these sections where the parameters of rate equations, residence time distributions, or effectiveness are to be found from rate or tracer data.

CHEMICAL KINETIC LAWS

The two basic laws of kinetics are the *law of mass action* for the rate of a reaction and the *Arrhenius equation* for its dependence on temperature. Both of these are strictly empirical. They depend on the structures of the molecules, but at present the constants of the equations cannot be derived from the structures of reacting molecules. For a reaction, $a\text{A} + b\text{B} \Rightarrow$ Products, the combined law is

$$r_a = -\frac{1}{V_r}\frac{dn_a}{dt} = \exp\left(\gamma + \frac{\delta}{T}\right) C_a^{\alpha} C_b^{\beta} \qquad (23\text{-}1)$$

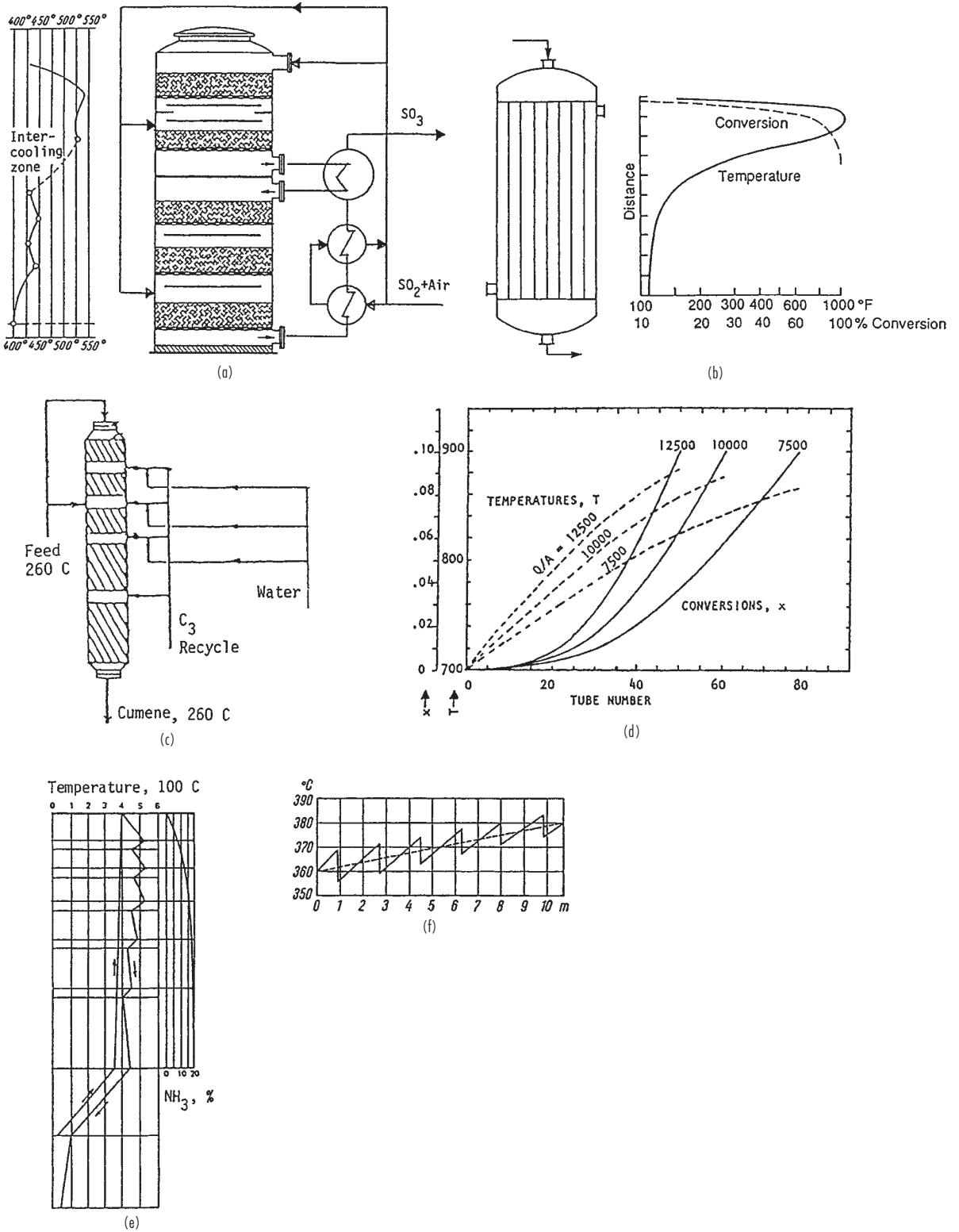

FIG. 23-3 Temperature and composition profiles. (*a*) Oxidation of SO_2 with intercooling and two cold shots. (*b*) Phosgene from CO and Cl_2, activated carbon in 2-in tubes, water cooled. (*c*) Cumene from benzene and propylene, phosphoric acid on quartz, with four quench zones, 260°C. (*d*) Mild thermal cracking of a heavy oil in a tubular furnace, back pressure of 250 psig and several heat fluxes, Btu/(ft²·h), *T* in °F. (*e*) Vertical ammonia synthesizer at 300 atm, with five cold shots and an internal exchanger. (*f*) Vertical methanol synthesizer at 300 atm, Cr_2O_3-ZnO catalyst, with six cold shots totaling 10 to 20 percent of the fresh feed. To convert psi to kPa, multiply by 6.895; atm to kPa, multiply by 101.3.

TABLE 23-1 Residence Times and/or Space Velocities in Industrial Chemical Reactors*

Product (raw materials)	Type	Reactor phase	Catalyst	*T*, °C	*P*, atm	Residence time or space velocity	Source and page†
Acetaldehyde (ethylene, air)	FB	L	Cu and Pd chlorides	50–100	8	6–40 min	[2] 1, [7] 3
Acetic anhydride (acetic acid)	TO	L	Triethylphosphate	700–800	0.3	0.25–5 s	[2]
Acetone (*i*-propanol)	MT	LG	Ni	300	1	2.5 h	[1] 1 314
Acrolein (formaldehyde, acetaldehyde)	FL	G	MnO, silica gel	280–320	1	0.6 s	[1] 1 384, [7] 33
Acrylonitrile (air, propylene, ammonia)	FL	G	Bi phosphomolybdate	400	1	4.3 s	[3] 684, [2] 47
Adipic acid (nitration of cyclohexanol)	TO	L	Co naphthenate	125–160	4–20	2 h	[2] 51, [7] 49
Adiponitrile (adipic acid)	FB	G	H_3BO_3 H_3PO_4	370–410	1	3.5–5 s 350–500 GHSV	[1] 2 152, [7] 52
Alkylate (*i*-C_4, butenes)	CST	L	H_2SO_4	5–10	2–3	5–40 min	[4] 223
Alkylate (*i*-C_4, butenes)	CST	L	HF	25–38	8–11	5–25 min	[4] 223
Allyl chloride (propylene, Cl_2)	TO	G	NA	500	3	0.3–1.5 s	[1] 2 416, [7] 67
Ammonia (H_2, N_2)	FB	G	Fe	450	150	28 s 7,800 GHSV	[6] 61
Ammonia (H_2, N_2)	FB	G	Fe	450	225	33 s 10,000 GHSV	[6] 61
Ammonia oxidation	Flame	G	Pt gauze	900	8	0.0026 s	[6] 115
Aniline (nitrobenzene, H_2)	B	L	$FeCl_2$ in H_2O	95–100	1	8 h	[1] 3 289
Aniline (nitrobenzene, H_2)	FB	G	Cu on silica	250–300	1	0.5–100 s	[7] 82
Aspirin (salicylic acid, acetic anhydride)	B	L	None	90	1	>1 h	[7] 89
Benzene (toluene)	TU	G	None	740	38	48 s 815 GHSV	[6] 36, [9] 109
Benzene (toluene)	TU	G	None	650	35	128 s	[1] 4 183, [7] 98
Benzoic acid (toluene, air)	SCST	LG	None	125–175	9–13	0.2–2 h	[7] 101
Butadiene (butane)	FB	G	Cr_2O_3, Al_2O_3	750	1	0.1–1 s	[7] 118
Butadiene (1-butene)	FB	G	None	600	0.25	0.001 s 34,000 GHSV	[3] 572
Butadiene sulfone (butadiene, SO_2)	CST	L	*t*-Butyl catechol	34	12	0.2 LHSV	[1] 5 192
i-Butane (*n*-butane)	FB	L	$AlCl_3$ on bauxite	40–120	18–36	0.5–1 LHSV	[4] 239, [7] 683
i-Butane (*n*-butane)	FB	L	Ni	370–500	20–50	1–6 WHSV	[4] 239
Butanols (propylene hydroformylation)	FB	L	PH_3-modified Co carbonyls	150–200	1,000	100 g L·h	[1] 5 373
Butanols (propylene hydroformylation)	FB	L	Fe pentacarbonyl	110	10	1 h	[7] 125
Calcium stearate	B	L	None	180	5	1–2 h	[7] 135
Caprolactam (cyclohexane oxime)	CST	L	Polyphosphoric acid	80–110	1	0.25–2 h	[1] 6 73, [7] 139
Carbon disulfide (methane, sulfur)	Furn.	G	None	500–700	1	1.0 s	[1] 6 322, [7] 144
Carbon monoxide oxidation (shift)	TU	G	Cu-Zn or Fe_2O_3	390–220	26	4.5 s 7,000 GHSV	[6] 44
Portland cement	Kiln	S		1,400–1,700	1	10 h	[11]
Chloral (Cl_2, acetaldehyde)	CST	LG	None	20–90	1	140 h	[7] 158
Chlorobenzenes (benzene, Cl_2)	SCST	LG	Fe	40	1	24 h	[1] 8 122
Coking, delayed (heater)	TU	LG	None	490–500	15–4	250 s	[1] 10 8
Coking, delayed (drum, 100 ft max height)	B	LG	None	500–440	4	0.3–0.5 ft/s vapor	[1] 10 8
Cracking, fluid catalytic	Riser	G	Zeolite	520–540	2–3	2–4 s	(14) 353
Cracking, hydro (gas oils)	FB	LG	Ni, SiO_2, Al_2O_3	350–420	100–150	1–2 LHSV	[11]
Cracking (visbreaking residual oils)	TU	LG	None	470–495	10–30	450 s, 8 LHSV	[11]
Cumene (benzene, propylene)	FB	G	H_3PO_4	260	35	23 LHSV	[11]
Cumene hydroperoxide (cumene, air)	CST	L	Metal porphyrins	95–120	2–15	1–3 h	[7] 191
Cyclohexane (benzene, H_2)	FB	G	Ni on Al_2O_3	150–250	25–55	0.75–2 LHSV	[7] 201
Cyclohexanol (cyclohexane, air)	SCST	LG	None	185–200	48	2–10 min	[7] 203
Cyclohexanone (cyclohexanol)	CST	L	N.A.	107	1	0.75 h	[8] (1963)
Cyclohexanone (cyclohexanol)	MT	G	Cu on pumice	250–350	1	4–12 s	[8] (1963)
Cyclopentadiene (dicyclopentadiene)	TJ	G	None	220–300	1–2	0.1–0.5 LHSV	[7] 212
DDT (chloral, chlorobenzene)	B	L	Oleum	0–15	1	8 h	[7] 233
Dextrose (starch)	CST	L	H_2SO_4	165	1	20 min	[8] (1951)
Dextrose (starch)	CST	L	Enzyme	60	1	100 min	[7] 217
Dibutylphthalate (phthalic anhydride, butanol)	B	L	H_2SO_4	150–200	1	1–3 h	[7] 227
Diethylketone (ethylene, CO)	TO	L	Co oleate	150–300	200–500	0.1–10 h	[7] 243
Dimethylsulfide (methanol, CS_2)	FB	G	Al_2O_3	375–535	5	150 GHSV	[7] 266
Diphenyl (benzene)	MT	G	None	730	2	0.6 s 3.3 LHSV	[7] 275, [8] (1938)
Dodecylbenzene (benzene, propylene tetramer)	CST	L	$AlCl_3$	15–20	1	1–30 min	[7] 283
Ethanol (ethylene, H_2O)	FB	G	H_3PO_4	300	82	1,800 GHSV	[2] 356, [7] 297
Ethyl acetate (ethanol, acetic acid)	TU, CST	L	H_2SO_4	100	1	0.5–0.8 LHSV	[10] 45, 52, 58
Ethyl chloride (ethylene, HCl)	TO	G	$ZnCl_2$	150–250	6–20	2 s	[7] 305
Ethylene (ethane)	TU	G	None	860	2	1.03 s 1,880 GHSV	[3] 411, [6] 13
Ethylene (naphtha)	TU	G	None	550–750	2–7	0.5–3 s	[7] 254
Ethylene, propylene chlorohydrins (Cl_2, H_2O)	CST	LG	None	30–40	3–10	0.5–5 min	[7] 310, 580
Ethylene glycol (ethylene oxide, H_2O)	TO	LG	1% H_2SO_4	50–70	1	30 min	[2] 398
Ethylene glycol (ethylene oxide, H_2O)	TO	LG	None	195	13	1 h	[2] 398
Ethylene oxide (ethylene, air)	FL	G	Ag	270–290	1	1 s	[2] 409, [7] 322
Ethyl ether (ethanol)	FB	G	WO_3	120–375	2–100	30 min	[7] 326
Fatty alcohols (coconut oil)	B	L	Na, solvent	142	1	2 h	[8] (1953)

TABLE 23-1 Residence Times and/or Space Velocities in Industrial Chemical Reactors (*Concluded*)

Product (raw materials)	Type	Reactor phase	Catalyst	T, °C	P, atm	Residence time or space velocity	Source and page†
Formaldehyde (methanol, air)	FB	G	Ag gauze	450–600	1	0.01 s	[2] 423
Glycerol (allyl alcohol, H_2O_2)	CST	L	H_2WO_4	40–60	1	3 h	[7] 347
Hydrogen (methane, steam)	MT	G	Ni	790	13	5.4 s 3,000 GHSV	[6] 133
Hydrodesulfurization of naphtha	TO	LG	Co-MO	315–500	20–70	1.5–8 LHSV 125 WHSV	[4] 285, [6] 179, [9] 201
Hydrogenation of cottonseed oil	SCST	LG	Ni	130	5	6 h	[6] 161
Isoprene (*i*-butene, formaldehyde)	FB	G	HCl, silica gel	250–350	1	1 h	[7] 389
Maleic anhydride (butenes, air)	FL	G	V_2O_5	300–450	2–10	0.1–5 s	[7] 406
Melamine (urea)	B	L	None	340–400	40–150	5–60 min	[7] 410
Methanol (CO, H_2)	FB	G	ZnO, Cr_2O_3	350–400	340	5,000 GHSV	[7] 421
Methanol (CO, H_2)	FB	G	ZnO, Cr_2O_3	350–400	254	28,000 GHSV	[3] 562
o-Methyl benzoic acid (xylene, air)	CST	L	None	160	14	0.32 h 3.1 LHSV	[3] 732
Methyl chloride (methanol, Cl_2)	FB	G	Al_2O_3 gel	340–350	1	275 GHSV	[2] 533
Methyl ethyl ketone (2-butanol)	FB	G	ZnO	425–475	2–4	0.5–10 min	[7] 437
Methyl ethyl ketone (2-butanol)	FB	G	Brass spheres	450	5	2.1 s 13 LHSV	[10] 284
Nitrobenzene (benzene, HNO_3)	CST	L	H_2SO_4	45–95	1	3–40 min	[7] 468
Nitromethane (methane, HNO_3)	TO	G	None	450–700	5–40	0.07–0.35 s	[7] 474
Nylon-6 (caprolactam)	TU	L	Na	260	1	12 h	[7] 480
Phenol (cumene hydroperoxide)	CST	L	SO_2	45–65	2–3	15 min	[7] 520
Phenol (chlorobenzene, steam)	FB	G	Cu, Ca phosphate	430–450	1–2	2 WHSV	[7] 522
Phosgene (CO, Cl_2)	MT	G	Activated carbon	50	5–10	16 s 900 GHSV	[11]
Phthalic anhydride (*o*-xylene, air)	MT	G	V_2O_5	350	1	1.5 s	[3] 482, 539, [7] 529
Phthalic anhydride (naphthalene, air)	FL	G	V_2O_5	350	1	5 s	[9] 136, [10] 335
Polycarbonate resin (bisphenol-A, phosgene)	B	L	Benzyltriethylammonium chloride	30–40	1	0.25–4 h	[7] 452
Polyethylene	TU	L	Organic peroxides	180–200	1,000–1,700	0.5–50 min	[7] 547
Polyethylene	TU	L	Cr_2O_3, Al_2O_3, SiO_2	70–200	20–50	0.1–1,000 s	[7] 549
Polypropylene	TO	L	R_2AlCl, $TiCl_4$	15–65	10–20	15–100 min	[7] 559
Polyvinyl chloride	B	L	Organic peroxides	60	10	5.3–10 h	[6] 139
i-Propanol (propylene, H_2O)	TO	L	H_2SO_4	70–110	2–14	0.5–4 h	[7] 393
Propionitrile (propylene, NH_3)	TU	G	CoO	350–425	70–200	0.3–2 LHSV	[7] 578
Reforming of naphtha (H_2/hydrocarbon = 6)	FB	G	Pt	490	30–35	3 LHSV 8,000 GHSV	[6] 99
Starch (corn, H_2O)	B	L	SO_2	25–60	1	18–72 h	[7] 607
Styrene (ethylbenzene)	MT	G	Metal oxides	600–650	1	0.2 s 7,500 GHSV	[5] 424
Sulfur dioxide oxidation	FB	G	V_2O_5	475	1	2.4 s 700 GHSV	[6] 86
t-Butyl methacrylate (methacrylic acid, *i*-butene)	CST	L	H_2SO_4	25	3	0.3 LHSV	[1] 5 328
Thiophene (butane, S)	TU	G	None	600–700	1	0.01–1 s	[7] 652
Toluene diisocyanate (toluene diamine, phosgene)	B	LG	None	200–210	1	7 h	[7] 657
Toluene diamine (dinitrotoluene, H_2)	B	LG	Pd	80	6	10 h	[7] 656
Tricresyl phosphate (cresyl, $POCl_3$)	TO	L	$MgCl_2$	150–300	1	0.5–2.5 h	[2] 850, [7] 673
Vinyl chloride (ethylene, Cl_2)	FL	G	None	450–550	2–10	0.5–5 s	[7] 699
Aldehydes (diisobutene, CO)	CST	LG	Co Carbonyl	150	200	1.7 h	(12) 173
Allyl alcohol (propylene oxide)	FB	G	Li phosphate	250	1	1.0 LHSV	(15) 23
Automobile exhaust	FB	G	Pt-Pd: 1–2 g/unit	400–600+	1		
Gasoline (methanol)	FB	G	Zeolite	400	20	2 WHSV	(13)3 383
Hydrogen cyanide (NH_3, CH_4)	FB	G	Pt-Rh	1150	1	0.005 s	(15) 211
Isoprene, polymer	B	L	$Al(i\text{-}Bu)_3{\cdot}TiCl_4$	20–50	1–5	1.5–4 h	(15) 82
NO_x pollutant (with NH_3)	FB	G	$V_2O_5{\cdot}TiO_2$	300–400	1–10		(14) 332
Vinyl acetate (ethylene + CO)	TO	LG	Cu-Pd	130	30	1 h L, 10 s G	(12) 140

*Abbreviations: reactors: batch (B), continuous stirred tank (CST), fixed bed of catalyst (FB), fluidized bed of catalyst (FL), furnace (Furn.), multitubular (MT), semicontinuous stirred tank (SCST), tower (TO), tubular (TU). Phases: liquid (L), gas (G), both (LG). Space velocities (hourly): gas (GHSV), liquid (LHSV), weight (WHSV). Not available, NA. To convert atm to kPa, multiply by 101.3.

†1. J. J. McKetta, ed., *Encyclopedia of Chemical Processing and Design,* Marcel Dekker, 1976 to date (referenced by volume).
2. W. L. Faith, D. B. Keyes, and R. L. Clark, *Industrial Chemicals,* revised by F. A. Lowenstein and M. K. Moran, John Wiley & Sons, 1975.
3. G. F. Froment and K. B. Bischoff, *Chemical Reactor Analysis and Design,* John Wiley & Sons, 1979.
4. R. J. Hengstebeck, *Petroleum Processing,* McGraw-Hill, New York, 1959.
5. V. G. Jenson and G. V. Jeffreys, *Mathematical Methods in Chemical Engineering,* 2d ed., Academic Press, 1977.
6. H. F. Rase, *Chemical Reactor Design for Process Plants,* Vol. 2: Case Studies, John Wiley & Sons, 1977.
7. M. Sittig, *Organic Chemical Process Encyclopedia,* Noyes, 1969 (patent literature exclusively).
8. Student Contest Problems, published annually by AIChE, New York (referenced by year).
9. M. O. Tarhan, *Catalytic Reactor Design,* McGraw-Hill, 1983.
10. K. R. Westerterp, W. P. M. van Swaaij, and A. A. C. M. Beenackers, *Chemical Reactor Design and Operation,* John Wiley & Sons, 1984.
11. Personal communication (Walas, 1985).
12. B. C. Gates, J. R. Katzer, and G. C. A. Schuit, *Chemistry of Catalytic Processes,* McGraw-Hill, 1979.
13. B. E. Leach, ed., *Applied Industrial Catalysts,* 3 vols., Academic Press, 1983.
14. C. N. Satterfield, *Heterogeneous Catalysis in Industrial Practice,* McGraw-Hill, 1991.
15. C. L. Thomas, *Catalytic Processes and Proven Catalysts,* Academic Press, 1970.

When the density is constant, replace $n_a/V_r = C_a$. How the constants α, β, γ, and δ are found from experimental conversion data is explained in Sec. 7.

BASIC REACTOR ELEMENTS

Reactions are carried out as batches or with continuous streams through a vessel. Flow reactors are distinguished by the degree of mixing of successive inputs. The limiting cases are: (1) with complete mixing, called an *ideal continuous stirred tank reactor* (CSTR), and (2) with no axial mixing, called a *plug flow reactor* (PFR).

Real reactors deviate more or less from these ideal behaviors. Deviations may be detected with *residence time distributions* (RTD) obtained with the aid of tracer tests. In other cases a mechanism may be postulated and its parameters checked against test data. The commonest models are combinations of CSTRs and PFRs in series and/or parallel. Thus, a stirred tank may be assumed completely mixed in the vicinity of the impeller and in plug flow near the outlet.

The combination of reactor elements is facilitated by the concept of *transfer functions.* By this means the Laplace transform can be found for the overall model, and the residence time distribution can be found after inversion. Finally, the chemical conversion in the model can be developed with the *segregation* and *maximum mixed* models.

Simple combinations of reactor elements can be solved directly. Figure 23-8, for instance, shows two CSTRs in series and with recycle through a PFR. The material balances with an n-order reaction $r = kC^n$ are

$$\frac{C_3}{C_2} = \frac{1}{1 + \dfrac{kV_rC_2}{RV'}}$$

$$V'C_f + RC_3 = (V' + R)C_1 + kV_{r1}C_1^n$$

$$(V' + R)C_1 = (V' + R)C_2 + kV_{r2}C_2^n \qquad (23\text{-}2)$$

Elimination of C_1 and C_3 from these equations will result in the desired relation between inlet C_f and outlet C_2 concentrations, although not in an explicit form except for zero or first-order reactions. Alternatively, the Laplace transform could be found, inverted and used to evaluate segregated or max mixed conversions that are defined later. Inversion of a transform like that of Fig. 23-8 is facilitated after replacing the exponential by some ratio of polynomials, a Padé approximation, as explained in books on linear control theory. Numerical inversion is always possible.

A stirred tank sometimes can be modeled as having a fraction α in bypass and a fraction β of the reactor volume stagnant. The material balance then is made up of

$$C = \alpha C_0 + (1 - \alpha)C_1 \qquad (23\text{-}3)$$

$$(1 - \alpha)V'C_0 = (1 - \alpha)V'C_1 + (1 - \beta)\,kV_rC_1^n \qquad (23\text{-}4)$$

where C_1 is the concentration leaving the active zone of the tank. Elimination of C_1 will relate the input and overall output concentrations. For a first-order reaction,

$$\frac{C_0}{C} = 1 + \frac{kV_r(1 - \beta)}{V'(1 - \alpha)} \qquad (23\text{-}5)$$

The two parameters α and β may be expected to depend on the amount of agitation.

A flow reactor with some deviation from plug flow, a quasi-PFR, may be modeled as a CSTR battery with a characteristic number n of stages, or as a dispersion model with a characteristic value of the dispersion coefficient or Peclet number. These models are described later.

MATERIAL BALANCES

Material and energy balances of common types of reactors are summarized in several tables of Sec. 7. For review purposes some material balances are restated here. For the nth stage of a CSTR battery,

$$V'_{n-1}C_{n-1} = V'_nC_n + V_rr_n \qquad (23\text{-}6)$$

or at constant density and a power law rate,

$$C_{n-1} = C_n + k\bar{t}_nC_n^\alpha \qquad (23\text{-}7)$$

The concentrations of all stages are found in succession when C_0 is known. For a PFR,

$$-V'\,dn_a = r_a\,dV_r = k\left(\frac{n_a}{V'}\right)^\alpha dV_r$$

$$kV_r = \int_{n_a}^{n_{a_0}} V'\left(\frac{V'}{n_a}\right)^\alpha dn_a \qquad (23\text{-}8)$$

For operation with an inert tracer, the material balances are conveniently handled as Laplace transforms. For a stirred tank, the differential equation

$$C_0 = C + \bar{t}\,\frac{dC}{dt}, \qquad C = 0 \quad \text{when} \quad t = 0 \qquad (23\text{-}9)$$

becomes

$$\frac{\overline{C}}{\overline{C}_0} = \frac{1}{1 + \bar{t}s} \qquad (23\text{-}10)$$

and the partial differential equation of a plug flow vessel becomes

$$\frac{\overline{C}}{\overline{C}_0} = \exp(-\bar{t}s) \qquad (23\text{-}11)$$

The terms on the right are the transfer functions.

With the two units in series,

$$\frac{\overline{C}_2}{\overline{C}_0} = \left(\frac{\overline{C}_2}{\overline{C}_1}\right)\left(\frac{\overline{C}_1}{\overline{C}_0}\right) = \frac{\exp(-\bar{t}_2s)}{1 + \bar{t}_1s} \qquad (23\text{-}12)$$

and in parallel with a fraction β going to the mixed unit

$$\frac{\overline{C}}{\overline{C}_0} = \frac{\beta}{1 + \bar{t}_1s} + (1 - \beta)\exp(-\bar{t}_2s) \qquad (23\text{-}13)$$

where $\bar{t}_1 = \dfrac{V_{r1}}{\beta V'}$, $\quad \bar{t}_2 = \dfrac{V_{r2}}{(1 - \beta)V'}$

HEAT TRANSFER AND MASS TRANSFER

Temperature affects rates of reaction, degradation of catalysts, and equilibrium conversion. Some of the modes of heat transfer applied in reactors are indicated in Figs. 23-1 and 23-2. Profiles of some temperatures and compostions in reactors are in Figs. 23-3 to 23-6, 23-22, and 23-40. Many reactors with fixed beds of catalyst pellets have divided beds, with heat transfer between the individual sections. Such units can take advantage of initial high rates at high temperatures and higher equilibrium conversions at lower temperatures. Data for two such cases are shown in Table 23-2. For SO_2 the conversion attained in the fourth bed is 97.5 percent, compared with an adiabatic single bed value of 74.8 percent. With the three-bed ammonia reactor, final ammonia concentration is 18.0 percent, compared with the one-stage adiabatic value of 15.4 percent. Some catalysts deteriorate at much above 500°C, another reason for limiting temperatures.

Since reactors come in a variety of configurations, use a variety of operating modes, and may handle mixed phases, the design of provisions for temperature control draws on a large body of heat transfer theory and data. These extensive topics are treated in other sections of this Handbook and in other references. Some of the high points pertinent to reactors are covered by Rase (*Chemical Reactor Design for Process Plants,* Wiley, 1977). Two encyclopedic references are *Heat Exchanger Design Handbook* (5 vols., Hemisphere, 1983–date), and Cheremisinoff, ed. (*Handbook of Heat and Mass Transfer,* 4 vols., Gulf, 1986–1990), which has several articles addressed specifically to reactors.

References to mass transfer are made throughout this section wherever multiple phases are discussed.

CASE STUDIES

Exploration for an acceptable or optimum design of a new reaction process may need to consider reactor types, several catalysts, specifications of feed and product, operating conditions, and economic evaluations. Modifications to an existing process likewise may need to consider many cases. These efforts can be eased by commercial kinetics services. A typical one can handle up to 20 reactions in CSTRs or

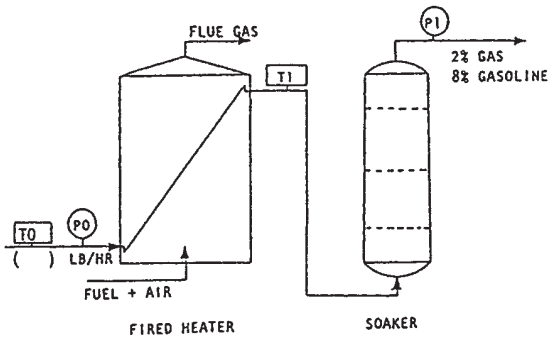

(a)

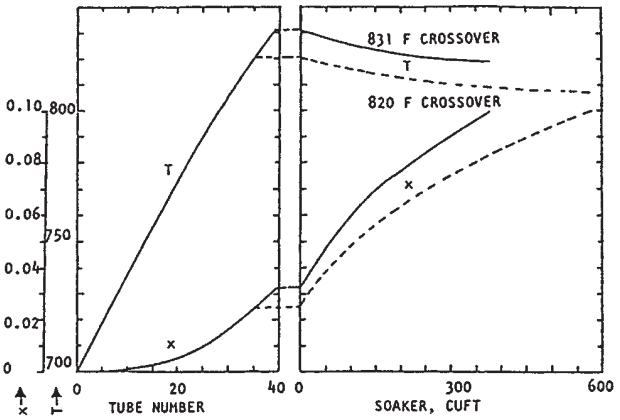

(b)

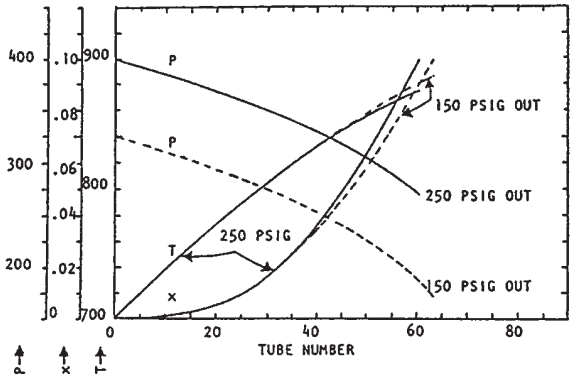

(c)

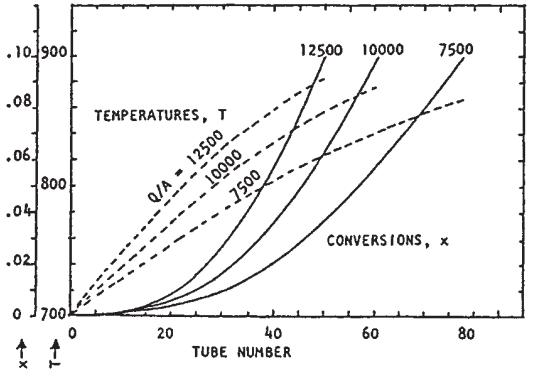

(d)

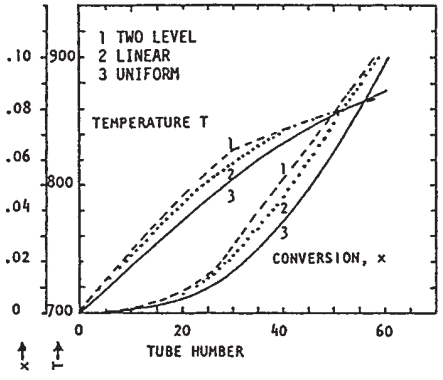

(e)

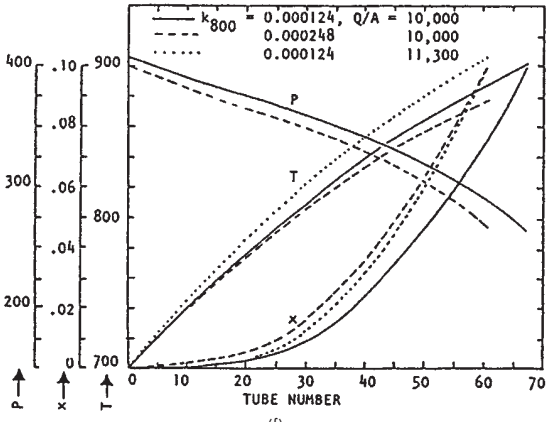

(f)

FIG. 23-4 (*a*) Visbreaking flowsketch, feed 160,000 lbm/h, $k_{800} = 0.000248$/s, tubes 5.05 in ID by 40 ft; (*b*) $Q/A = 10{,}000$ Btu/(ft^2·h), $P_{out} = 250$ psig; (*c*) $Q/A = 10{,}000$ Btu/(ft^2·h), $P_{out} = 150$ or 250 psig; (*d*) three different heat fluxes, $P_{out} = 250$ psig; (*e*) variation of heat flux, average 10,000 Btu/(ft^2·h), $P_{out} = 250$ psig; (*f*) halving the specific rate. *T* in °F. To convert psi to kPa, multiply by 6.895; ft to m, multiply by 0.3048; in to cm, multiply by 2.54.

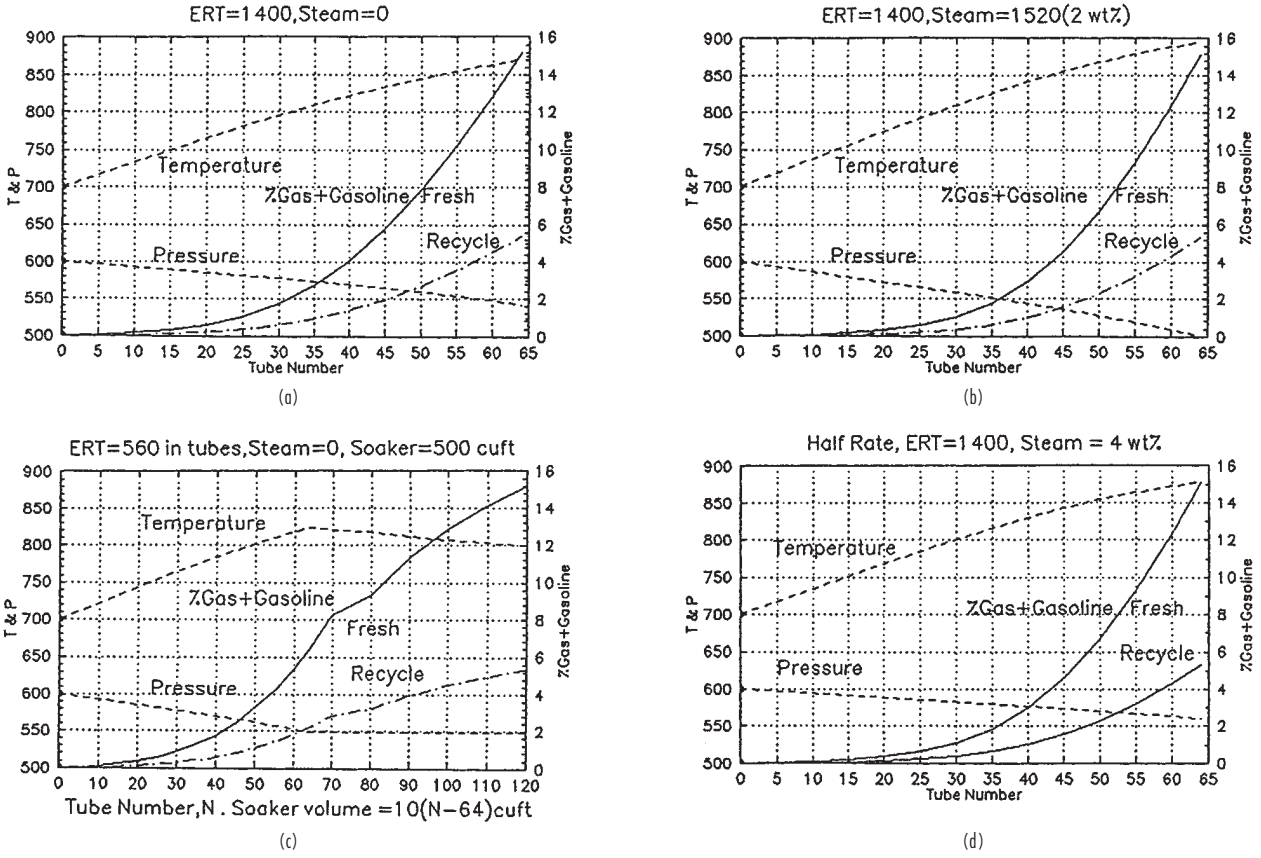

FIG. 23-5 Visbreaking fresh oil at 38,000 lbm/h, $k_{800} = 0.00012$/s, plus heavy gas oil at 38,000 lbm/h, $k_{800} = 0.00004$/s, 2% steam to put flow in the turbulent range. Tubes 4.25 in ID by 69 ft. (*a*) Heat flux 2,300 without steam. (*b*) Heat flux 2,600 with steam. (*c*) Soaker operation cuts the peak temperature by 50 ft and the heat flux by 30%. (*d*) When the feed rate turndown is 50%, steam rate is increased to 4% to keep flow turbulent. To convert ft to m, multiply by 0.3048; in to cm, multiply by 2.54; lb to kg/h, multiply by 0.454; Δt°F to Δt°C, multiply by 0.556.

PFRs, under isothermal, adiabatic, or heat transfer conditions in one or two phases. Outputs can provide profiles of composition, pressure, and temperature as well as vessel size.

When the kinetics are unknown, still-useful information can be obtained by finding equilibrium compositions at fixed temperature or adiabatically, or at some specified approach to the adiabatic temperature, say within 25°C (45°F) of it. Such calculations require only an input of the components of the feed and products and their thermodynamic properties, not their stoichiometric relations, and are based on Gibbs energy minimization. Computer programs appear, for instance, in Smith and Missen (*Chemical Reaction Equilibrium Analysis Theory and Algorithms,* Wiley, 1982), but the problem often is laborious enough to warrant use of one of the several available commercial services and their data banks. Several simpler cases with specified stoichiometries are solved by Walas (*Phase Equilibria in Chemical Engineering,* Butterworths, 1985).

For some widely practiced processes, especially in the petroleum industry, reliable and convenient computerized models are available from a number of vendors or, by license, from proprietary sources. Included are reactor-regenerator of fluid catalytic cracking, hydrotreating, hydrocracking, alkylation with HF or H_2SO_4, reforming with Pt or Pt-Re catalysts, tubular steam cracking of hydrocarbon fractions, noncatalytic pyrolysis to ethylene, ammonia synthesis, and other processes by suppliers of catalysts. Vendors of some process simulations are listed in the *CEP Software Directory* (AIChE, 1994).

Several excellent case studies that appear in the literature are listed, following.

Rase (*Case Studies and Design Data,* vol. 2 of *Chemical Reactor Design for Process Plants,* Wiley, 1977) has these items:

Styrene polymerization
Cracking of ethane to ethylene
Quench cooling in the ethylene process
Toluene dealkylation
Shift conversion
Ammonia synthesis
Sulfur dioxide oxidation
Catalytic reforming
Ammonia oxidation
Phthalic anhydride production
Steam reforming
Vinyl chloride polymerization
Batch hydrogenation of cottonseed oil
Hydrodesulfurization

Rase (*Fixed Bed Reactor Design and Diagnostics,* Butterworths, 1990) has a general computer program for reactor design and these case studies:

Methane-steam reaction
Hydrogenation of benzene to cyclohexane
Dehydrogenation of ethylbenzene to styrene

Tarhan (*Catalytic Reactor Design,* McGraw-Hill, 1983) has computer programs and results for these cases:

Toluene hydrodealkylation to benzene and methane
Phthalic anhydride by air oxidation of naphthalene
Trickle bed reactor for hydrodesulfurization

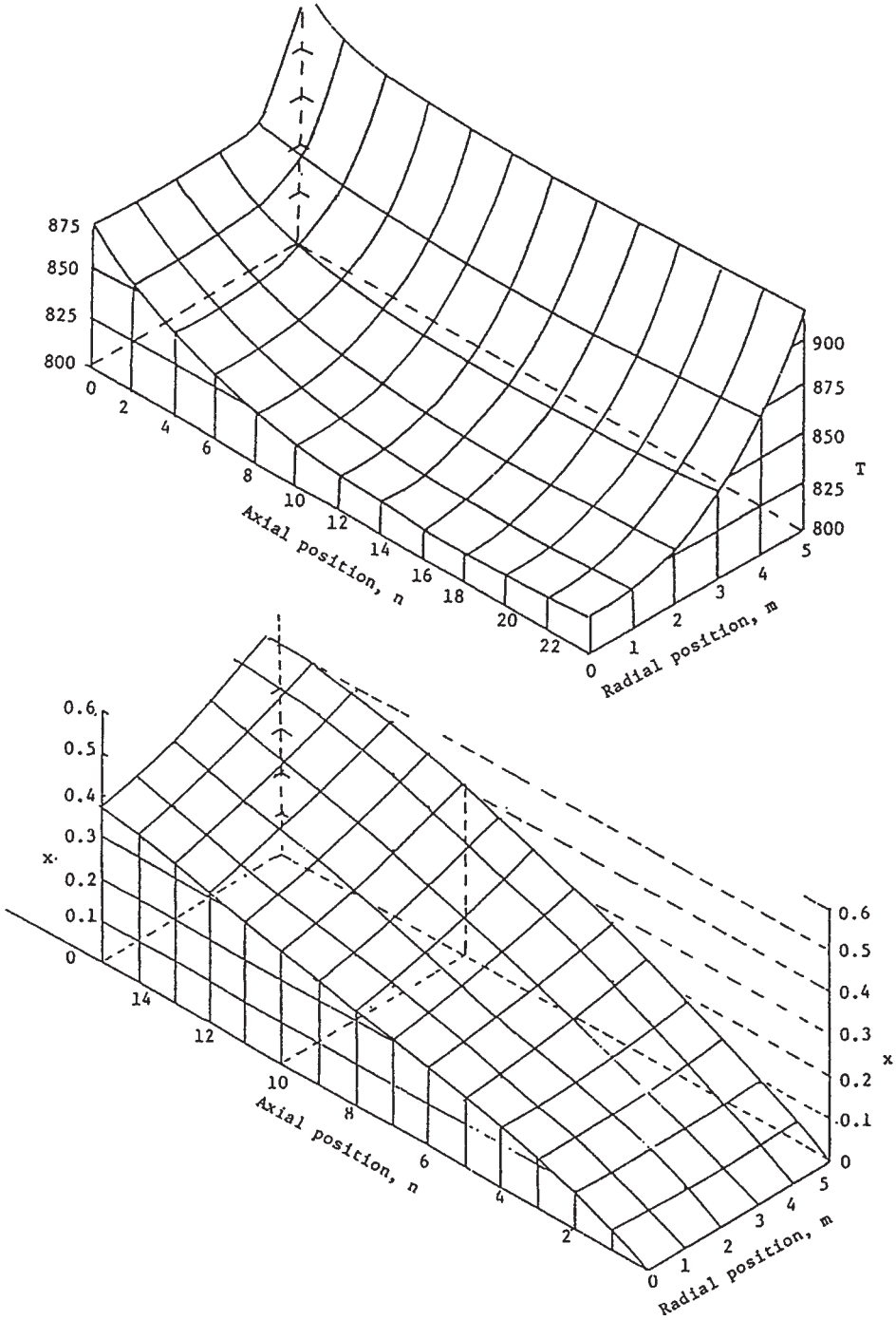

FIG. 23-6 Temperature in K and composition profiles in the styrene reactor. (*a*) Temperature profiles with $T' = 1000$, $T_{5.0} = 936.5$, and $hU/k_E = 0.5$. (*b*) Composition profiles with $T' = 1000$, $hU/k_E = 1000$. h = radial increment, U = heat-transfer coefficient at the wall, k_E = thermal conductivity, T in K. To convert K to R, multiply by 1.8.

T_0	T'	hU/k_E	$T_{5.0}$	n at 50% conversion
873	1000	0	873	—*
873	1000	0.5	936.5	25.3
873	1000	0.5	873	26.1
873	1000	1000	1000	15.6
873	1050	0.5	962.5	21.6
873	873	0.5	873	51.2

*The adiabatic reaction temperature reaches essentially the steady conditions, $x = 0.426$ and $T = 784$, after about 70 axial increments.

TABLE 23-2 Multibed Reactors, Adiabatic Temperature Rises and Approaches to Equilibrium*

Oxidation of SO_2 at atmospheric pressure in a four-bed reactor. Feed 6.26% SO_2, 8.3% O_2, 5.74% CO_2, and 79.7% N_2.

°C		Conversion, %	
In	Out	Plant	Equilibrium
463.9	592.8	68.7	74.8
455.0	495.0	91.8	93.4
458.9	465.0	96.0	96.1
435.0	437.2	97.5	97.7

Ammonia synthesis in a three bed reactor at 225 atm. Feed 22% N_2, 66% H_2, 12% inerts.

°C		Ammonia, %	
In	Out	Calculated	Equilibrium
399	518.9	13.0	15.4
427	488.9	16.0	19.0
427	470.0	18.0	21.7

*To convert atm to kPa multiply by 101.3.

SOURCE: Plant data and calculated design values from Rase, *Chemical Reactor Design for Process Plants,* Wiley, 1977.

Ramage, Graziani, Schipper, Krambeck, and Choi (*Advances in Chemical Engineering,* vol. 13, Academic Press, 1987, pp. 193–266):

Mobil's Kinetic Reforming Model

Dente and Ranzi (in Albright et al., eds., *Pyrolysis Theory and Industrial Practice,* Academic Press, 1983, pp. 133–175):

Mathematical modeling of hydrocarbon pyrolysis reactions

Shah and Sharma (in Carberry and Varma, eds., *Chemical Reaction and Reaction Engineering Handbook,* Dekker, 1987, pp. 713–721):

Hydroxylamine phosphate manufacture in a slurry reactor

Some aspects of a kinetic model of methanol synthesis are described in the first example, which is followed by a second example that describes coping with the multiplicity of reactants and reactions of some petroleum conversion processes. Then two somewhat simplified industrial examples are worked out in detail: mild thermal cracking and production of styrene. Even these calculations are impractical without a computer. The basic data and mathematics and some of the results are presented.

Example 1: Kinetics and Equilibria of Methanol Synthesis Although methanol from synthesis gas has been a large-scale industrial chemical for 70 years, the scientific basis of the manufacture apparently can stand some improvement, which was undertaken by Beenackers, Graaf, and Stamhuis (in Cheremisinoff, ed., *Handbook of Heat and Mass Transfer,* vol. 3, Gulf, 1989, pp. 671–699). The process occurs at 50 to 100 atm with catalyst of oxides of Cu-Zn-Al and a feed stream of H_2, CO, and CO_2. Three reactions were taken for the process:

$$CO + 3H_2 \Leftrightarrow CH_3OH$$

$$CO_2 + H_2 \Leftrightarrow CO + H_2O \qquad \text{(shift reaction)}$$

$$CO_2 + 3H_2 \Leftrightarrow CH_3OH$$

In some earlier work the shift reaction was assumed always at equilibrium. Fugacities were calculated with the SRK and Peng-Robinson equations of state, and correlations were made of the equilibrium constants.

Various Langmuir-Hinshelwood mechanisms were assumed. CO and CO_2 were assumed to adsorb on one kind of active site, s1, and H_2 and H_2O on another kind, s2. The H_2 adsorbed with dissociation and all participants were assumed to be in adsorptive equilibrium. Some 48 possible controlling mechanisms were examined, each with 7 empirical constants. Variance analysis of the experimental data reduced the number to three possibilities. The rate equations of the three reactions are stated for the mechanisms finally adopted, with the constants correlated by the Arrhenius equation.

Kinetic studies were made with a spinning basket reactor using catalyst HaldorTopsoe MK 101, at three pressures and three temperatures.

Effectiveness factors of the porous catalyst were found by comparison with crushed particles 0.15 to 0.2 mm in diameter. For methanol formation the range of effectiveness was from approximately 0.9 at 490 K to 0.5 at 560 K, and for water formation 0.8 at 490 K and 0.5 at 560 K.

Simpler, mostly power law rate equations for the production of mixed alcohols from synthesis gas are cited by Forzatti, Tronconi, and Villa (in *Handbook of Heat & Mass Transfer,* vol. 4, Gulf, 1990, pp. 289–311). Agreements between their correlations and some data were deemed satisfactory. Rate equations are not necessarily the same on different catalysts.

Example 2: Coping with Multiple Reactants and Reactions (*a*) Thermal cracking of ethane and propane is done to make primarily olefins but other products also are formed. A number of simplified reaction models are in use. One of these (Sundaram and Froment, *Chem. Eng. Sci.,* **32,** 601–617 [1977]; *Ind. Eng. Chem. Fund.,* **17,** 174–182 [1978]) takes these reactions to represent the cracking processes:

Ethane cracking

$$C_2H_6 \overset{k_1}{\rightleftharpoons} C_2H_4 + H_2$$

$$2C_2H_6 \overset{k_2}{\longrightarrow} C_3H_8 + CH_4$$

$$C_3H_8 \overset{k_3}{\longrightarrow} C_3H_6 + H_2$$

$$C_3H_8 \overset{k_4}{\longrightarrow} C_2H_4 + CH_4$$

$$C_3H_6 \overset{k_5}{\rightleftharpoons} C_2H_2 + CH_4$$

$$C_2H_2 + C_2H_4 \overset{k_6}{\longrightarrow} C_4H_6$$

Propane cracking

$$C_3H_8 \longrightarrow C_2H_4 + CH_4$$

$$C_3H_8 \rightleftharpoons C_3H_6 + H_2$$

$$C_3H_8 + C_2H_4 \longrightarrow C_2H_6 + C_3H_6$$

$$2C_3H_6 \longrightarrow 3C_2H_4$$

$$2C_3H_6 \longrightarrow 0.5C_6 + 3CH_4$$

$$C_3H_6 \rightleftharpoons C_2H_2 + CH_4$$

$$C_3H_6 + C_2H_6 \longrightarrow C_4H_8 + CH_4$$

$$C_2H_6 \rightleftharpoons C_2H_4 + H_2$$

$$C_2H_4 + C_2H_2 \longrightarrow C_4H_6$$

In the second paper the models were amplified: for ethane, 49 reactions with 11 molecular species and 9 free radicals; for propane, 80 reactions with 11 molecular species and 11 free radicals. The second paper has a list of 133 reactions involving light hydrocarbons and their first- or second-order specific rates.

(*b*) The feed to a typical fluidized catalytic cracking unit consists of liquid C_5 to C_{40} and contains thousands of individual species. This stream is made amenable to kinetic modeling by a process of lumping. A Mobil Corporation model (Weekman, "Lumps Models and Kinetics in Practice," *AIChE Monograph Series* No. 11, 1979) employs 10 lumps and 20 reactions. There are four lumps each in the boiling range, 222 to 342°C, of paraffins, naphthenes, aromatics, and aromatic substituents and also four above 342°C. The other two lumps are total C_1 to C_4 plus coke, and C_5 to 222°C. The specific rates are presumably proprietary data. In 1991, a seventh generation of this model was said to be in use.

(*c*) Commercial catalytic reformers upgrade naphthas in the C_5 to C_{12} range to high-octane gasoline with coproducts. Some 300 participants have been identified. In a Mobil Corporation model (Ramage et al., *Advances in Chemical Engineering,* vol. 13, Academic Press, 1987, pp. 193–266; Sapre, in Sapre and Krambeck, eds., *Chemical Reactions in Complex Mixtures,* Van Nostrand Reinhold, 1991, pp. 222–253) these have been lumped into pseudocomponents identified by carbon number and chemical nature. These lumps vary with the age of the catalyst. The table shows the 13 lumps adopted for the "start of the kinetic cycle."

Carbon number	Six-carbon-ring naphthenes, N_6	Five-carbon-ring naphthenes, N_5	Paraffins, P	Aromatics, A
C_{8-} C_7	C_{8-} cyclohexanes (1) Methylcyclohexane (5)	C_{8-} cyclopentanes (2) Cyclopentanes (6)	C_{8-} paraffins (3) Heptanes (7)	C_{8-} aromatics (4) Toluene (8)
C_6	Cyclohexane (9)	Methylcyclopentane (10)	Hexanes (11)	Benzene (12)
C_{5-}				C_{5-} hydrocarbons (13)

The reaction network is shown in the paper. The kinetic characteristics of the lumps are proprietary. Originally, the model required 30 person-years of effort on paper and in the laboratory, and it is kept up to date.

Example 3: Thermal Cracking of Heavy Oils (Visbreaking) Mild thermal cracking is conducted in the tubes of a fired heater, sometimes fol-

lowed by an adiabatic holding drum. The cases to be studied are for making a product with reduced viscosity and with 8 percent gasoline plus 2 percent gas. A tube diameter is first selected with the rule that the cold oil velocity be 5 to 6 ft/s; this diameter is subject to change during the course of the calculation. For a specified heat flux, Q/A Btu/(h·ft^2 of tube surface), a number of parameters can be explored:

- Number of tubes of a given length, with and without a soaking drum
- Profiles of T, P, and fractional conversion x

A key consideration is that coking becomes likely in the vicinity of 900°F.

For the process of the flowsketch two different cases will be examined:

(*a*) Oil feed 160,000 lbm/h, $k_{800} = 0.000248$/s, tubes 5.05 in ID, 40 ft long.

(*b*) 38,000 lbm/h of fresh oil, $k_{800} = 0.00012$/s, + 38,000 lbm/h heavy gas oil, $k_{800} = 0.00004$/s, + 1,520 lbm/h steam; 64 tubes in series, 4.25 in ID, each 69 ft long.

In view of the necessity to be able to design for charge stocks of varied and not-well-characterized properties, some approximations are made. The main properties and operating variables are listed. n is the increment number of the integration and x is the fraction decomposed to gas + gasoline.

1. The components are original oil M, lbm/h, 10°API; cracked oil, 30°API; steam S, lbm/h; gasoline product 114 mol wt; gas product 28 mol wt.
2. The gas produced is a fraction $y = 0.2$ of the gas + gasoline made.
3. The specific rate at temperature T_n is

$$k = k_{800} \exp\left[50{,}000\left(\frac{1}{1{,}260} - \frac{1}{T_n + 460}\right)\right]$$

4. The mean density is figured on the assumption that the gas and gasoline are in the vapor phase and the cracked oil is in the liquid phase:

$$\rho_n = f(T_n, P_n, x_n) \tag{A}$$

5. The viscosity is that of the 30°API stock. $\nu_n = f(T_n)$, cSt.
6. Heat of reaction $\Delta H_r = 332$ Btu/(lbm gas + gasoline)
7. $Q_t A_t / M$ = heat input per increment of reactor, Btu/(h·lbm feed).
8. Each component of the feed has the enthalpy equation $H_i = A_i + B_i(T - 800)$.
9. The enthalpies of the mixtures leaving increments n and $n + 1$ of the reaction are expressed per unit mass of fresh oil,

$$H_n = f(T_n, x_n), \qquad H_{n+1} = f(T_{n+1}, x_{n+1})$$

10. The enthalpy balance over an increment of tubes is

$$H_n + \frac{Q_t A_t}{M} = H_{n+1} + \Delta H_r (x_{n+1} - x_n)$$

11. The temperature is derived from the enthalpy balance and is

$$T_{n+1} = T_0 + f(T_n, x_n, x_{n+1}) \tag{B}$$

where $T_0 = 800$ is the reference temperature for enthalpy.

12. The Reynolds number is

$$\mathrm{Re}_n = \frac{6.316\,(M + S)}{D\rho_n \nu_n}$$

D, in; ρ, lbm/ft^3; ν, cSt

13. The friction factor is given by Round's equation with a roughness factor $\varepsilon = 0.00015$ ft,

$$f_n = \frac{1.6434}{\ln(0.000243/D + 6.5/\mathrm{Re}_n)}$$

14. The pressure relation, lbm/in^2 is

$$P_{n+1} = P_n + \frac{3.356(10^{-6})L_t}{D^5}(M + S)^2\left(\frac{f_n}{\rho_n} + \frac{f_{n+1}}{\rho_{n+1}}\right) \tag{C}$$

The differential material balance of the first-order flow reaction is

$$M dx = r dV_r = kC dV_r = \frac{kM(1-x)}{V'} dV_r = \frac{kM(1-x)}{(M+S)/\rho} dV_r$$

$$= k\rho\left(\frac{M}{M+S}\right)(1-x)\, V_t\, dN$$

The integral is rearranged to

$$x_{n+1} = 1 - (1 - x_n) \exp\left[-\frac{V_t}{M+S}\int_N^{N+\Delta N} k\rho\, dN\right]$$

Integration is by successive approximation, using essentially Euler's method. For the first trial,

$$x_{n+1}^{(1)} = 1 - (1 - x_n) \exp\left(-\frac{3600 V_t}{M+S}(k\rho)_n \Delta N\right) \tag{D}$$

and for subsequent trials,

$$x_{n+1}^{(i+1)} = 1 - (1 - x_n) \exp\left\{-\frac{1800 V_t}{M+S}[(k\rho)_n + (k\rho)_{n+1}^{(i)}]\right\} \tag{E}$$

Here,

k_n is a function of T_n

ρ_n is a function of T_n, P_n and x_n

V_t is the volume of one tube

ΔN is the number of tubes per reactor increment

3,600 compensates for the fact that k_n is per s and $M + S$ is per h

Calculation procedure

(*a*) In the preheat zone of the reactor, before cracking is appreciable, usually below 800°F, the pressure drop is found adequately enough by taking average densities and Reynolds numbers over this zone. The conditions at the inlet to the reaction zone are designated x_0, T_0, and P_0.

(*b*) Evaluate k_n, H_n, ρ_n, and ν_n at the inlet, where $n = 0$.

(c) Apply Eq. (D) to find the first approximation $x_{n+1}^{(1)}$ at the end of the first reactor increment.

(*d*) Find the next approximation $x_{n+1}^{(2)}$ with Eq. (E).

(*e*) If the condition

$$\frac{|x_{n+1}^{(2)} - x_{n+1}^{(1)}|}{x_{n+1}^{(2)} + x_{n+1}^{(1)}} \overset{?}{\leq} 0.01$$

is not satisfied, repeat the process; otherwise, continue with the next increment until the specified conversion is attained or some other specification is met or violated.

Equivalent residence time (ERT) can be found after the temperature profile has been established:

$$\mathrm{ERT} = \frac{V_r}{V'\rho_0}\int_0^1 \left(\frac{k}{k_{800}}\right)\rho\, dz \tag{F}$$

where z is the fractional distance along the total tube length. Engineers in the industry have a feel for what value of ERT is desirable with particular stocks and their conversion. The number usually is in the range of 500 to 1,500.

Results The results of computer calculations are summarized for the two operations by Figs. 23-4 and 23-5. In the second design, the equations had to be modified to take account of two feeds with different specific rates.

Example 4: Styrene from Ethylbenzene The principal reaction in the dehydrogenation of ethylbenzene is to styrene and hydrogen,

$$C_6H_5C_2H_5 \Leftrightarrow C_6H_5C_2H_3 + H_2$$

For a catalyst packed reactor, a rate equation was found by Wenner and Dybdal (*Chem. Eng. Prog.*, **44,** 275–286 [1948]):

$$R_c = k_r\left(P_E - \frac{(P_S P_H)^2}{K_e}\right) \text{ kg mol/(h·kg catalyst)} \tag{A}$$

$$k_r = \exp\left(9.44 - \frac{11{,}000}{T}\right) \tag{B}$$

$$K_e = \exp\left(15.69 - \frac{15{,}000}{T}\right) \tag{C}$$

where the pressures are in bar and temperatures in K.

The material balance with bulk flow in the axial direction z and diffusion in the radial direction r with diffusivity D gives rise to the equation

$$\frac{\partial(uC)}{\partial z} - \frac{D}{u}\left[\frac{\partial^2(uC)}{\partial r^2} + \frac{1}{r}\frac{\partial(uC)}{\partial r}\right] + \rho R_c = 0 \tag{D}$$

In terms of the fraction converted, the material balance becomes

$$\frac{\partial x}{\partial z} - \frac{D}{u}\left[\frac{\partial^2 x}{\partial r^2} + \frac{1}{r}\frac{\partial x}{\partial r}\right] - \frac{\rho}{u_0 C_0} R_c = 0 \tag{E}$$

Similarly, the heat balance gives rise to

$$\frac{\partial T}{\delta z} - \frac{k_e}{GC_p}\left[\frac{\partial^2 T}{\partial r^2} + \frac{1}{r}\frac{\partial T}{\partial r}\right] + \frac{\Delta H_r \rho}{GC_p} R_c = 0 \tag{F}$$

where G is the mass flow rate (2,500 kg/h as developed later).

Operating conditions The reactor is 10 cm ID, input of ethylbenzene is 0.069 kg mol/h, input of steam is 0.69 kgmol/h, total of 2,500 kg/h. Pressure is 1.2 bar, inlet temperature is 600°C. Heat is supplied at some constant temperature in a jacket. Performance is to be found with several values of heat transfer coefficient at the wall, including the adiabatic case.

Data

Bulk density of catalyst	$\rho = 1{,}440$ kg/m^3
Heat of reaction	$\Delta H_r = 140{,}000$ kJ/kg mol
Thermal conductivity	$k_e = 0.45$ W/m K
Ratio of diffusivity to linear velocity	$D/u = 0.000427$ m
Specific heat of the mixture	$C_p = 2.18$ kJ/kg K

In terms of the fractional conversion and the ideal gas law, the rate equation becomes

$$R_c = 1.2 \exp\left(9.44 - \frac{11{,}000}{T}\right)\left[\frac{1-x}{11+x} - \frac{1.2}{K_e}\left(\frac{x}{11+x}\right)^2\right] \tag{G}$$

Substitution of the data transforms the heat and material balances into Eqs. (H) and (I):

$$\frac{\partial T}{\partial z} = a\left(\frac{\partial^2 T}{\partial r^2} + \frac{1}{r}\frac{\partial T}{\partial r}\right) - bR_c, \qquad a = 0.000297, \qquad b = 37{,}000 \tag{H}$$

$$\frac{\partial x}{\partial z} = c\left(\frac{\partial^2 x}{\partial r^2} + \frac{1}{r}\frac{\partial x}{\partial r}\right) + dR_c, \qquad c = 0.000427, \qquad d = 164 \tag{I}$$

At the center, Eqs. (H) and (I) become, after application of l'Hopital's rule,

$$\frac{\partial T}{\partial z} = 2a\frac{\partial^2 T}{\partial r^2} - bR_c \tag{J}$$

$$\frac{\partial x}{\partial r} = 2c\frac{\partial^2 T}{\partial r^2} + dR_c \tag{K}$$

At the wall,

$$-k_e\frac{\partial T}{\partial r} = U(T - T') \tag{L}$$

Eqs. (H) through (L) will be solved by the explicit finite difference method. Substitute

$$\frac{\partial T}{\partial z} = \frac{T_{m,n+1} - T_{m,n}}{k}, \qquad k = \Delta z \tag{M}$$

$$\frac{\partial T}{\partial r} = \frac{T_{m,n+1} - T_{m,n-1}}{2h}, \qquad h = \Delta r \tag{N}$$

$$\frac{\partial^2 T}{\partial r^2} = \frac{T_{m+1,n} - 2T_{m,n} + T_{m-1,n}}{h^2} \tag{O}$$

and similarly for variable x.

The substituted finite difference equations will contain the terms

$$M' = \frac{0.000427k}{h^2} = 0.250, \qquad \text{for stability} \tag{P}$$

$$M = \frac{0.000297k}{h^2} = 0.174$$

The choice $M' = 0.250$ is to prevent negative coefficients and thus an unstable iterative process.

The finite difference equations will be formulated with five radial increments $m = 0, 1, 2, 3, 4, 5$, and for as many axial increments as necessary to obtain 50 percent conversion. Accordingly,

$$h = \Delta r = 1 \text{ cm}$$

$$k = \Delta z = \frac{0.250}{0.000427} = 585 \text{ cm}$$

At the center, $m = 0$, the finite difference equations become

$$T_{0,n+1} = 4MT_{1,n} + (1 - 4M)T_{0,n} - kbR_{c0,n} \tag{Q}$$

$$x_{0,n+1} = 4M'x_{1,n} + (1 - 4M')x_{0,n} + kdR_{c0,n} \tag{R}$$

When $m = 1, 2, 3$, or 4,

$$T_{m,n+1} = M\left(1 + \frac{1}{2m}\right)T_{m+1,m} + (1 - 2M)\,T_{m,n} + M\left(1 - \frac{1}{2m}\right)T_{m-1,n} - kbR_{cm,n} \tag{S}$$

$$x_{m,n+1} = M\left(1 + \frac{1}{2m}\right)x_{m+1,n} + (1 - 2M)\,x_{m,n} + M\left(1 - \frac{1}{2m}\right)x_{m-1,n} + kdR_{cm,n} \tag{T}$$

At the wall, $m = 5$, the heat-transfer coefficient is U and the heating gas has temperature T'_n,

$$T_{5,n} = \frac{T_{4,n} + (hU/k_e)T'_n}{1 + hU/k_e} \tag{U}$$

$$x_{5,n} = x_{4,n} \tag{V}$$

The rate equation becomes

$$R_{cm,n} = 1.2\,k_r\left[\frac{1 - x_{m,n}}{11 + x_{m,n}} - \frac{1.2}{K_e}\left(\frac{x_{m,n}}{11 + x_{m,n}}\right)^2\right] \tag{W}$$

$$k_r = \exp\left(9.44 - \frac{11{,}000}{T_{m,n}}\right) \tag{X}$$

$$K_e = \exp\left(15.69 - \frac{15{,}000}{T_{m,n}}\right) \tag{Y}$$

At this point the computer takes over. Cases with several values of jacket temperature and several values of heat-transfer coefficient, or hU/k_e, are examined, and also several assumptions about the temperature at the wall at the inlet. Eq. (U) with $n = 0$ could be used. The number of axial increments are found for several cases of 50% conversion. Two of the profiles of temperature or conversion are shown in Fig. 23-6.

The Crank-Nicholson implicit method and the method of lines for numerical solution of these equations do not restrict the radial and axial increments as Eq. (P) does. They are more involved procedures, but the burden is placed on the computer in all cases.

A version of this problem is solved by Jenson and Jeffreys (*Mathematical Methods in Chemical Engineering,* Academic Press, 1977).

More up-to-date data of this process are employed in a study by Rase (*Fixed Bed Reactor Design and Diagnostics,* Butterworths, 1990, pp. 275–286). In order to keep the pressure drop low, radial flow reactors are used, two units in series with reheating between them. Simultaneous formation of benzene, toluene, and minor products is taken into account. An economic comparison is made of two different catalysts under a variety of operating conditions. Some of the computer printouts are shown there.

RESIDENCE TIME DISTRIBUTION (RTD) AND REACTOR EFFICIENCY

The distribution of residence times of reactants or tracers in a flow vessel, the RTD, is a key datum for determining reactor performance, either the expected conversion or the range in which the conversion must fall. In this section it is shown how tracer tests may be used to establish how nearly a particular vessel approaches some standard ideal behavior, or what its efficiency is. The most useful comparisons are with complete mixing and with plug flow. A glossary of special terms is given in Table 23-3, and major relations of tracer response functions are shown in Table 23-4.

TRACERS

Nonreactive substances that can be used in small concentrations and that can easily be detected by analysis are the most useful tracers. When making a test, tracer is injected at the inlet of the vessel along with the normal charge of process or carrier fluid, according to some definite time sequence. The progress of both the inlet and outlet concentrations with time is noted. Those data are converted to a residence time distribution (RTD) that tells how much time each fraction of the charge spends in the vessel.

An RTD, however, does not represent the mixing behavior in a vessel uniquely, because several arrangements of the internals of a vessel may give the same tracer response, for example, any series arrangements of reactor elements such as plug flow or complete mixing. This is a consequence of the fact that tracer behavior is represented by linear differential equations. The lack of uniqueness limits direct application of tracer studies to first-order reactions with constant specific rates. For other reactions, the tracer curve may determine the upper and lower limits of reactor performance. When this range is not too broad, the result can be useful. Tracer data also may be taken at several representative positions in the vessel in order to develop a realistic model of the reactor.

REACTOR EFFICIENCY

One quantitative measure of reactor efficiency at a conversion level x is the ratio of the mean residence time or the reactor volume in a plug flow reactor to that of the reactor in question,

$$\eta_x = \left(\frac{\bar{t}_{pf}}{\bar{t}}\right)_x = (V_{pf}/V)_x \tag{23-14}$$

TABLE 23-3 Glossary of RTD Terms

Closed end vessel One in which the inlet and outlet streams are completely mixed and dispersion occurs only between the terminals. At the inlet where $z = 0$, $uC_0 = [uC - D_e(\partial C/\partial z)]_{z=0}$; at the outlet where $x = L$, $(\partial C/\partial z)_{z=L} = 0$. These are called *Danckwerts' boundary conditions.*

Concentration The main special kinds are: C_δ, that of the effluent from a vessel with impulse input of tracer; $C^0 = m/V_r$, the initial mean concentration resulting from impulse input of magnitude m; C_u, that of the effluent from a vessel with a step input of magnitude C_f.

Dispersion The movement of aggregates of molecules under the influence of a gradient of concentration, temperature, and so on. The effect is represented by Fick's law with a dispersion coefficient substituted for molecular diffusivity. Thus, rate of transfer $= -D_e(\partial C/\partial z)$.

Impulse An amount of tracer injected instantaneously into a vessel at time zero. The symbol $m\delta(t - a)$ represents an impulse of magnitude m injected at time $t = a$. The effluent concentration resulting from an impulse input is designated C_δ.

Maximum mixedness Exists when any molecule that enters a vessel immediately becomes associated with those molecules with which it will eventually leave the vessel; that is, with those molecules that have the same life expectation. A state of MM is associated with every RTD.

Mixing, ideal or complete A state of complete uniformity of composition and temperature in a vessel. In flow, the residence time varies exponentially, from zero to infinity.

Peclet number for dispersion $\mathrm{Pe} = uL/D_e$ where u is a linear velocity, L is a linear dimension, and D_e is the dispersion coefficient. In packed beds, $\mathrm{Pe} = ud_p/D_e$, where u is the interstitial velocity and d_p is the pellet diameter.

Plug flow A condition in which all effluent molecules have had the same residence time.

Residence time distribution (RTD) In the case of elutriation of tracer from a vessel that contained an initial average concentration C^0, the area under a plot of $E(t) = C_{\text{effluent}}/C^0$ between the ordinates at t_1 and t_2 is the fraction of the molecules that have residence times in this range. In the case of constant input of concentration C_f to a vessel with zero initial concentration, the ratio $F(t) = C_{\text{effluent}}/C_f$ at t_1 is the fraction of molecules with residence times less than t_1.

Residence time, mean The average time spent by the molecules in a vessel. Mathematically, it is the first moment of the effluent concentration from a vessel with impulse input, or

$$\bar{t} = \frac{\int_0^\infty tC_\delta\,dt}{\int_0^\infty C_\delta\,dt.}$$

Segregated flow Occurs when all molecules that enter together also leave together. A state of aggregation is associated with every RTD. Each aggregate of molecules reacts independently of every other aggregate; thus, as an individual batch reactor.

Skewness The third moment of a residence time distribution:

$$\gamma^3(t) = \int_0^\infty (t - \bar{t})^3 E(t)\,dt.$$

It is a measure of asymmetry.

Step An input in which the concentration of tracer is changed to some constant value C_f at time zero and maintained at this level indefinitely. The symbol $C_f u(t - a)$ represents a step of magnitude C_f beginning at $t = a$. The resulting effluent concentration is designated C_u.

Variance The second moment of the RTD. There are two forms: one in terms of the absolute time, designated $\sigma^2(t)$; and the other in terms of reduced time, $t_r = t/\bar{t}$, designated $\sigma^2(t_r)$.

$$\sigma^2(t) = \frac{\int_0^\infty (t - \bar{t})^2 C_\delta\,dt}{\int_0^\infty C_\delta\,dt} = \int_0^\infty (t - \bar{t})^2 E(t)\,dt$$

$$\sigma^2(t_r) = \frac{\sigma^2(t)}{\bar{t}^2} = \int_0^\infty (t_r - 1)^2 E(t_r)\,dt_r$$

TABLE 23-4 Tracer Response Functions

Mean residence time:

$$\bar{t} = \frac{\int_0^\infty tC_\delta\,dt}{\int_0^\infty C_\delta\,dt} = \frac{\int_0^{C_{u\infty}} t\,dC_u}{C_{u\infty}}$$

Initial mean concentration with impulse input,

$$C^0 = \frac{m}{V_r} = \left(\frac{V'}{V_r}\right)\int_0^\infty C_\delta\,dt = \frac{\int_0^\infty C_\delta\,dt}{\bar{t}}$$

Reduced time:

$$t_r = \frac{t}{\bar{t}}$$

Residence time distribution:

$$E(t) = \frac{C_\delta}{\int_0^\infty C_\delta\,dt} = \frac{E(t_r)}{\bar{t}} = \frac{dF(t)}{dt}$$

Residence time distribution, normalized,

$$E(t_r) = \frac{\text{impulse output}}{\text{initial mean concentration}}$$

$$= \frac{C_\delta}{C^0} = \frac{\bar{t}C_\delta}{\int_0^\infty C_\delta\,dt} = \bar{t}\,E(t) = \frac{dF(t)}{dt}$$

Age:

$$F(t) = \frac{\text{step output}}{\text{step input}}$$

$$= \frac{C_u}{C_f} = \frac{\int_0^t C_\delta\,dt}{\int_0^\infty C_\delta\,dt} = F(t_r)$$

Internal age:

$$I(t) = 1 - F(t)$$

Intensity:

$$\Lambda(t) = \frac{E(t)}{1 - F(t)} = \frac{E(t)}{I(t)}$$

Variance:

$$\sigma^2(t) = \int_0^\infty (t - \bar{t})^2 E(t)\,dt = -\bar{t}^2 + \frac{\int_0^\infty t^2 C_\delta\,dt}{\int_0^\infty C_\delta\,dt}$$

Variance, normalized:

$$\sigma^2(t_r) = \frac{\sigma^2(t)}{\bar{t}^2} = -1 + \frac{\int_0^\infty t^2 C_\delta\,dt}{\int_0^\infty C_\delta\,dt}$$

$$= \int_0^1 (t_r - 1)^2\,dF(t_r)$$

Skewness, third moment:

$$\gamma^3(t_r) = \int_0^\infty (t_r - 1)^3 E(t_r)\,dt_r$$

The conversion level sometimes is taken at 95 percent of equilibrium, but there is no universal standard.

Other measures of efficiency are derived from the experimental RTD, which is characterized at least approximately by the variance $\sigma^2(t_r)$. This quantity is zero for plug flow and unity for complete mixing, and thus affords natural bounds to an efficiency equated to the variance. It is possible, however, for the variance to fall out of the range (0,1) when stagnancy or bypassing occurs.

A related measure of efficiency is the equivalent number of stages n_{erlang} of a CSTR battery with the same variance as the measured RTD. Practically, in some cases 5 or 6 stages may be taken to approximate plug flow. The dispersion coefficient D_e also is a measure of deviation from plug flow and has the merit that some limited correlations in terms of operating conditions have been obtained.

No correlations of $\sigma^2(t_r)$ or n_{erlang} have been achieved in terms of operating variables. At present, the chief value of RTD studies is for the diagnosis of the performance of existing equipment; for instance, maldistribution of catalyst in a packed reactor, or bypassing or stagnancy in stirred tanks. Reactor models made up of series and/or parallel elements also can be handled theoretically by these methods.

TRACER RESPONSE

The unsteady material balances of tracer tests are represented by linear differential equations with constant coefficients that relate an input function $C_f(t)$ to a response function of the form

$$\sum_0^n a_n \frac{dC^n}{dt^n} = C_f \qquad (23\text{-}15)$$

The general form of the material balance is the familiar one,

Inputs + Sources = Outputs + Sinks + Accumulations

as described in the "Modeling Chemical Reactors" section. For the special case of initial equilibrium or dead state (all derivatives = 0 at time 0), the transformed function of the preceding equation is

$$\overline{C} = \frac{\overline{C}_f}{\Sigma\, a_n s^n} \tag{23-16}$$

and $C(t)$ is found by inversion with a table of Laplace transform pairs. The individual transform is defined as

$$\overline{C} = C(s) = \int_0^\infty \exp(-st) C(t)\, dt \tag{23-17}$$

The ratio of transforms,

$$G(s) = \frac{C(s)}{C_f(s)} \tag{23-18}$$

is called a *transfer function.* The concept is useful in the representation of systems consisting of several elements in series and parallel.

A particularly useful property of linear differential equations may be explained by comparing an equation and its derivative in operator form,

$$f(D)y = g(t) \qquad \text{and} \qquad f(D)z = \frac{dg(t)}{dt} \tag{23-19}$$

where the RHS of the second equation is the derivative of the RHS of the first. The property in question is that $z = dy/dt$. The chief use of this property in this area is with the step and impulse functions, the impulse being the derivative of the step. Often problems are easier to visualize and formulate in terms of the step input, but the desired solution may be for the impulse input which gives the RTD directly.

Kinds of Inputs Since a tracer material balance is represented by a linear differential equation, the response to any one kind of input is derivable from some other known input, either analytically or numerically. Although in practice some arbitrary variation of input concentration with time may be employed, five mathematically simple input signals supply most needs. *Impulse* and *step* are defined in the Glossary (Table 23-3). *Square pulse* is changed at time a, kept constant for an interval, then reduced to the original value. *Ramp* is changed at a constant rate for a period of interest. A *sinusoid* is a signal that varies sinusoidally with time. Sinusoidal concentrations are not easy to achieve, but such variations of flow rate and temperature are treated in the vast literature of automatic control and may have potential in tracer studies.

RESPONSE FUNCTIONS

The chief quantities based on tracer tests are summarized in Table 23-4. Effluent concentrations resulting from impulse and step inputs are designated C_δ and C_u, respectively. The initial mean concentration resulting from an impulse of magnitude m into a vessel of volume V_r is $C^0 = m/V_r$. The mean residence time is the ratio of the vessel volume to the volumetric flow rate, $\bar{t} = V_r/V'$ or $\bar{t} = \int_0^\infty tC_\delta\, dt / \int_0^\infty C_\delta\, dt$. The reduced time is $t_r = t/\bar{t}$.

Residence time distributions are used in two forms: Normalized, $E(t_r) = C_\delta/\underline{C}^0$; or plain, $E(t) = C_\delta/\int_0^\infty C_\delta\, dt$. The relation between them is $E(t_r) = \bar{t}E(t)$. On time plots, the area under either RTD is unity: $\int_0^\infty E(t_r)\, dt_r = \int_0^\infty E(t)\, dt = 1$. Moreover, the area between the ordinates at t_1 and t_2 is the fraction of the total effluent that has spent the period between those times in the vessel.

The *age function* is defined in terms of the step input as

$$F(t) = \frac{C_u}{C_f} = \int_0^t E(t)\, dt$$

Relations to other functions are in Table 23-3.

The intensity function $\Lambda(t) = E(t)/[1 - F(t)]$ occurs in the maximum mixing concept and is of value, for instance, in detecting maldistributions of catalyst and channeling in a packed vessel.

The Erlang number n_{erlang} and the variances $\sigma^2(t_r)$ and $\sigma^2(t)$ are single parameter characterizations of RTD curves. The skewness $\gamma^3(t)$, and higher moments can be used to represent RTD curves more closely if the data are accurate enough.

ELEMENTARY MODELS

Real reactors may conform to some sort of ideal mixing patterns, or their performance may be simulated by combinations of ideal models. The commonest ideal models are the following:

- *Plug flow reactor* (*PFR*), in which all portions of the charge have the same residence time. The concentration varies with time and position, according to the equation,

$$\frac{\partial C}{\partial t} + V' \frac{\partial C}{\partial V_r} = 0$$

- *Continuous stirred tank reactor* (*CSTR*), with the effluent concentration the same as the uniform vessel concentration. With a mean residence time $\bar{t} = V_r/V'$, the material balance is

$$\bar{t}\, \frac{dC}{dt} + C = \text{Input concentration}$$

- *Dispersion model* is based on Fick's diffusion law with an empirical dispersion coefficient D_e substituted for the diffusion coefficient. The material balance is

$$\frac{\partial C}{\partial t} + V' \frac{\partial C}{\partial V_r} - D_e \frac{\partial^2 C}{\partial V_r^2} = 0$$

- *Laminar* or power law velocity distribution in which the linear velocity varies with radial position in a cylindrical vessel. Plug flow exists along any streamline and the mean concentration is found by integration over the cross section.
- *Distribution models* are curvefits of empirical RTDs. The Gaussian distribution is a one-parameter function based on the statistical rule with that name. The Erlang and gamma models are based on the concept of the multistage CSTR. RTD curves often can be well fitted by ratios of polynomials of the time.

Figure 23-7 illustrates the responses of CSTRs and PFRs to impulse or step inputs of tracers.

REAL BEHAVIOR

An empty tubular reactor often can be simulated as a PFR or by a dispersion model with a small value of the dispersion coefficient. Stirred tank performance often is nearly completely mixed (CSTR), or the model may be modified by taking account of bypass zones, stagnant zones, or other parameters associated with the geometry and operation of the vessel. The additional parameters contribute to the mathematical complexity of the model. Sometimes the vessel can be visualized as a zone of complete mixing in the vicinity of impellers followed by plug flow zones elsewhere; thus, CSTRs followed by PFRs. Packed beds usually deviate substantially from plug flow. The dispersion model and some combinations of PFRs and CSTRs or multiple CSTRs in series may approximate their behavior. Fluidized beds in small sizes approximate CSTR behavior, but large ones exhibit bypassing, stagnancy, nonhomogeneous regions, and several varieties of contact between particles and fluid.

The concept of transfer functions facilitates the combination of linear elements. The rule is:

Output transform = (Transfer function) (Input transform)

Figure 23-8 develops the overall transform of a process with a PFR in parallel with two CSTRs in series. $C(t)$ is found from $C(s)$ by inversion of the output transform.

TRACER EQUATIONS

Differential equations and their solutions will be stated for the elementary models with the main kinds of inputs. Since the ODEs are linear, solutions by Laplace transforms are feasible.

Ideal CSTR With a step input of magnitude C_f the unsteady material balance is

$$V_r \frac{dC}{dt} + V'C = V'C_f \tag{23-20}$$

whose integral is

$$\frac{C}{C_f} = F(t_r) = 1 - \exp(-t_r) \tag{23-21}$$

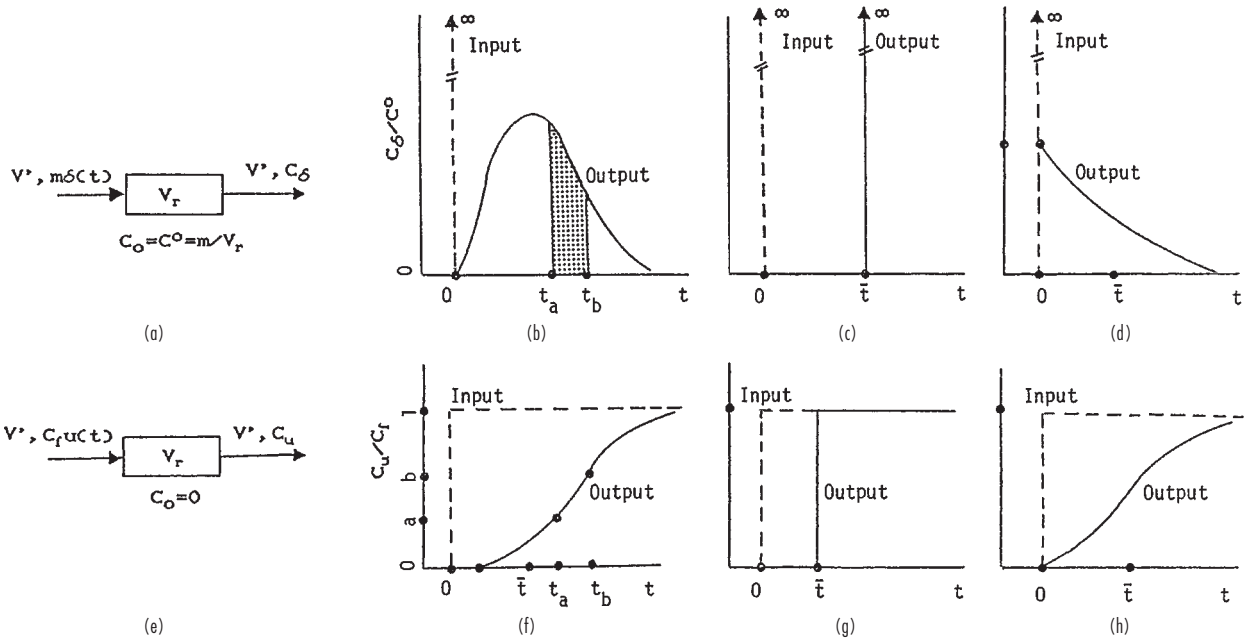

FIG. 23-7 Impulse and step inputs and responses. Typical, PFR and CSTR. (*a*) Experiment with impulse input of tracer. (*b*) Typical behavior; area between ordinates at t_a and t_b equals the fraction of the tracer with residence time in that range. (*c*) Plug flow behavior; all molecules have the same residence time. (*d*) Completely mixed vessel; residence times range between zero and infinity. (*e*) Experiment with step input of tracer; initial concentration zero. (*f*) Typical behavior; fraction with ages between t_a and t_b equals the difference between the ordinates, $b - a$. (*g*) Plug flow behavior; zero response until $t = \bar{t}$ has elapsed, then constant concentration C_f. (*h*) Completely mixed behavior; response begins at once, and ultimately reaches feed concentration.

With an impulse input of magnitude m or an initial mean concentration $C^0 = m/V_r$, the material balance is

$$\frac{dC}{dt_r} + C = 0 \qquad \text{when} \qquad C = C^0,\ t = 0 \tag{23-22}$$

and

$$\frac{C}{C^0} = E(t_r) = \exp(-t_r) \tag{23-23}$$

From these results it is clear that $E(t_r) = dF(t_r)/dt_r$.

Plug Flow Reactor (PFR) The material balance over a differential volume dV_r is

$$V'C = V'(C + dC) + dV_r \frac{\partial C}{\partial t}$$

or

$$\frac{\partial C}{\partial t} + V' \frac{\partial C}{V_r} = 0 \tag{23-24}$$

With step input the boundary conditions are

$$C(0,t) = C_f u(t) \qquad C(V_r,0) = 0 \tag{23-25}$$

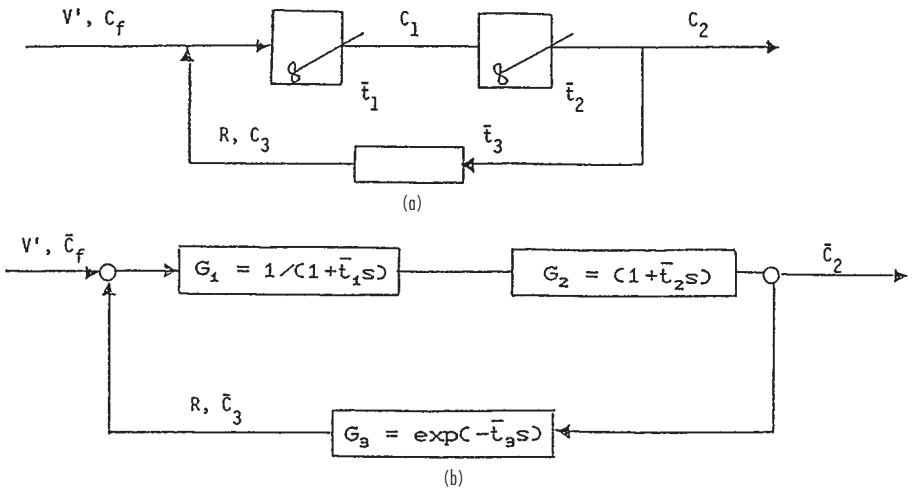

FIG. 23-8 Diagrams of a composite process: (*a*) process flow diagram, (*b*) transfer function diagram. The overall transfer function is:

$$\frac{\bar{C}_2}{\bar{C}_f} = \frac{1}{(1 + R/V')(1 + t_1 s)(1 + t_2 s) - (R/V')\exp(-t_3 s)}$$

By Laplace transform the solution is

$$\frac{C}{C_f} = F(t) = u(t-\bar{t}) = 0 \qquad \text{when} \qquad t \le \bar{t}$$
$$= 1 \qquad \text{when} \qquad t \ge \bar{t} \tag{23-26}$$

The response to impulse input is found by differentiation,

$$\frac{C}{C^0} = E(t_r) = \bar{t}\delta(t-\bar{t}) = \bar{t}\delta[\bar{t}(t_r-1)] = \delta(t_r-1) \tag{23-27}$$

that is, the effluent is an impulse that is delayed from the input impulse by $t_r = 1$ or $t = \bar{t}$.

Multistage CSTR This model has a particular importance because its RTD curve is bell-shaped like those of many experimental RTDs of packed beds and some empty tubes. The RTD is found by induction by solving the equations of one stage, two stages, and so on, with the result,

$$E(t_r) = \frac{C_n}{C^0} = \frac{n^n}{(n-1)!}\, t_r^{n-1} \exp(-nt_r) \tag{23-28}$$

Step response is found by integration, thus

$$F(t_r) = \int_0^{t_r} E(t_r)\, dt_r = 1 - \exp(-nt_r) \sum_{j=0}^{n-1} \frac{(nt_r)^j}{j!} \tag{23-29}$$

Plots of $E(t_r)$ and $f(t_r)$ for various values of n appear in Fig. 23-9. The bell shapes of $E(t_r)$ are more distinctive. The experimental curves of Figs. 23-10 and 23-11 clearly are of that family.

The peak of the E curve is reached at $t_r = (n-1)/n$ and has a magnitude

$$E(t_r)_{\max} = \frac{n(n-1)^{n-1}}{(n-1)!} \exp(1-n) \tag{23-30}$$

from which n can be found when $E(t_r)_{\max}$ has been measured.

Another significant characeristic of the E curve is the variance or the second moment which is

$$\sigma^2(t_r) = \int_0^{\infty} (t_r-1)^2 E(t_r)\, dt_r = \frac{1}{n} \tag{23-31}$$

The E equation can be rearranged into a linear form,

$$\ln[t_r E(t_r)] = \ln\left[\frac{n^n}{(n-1)!}\right] + n \ln[t_r \exp(-nt_r)] \tag{23-32}$$

With appropriate coordinates the slope of a loglog plot is n.

Combined Models, Transfer Functions The transfer function relation is

$$\overline{C}_{\text{output}} = (\text{Transfer function})\, \overline{C}_{\text{input}}$$
$$= G(s)\overline{C}_{\text{input}} \tag{23-33}$$

Some common transfer functions are

Element	*Transfer function, $G(s)$*
Ideal CSTR	$\dfrac{1}{(1+\bar{t}s)}$
PFR	$\exp(-\bar{t}s)$
n-stage CSTR (Erlang)	$\dfrac{1}{(1+\bar{t}s)^n}$
Erlang with time delay	$\dfrac{\exp(-\bar{t}_1 s)}{(1+\bar{t}_2 s)^n}$

The last item is of a PFR and an n-stage CSTR in series.

Although a transfer function relation may not be always invertible analytically, it has value in that the moments of the RTD may be derived from it, and it is thus able to represent an RTD curve. For instance, if G_0' and G_0'' are the limits of the first and second derivatives of the transfer function $G(s)$ as $s \Rightarrow 0$, the variance is

$$\sigma^2(t) = G_0'' - (G_0')^2$$

Characterization of RTD Curves An empirical RTD curve can be represented by equations of more than one algebraic form. The characteristic bell shape of many RTDs is evident in the real examples of Figs. 23-10 and 23-11. Such shapes invite comparison with some well-known statistical distributions and representation of the RTDs by their equations. Many of the standard statistical distributions are described by Hahn and Shapiro (*Statistical Models in Engineering*, Wiley, 1967) with their applicabilities. The most useful models in the present area are the gamma (or Erlang) and the Gaussian together with its Gram-Charlier extension. These distributions are representable by only a few parameters that define the asymmetry, the peak, and the shape in the vicinity of the peak. The moments—variance, skewness, and kurtosis—are such parameters.

Gamma or Erlang Distribution For nonintegral values, the factorial of the function $E(t_r)$ of Eq. (23-28) replaced as $(n-1)! = \Gamma(n)$. The result is called the gamma distribution,

$$E(t_r)_{\text{gamma}} = \frac{n^n}{\Gamma(n)}\, t_r^{n-1} \exp(-nt_r) \tag{23-34}$$

The value of n is the only parameter in this equation. Several procedures can be used to find its value when the RTD is known by experiment or calculation: from the variance, as in $n = 1/\sigma^2(t_r) = 1/\bar{t}^2\sigma^2(t)$, or from a suitable loglog plot or the peak of the curve as explained for the CSTR battery model. The Peclet number for dispersion is also related to n, and may be obtainable from correlations of operating variables.

Gaussian Distribution The best-known statistical distribution is the normal, or Gaussian, whose equation is

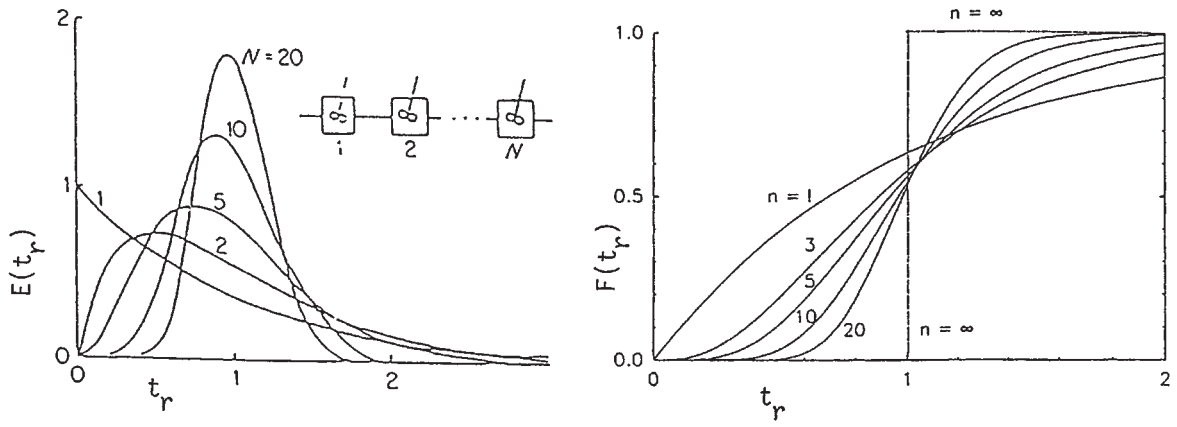

(a) (b)

FIG. 23-9 Tracer responses to n-stage continuous stirred tank batteries; the Erlang model: (*a*) impulse inputs, (*b*) step input.

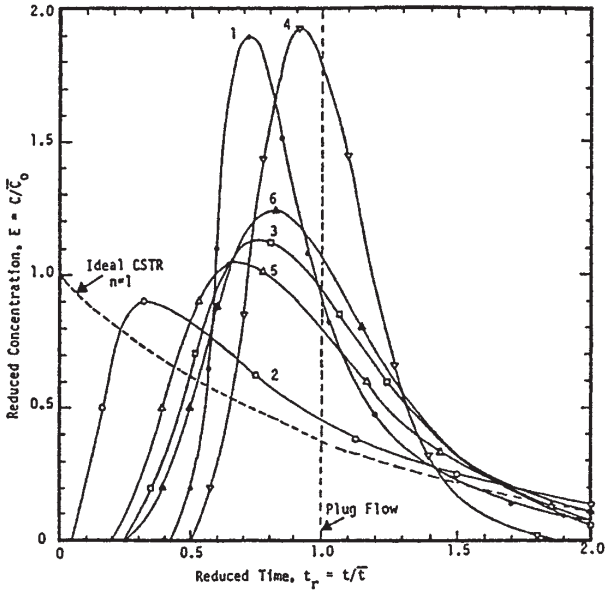

FIG. 23-10 Residence time distributions of pilot and commercial reactors. σ^2 = variance of the residence time distribution, n = number of stirred tanks with the same variance, Pe = Peclet number.

No.	Code	Process	σ^2	n	Pe
1	○	Aldolization of butyraldehyde	0.050	20.0	39.0
2	●	Olefin oxonation pilot plant	0.663	1.5	1.4
3	□	Hydrodesulfurization pilot plant	0.181	5.5	9.9
4	▽	Low-temp hydroisomerization pilot	0.046	21.6	42.2
5	△	Commercial hydrofiner	0.251	4.0	6.8
6	▲	Pilot plant hydrofiner	0.140	7.2	13.2

(*Walas,* Chemical Process Equipment, *Butterworths, 1990.*)

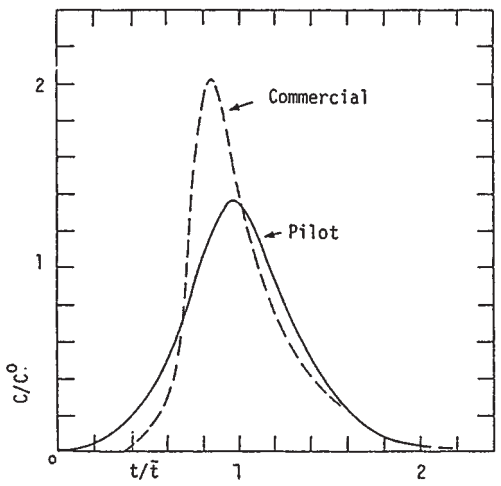

FIG. 23-11 Tracer tests on hydrodesulfurizers with 10-mm catalyst pellets. Commercial, 3 ft by 30 ft, $\bar{t}$ = 23 s, n = 12.9. Pilot, 4 in by 9 ft, $\bar{t}$ = 14 s, n = 9.3. To convert ft to m, multiply by 0.3048. (*Sherwood,* A Course in Process Design, *MIT Press, 1963.*)

$$C(t_r) = \frac{1}{\sigma\sqrt{2\pi}} \exp\left[-\frac{(t_r-1)^2}{2\sigma^2}\right], \qquad -\infty \le t_r \le +\infty \tag{23-35}$$

Since only positive values of t_r are of concern in RTD work, this function is normalized by dividing by the integral from 0 to ∞ with the result

$$E(t_r)_{\text{gauss}} = f(\sigma) \exp\left[-\frac{(t_r-1)^2}{2\sigma^2}\right] \tag{23-36}$$

where

$$f(\sigma) = \frac{\sqrt{2/\pi\sigma^2}}{1 + \text{erf}\,(1/\sigma\sqrt{2})} \tag{23-37}$$

Gram-Charlier Series This is an infinite series whose coefficients involve the Gaussian distribution and its derivatives (Kendall, *Advanced Theory of Statistics,* vol. 1, Griffin, 1958). The derivatives, in turn, are expressed in terms of the moments. The series truncated at the coefficient involving the fourth moment is

$$E(t_r)_{\text{GC}} = E(t_r)_{\text{gauss}}\left[\frac{1 - m_3(3z - z^3)}{6} + \frac{(m_4 - 3)\,(z^4 - 6z^2 + 3)}{24}\right] \tag{23-38}$$

where $z = \dfrac{(t_r - 1)}{\sigma}$

$$m_3 = \left(\frac{\gamma}{\sigma}\right)^3 = \int_0^\infty \left(\frac{t_r - 1}{\sigma}\right)^3 E(t_r)\,dt_r$$

$$m_4 = \left(\frac{\delta}{\sigma}\right)^4 = \int_0^\infty \left(\frac{t_r - 1}{\sigma}\right)^4 E(t_r)\,dt_r$$

More terms of the series are usually not justifiable because the higher moments cannot be evaluated with sufficient accuracy from experimental data. A comparison of the fourth-order GC with other distributions is shown in Fig. 23-12, along with calculated segregated conversions of a first-order reaction. In this case, the GC is the best fit to the original. At large variances the finite value of the ordinate at $t_r = 0$ appears to be a fatal objection to both the Gaussian and GC distributions. On the whole, the gamma distribution is perhaps the best representation of experimental RTDs.

Empirical Equations Tabular (C,t) data are easier to use when put in the form of an algebraic equation. Then necessary integrals and derivatives can be formed most readily and accurately. The calculation of chemical conversions by such mechanisms as segregation, maximum mixedness, or dispersion also is easier with data in the form of equations.

Procedures for curve fitting by polynomials are widely available. Bell-shaped curves, however, are fitted better and with fewer constants by ratios of polynomials. For figuring chemical conversions, the

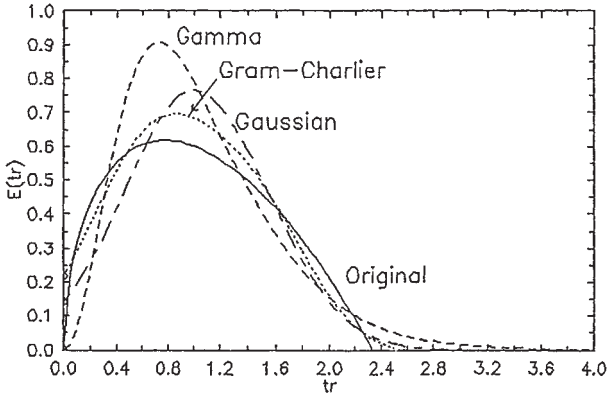

FIG. 23-12 Comparison of RTD models, all with the same variance and skewness. Values of C/C_0 of segregated conversion of a first-order reaction with $k\bar{t}$ = 3: original, 0.1408; gamma, 0.1158; Gauss, 0.1148; GC, 0.1418.

curve fit need not be accurate at small values of $E(t)$, since those regions do not affect the overall conversion significantly.

CHEMICAL CONVERSION

A distinction is to be drawn between situations in which (1) the flow pattern is known in detail, and (2) only the residence time distribution is known or can be calculated from tracer response data. Different networks of reactor elements can have similar RTDs, but fixing the network also fixes the RTD. Accordingly, reaction conversions in a known network will be unique for any form of rate equation, whereas conversions figured when only the RTD is known proceed uniquely only for linear kinetics, although they can be bracketed in the general case.

When the flow pattern is known, conversion in a known network and flow pattern is evaluated from appropriate material and energy balances. For first-order irreversible isothermal reactions, the conversion equation can be obtained from the transfer function by replacing s with the specific rate k. Thus, if $G(s) = \bar{C}/\bar{C}_0 = 1/(1 + \bar{t}s)$, then $C/C_0 = 1/(1 + k\bar{t})$. Complete knowledge of a network enables incorporation of energy balances into the solution, whereas the RTD approach cannot do that.

Segregated Flow In segregated flow the molecules travel as distinct groups, in which all molecules that enter the vessel together leave together. The groups are small enough so that the RTD of the whole system is represented by a smooth curve. For reaction orders above one, with a given RTD, the conversion is a maximum in segregated flow and a minimum under *maximum mixedness* conditions. This point is discussed in detail later.

Each group of molecules reacts independently of any other group, that is, as a batch reactor. Batch conversion equations for power law rate equations are:

$$\left(\frac{C}{C_0}\right)_{\text{batch}} = \exp(-kt) = \exp(-k\bar{t}t_r), \qquad \text{first order} \tag{23-39}$$

$$\left[\frac{1}{1 + (q-1)kC^{q-1}\bar{t}t_r}\right]^{1/(q-1)}, \qquad \text{order } q \tag{23-40}$$

For other rate equations a numerical solution may be needed.

The mean conversion of all the groups is the sum of the products of the individual conversions and their volume fractions of the total flow. Since the groups are small, the sum is replaced by the integal. Thus,

$$\left(\frac{C}{C_0}\right)_{\text{segregated}} = \int_0^\infty \left(\frac{C}{C_0}\right)_{\text{batch}} E(t)\,dt \tag{23-41}$$

$$= \int_0^\infty \left(\frac{C}{C_0}\right)_{\text{batch}} E(t_r)\,dt_r \tag{23-42}$$

Conversion in segregated flow is less than in plug flow and somewhat greater than in a CSTR battery with the same variance of the RTD.

When a conversion and an RTD are known, the specific rate can be found by trial: Values of k are estimated until one is found that makes the segregated integral equal to the known value. Moreover, if a series of conversions are known at several residence times, the order of the reaction can be found by trying different orders and noting which give a constant series of specific rates. A catch here, however, is that the RTD depends on the hydrodynamics of the process and may change with the residence time.

Maximum Mixedness The flow pattern for maximum mixedness is compared with segregated flow in Fig. 23-13. Segregated flow is in a vessel with multiple side *outlets* that result in a particular RTD. Maximum mixedness occurs in a plug flow vessel with multiple side *inlets* whose flow pattern is given by the same RTD. The main flow in the vessel is plug flow, but at each inlet the incoming material is completely mixed across the cross section with the axial flow. This means that each portion of fresh material is mixed with all the material that has the same life expectation, regardless of the actual residence time in the vessel up to the time of mixing. The life expectation under plug flow conditions is measured by the distance remaining to be traveled before leaving the vessel.

In contrast to segregated flow, in which the mixing occurs only after each sidestream leaves the vessel, under maximum mixedness mixing of all molecules having a certain period remaining in the vessel (the life expectation) occurs at the time of introduction of fresh material. These two mixing extremes—as late as possible and as soon as possible, both consistent with the same RTD—correspond to performance extremes of the vessel as a chemical reactor.

The differential equation of maximum mixedness was obtained by Zwietering (*Chem. Eng. Sci.*, **11**, 1 [1959]). It is:

$$\frac{dC}{dt} = R_c - \frac{E(t)}{1 - F(t)}(C_0 - C) \tag{23-43}$$

where R_c is the chemical rate equation; for an order q, $R_c = kC^q$. In the normalized units $f = C/C_0$ and $t_r = t/\bar{t}$,

$$\frac{df}{dt_r} = k\bar{t}C_0^{q-1}f^q - \frac{E(t_r)}{1 - F(t_r)}(1 - f) \tag{23-44}$$

The boundary condition is

$$\frac{df}{dt_r} = 0 \qquad \text{for} \qquad t_r \Rightarrow \infty \tag{23-45}$$

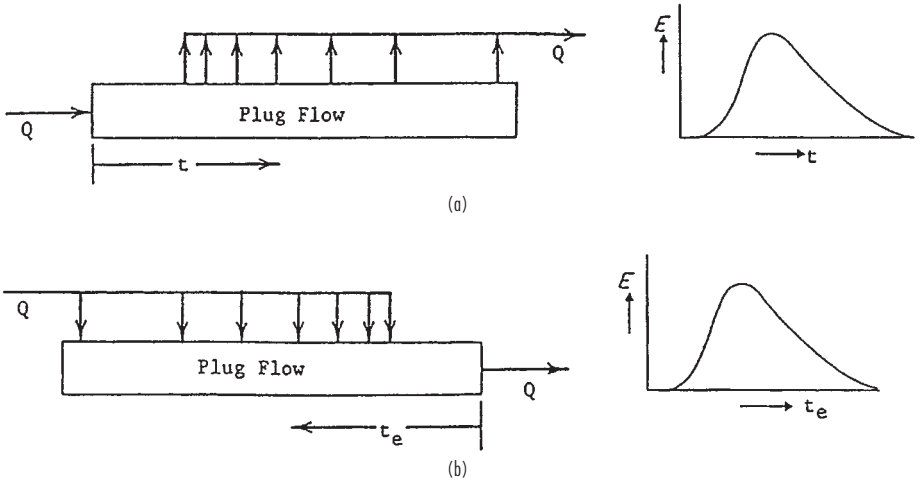

FIG. 23-13 The two limiting flow patterns with the same RTD. (*a*) Segregated flow, in which all molecules of any exit stream have the same residence time. (*b*) Maximum mixed flow, in which all molecules of an external stream with a certain life expectation are mixed with all molecules of the internal stream that have the same life expectation.

which makes

$$k\bar{t}C_0^{q-1}f_\infty^q - \frac{E(\infty)}{1-F(\infty)}(1-f_\infty) = 0 \qquad (23\text{-}46)$$

The conversion achieved in the vessel is obtained by the solution of the differential equation at the exit of the vessel where the life expectation is $t = 0$. The starting point for the integration is (f_∞, t_∞). When integrating numerically, however, the RTD becomes essentially 0 by the time t_r becomes 3 or 4, and the value of the integral beyond that point becomes nil. Accordingly, the integration interval is from $(f_\infty, t_r \le 3$ or 4) to $(f_{\text{effluent}}, t_r = 0)$. f_∞ is found from Eq. (23-46).

Numerical solutions of the maximum mixedness and segregated flow equations for the Erlang model have been obtained by Novosad and Thyn (*Coll. Czech. Chem. Comm.*, **31,** 3,710–3,720 [1966]). A few comparisons are made in Fig. 23-14. In some ranges of the parameters n or R_c the differences in conversion or reactor sizes for the same conversions are substantial. On the basis of only an RTD for the flow pattern, perhaps only an average of the two calculated extreme performances is justifiable.

Experimental confirmations of these mixing mechanisms are scarce. One study was with a 50-gal stirred tank reactor (Worrell and Eagleton, *Can. J. Chem. Eng.*, 254–258 [Dec. 1964]). They found seg-

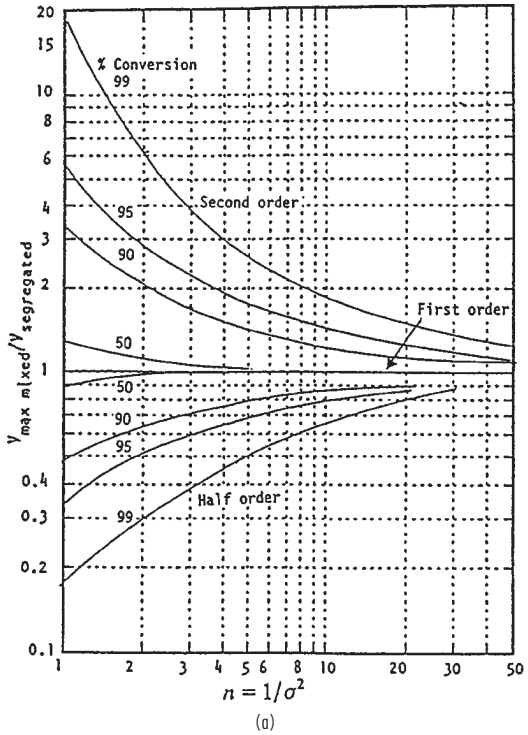

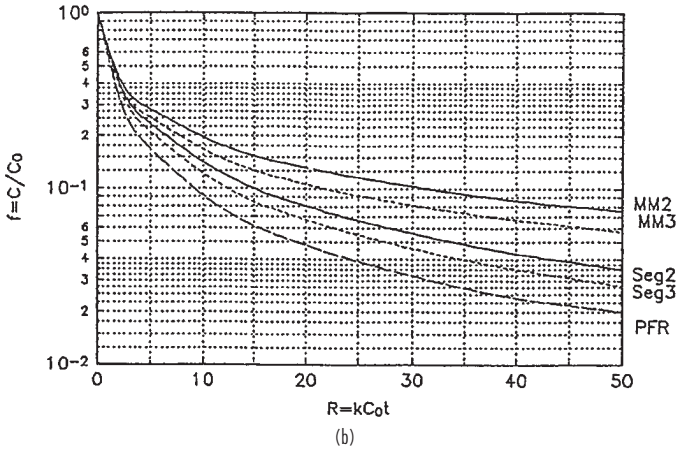

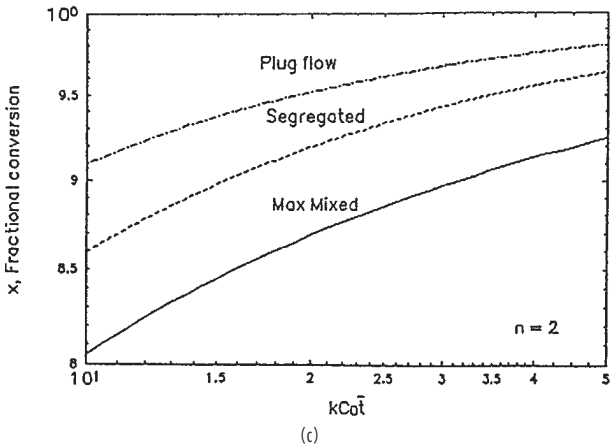

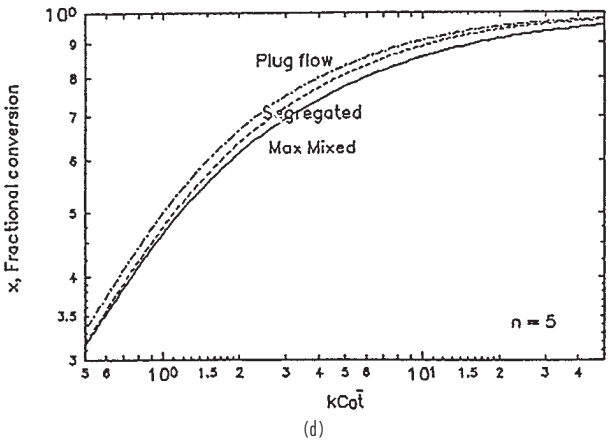

FIG. 23-14 Comparison of maximum mixed, segregated, and plug flows. (*a*) Relative volumes as functions of variance or n, for several reaction orders. (*b*) Second-order reaction with $n = 2$ or 3. (*c*) Second-order, $n = 2$. (*d*) Second-order, $n = 5$.

regation at low agitation, and were able to correlate complete mixing and maximum mixedness in terms of the power input and recirculation within the vessel.

Dispersion Model An impulse input to a stream flowing through a vessel may spread axially because of a combination of molecular diffusion and eddy currents that together are called *dispersion.* Mathematically, the process can be represented by Fick's equation with a dispersion coefficient replacing the diffusion coefficient. The dispersion coefficient D_e is associated with a linear dimension L and a linear velocity in the Peclet number, $\text{Pe} = uL/D_e$. In plug flow, $D_e = 0$ and $\text{Pe} \Rightarrow \infty$; and in a CSTR, $D_e \Rightarrow \infty$ and $\text{Pe} = 0$.

The dispersion coefficient is orders of magnitude larger than the molecular diffusion coefficient. Some rough correlations of the Peclet number are proposed by Wen (in Petho and Noble, eds., *Residence Time Distribution Theory in Chemical Engineering,* Verlag Chemie, 1982), including some for fluidized beds. Those for axial dispersion are:

1. Axial dispersion in empty tubes,

$$\frac{1}{\text{Pe}} = \frac{1}{(\text{Re})\,(\text{Sc})} + \frac{(\text{Re})\,(\text{Sc})}{192},$$

$$1 \le \text{Re} \le 2000, \qquad 0.2 \le \text{Sc} \le 1000 \qquad (23\text{-}47)$$

$$\frac{1}{\text{Pe}} = \frac{3(10^7)}{(\text{Re})^{2.1}} + \frac{1.35}{(\text{Re})^{0.125}}, \qquad \text{Re} \ge 2000 \qquad (23\text{-}48)$$

2. Axial dispersion of gases in packed tubes,

$$\frac{1}{\text{Pe}} = \frac{0.3}{(\text{Re})\,(\text{Sc})} + \frac{0.5}{1 + \dfrac{3.8}{(\text{Re})\,(\text{Sc})}},$$

$$0.008 \le \text{Re} \le 400, \qquad 0.28 \le \text{Sc} \le 2.2 \qquad (23\text{-}49)$$

where Pe = Peclet number, $d_p u_0/\varepsilon D$
Re = Reynolds number, $d_p s_p u_0/\nu$
Sc = Schmidt number, ν/D
D = axial dispersion coefficient
d_p = Diameter of particle or empty tube
ε = Fraction voids in packed bed
u_0 = Superficial velocity in the vessel.

In a vessel with axial dispersion, the steady-state equation for a reaction of order q is

$$\frac{d^2f}{dz^2} = \text{Pe}\left(\frac{df}{dz} - R_c\right) = \text{Pe}\left(\frac{df}{dz} - k\bar{t}C_0^{q-1}f^q\right) \qquad (23\text{-}50)$$

where the normalized variables are $f = C/C_0$ and $z = x/L$. For tracer flow, $R_c = 0$ and the time derivative appears,

$$\frac{\partial f}{\partial t_r} = \frac{1}{\text{Pe}}\frac{\partial^2 f}{\partial z^2} - \frac{\partial f}{\partial z} \qquad (23\text{-}51)$$

The solution of this partial differential equation is recorded in the literature (Otake and Kunigata, *Kagaku Kogaku,* **22,** 144 [1958]). The plots of $E(t_r)$ against t_r are bell-shaped, resembling the corresponding Erlang plots. A relation is cited later between the Peclet number, n_{erlang}, and $\sigma^2(t_r)$.

Boundary Conditions In normal operation with "closed ends," reactant is brought in by bulk flow and carried away by both bulk and dispersion flow. At the inlet where $L = 0$ or $z = 0$,

$$uC_0 = \left(uC - D\frac{\partial C}{\partial L}\right)_{L=0} \qquad (23\text{-}52)$$

or

$$f_0 = \left(f - \frac{1}{\text{Pe}}\frac{\partial f}{\partial z}\right)_{z=0} \qquad (23\text{-}53)$$

At the exit where $z = 1$,

$$\left(\frac{\partial f}{\partial z}\right)_{z=1} = 0 \qquad (23\text{-}54)$$

With these two-point boundary conditions the dispersion equation, Eq. (23-50), may be integrated by the *shooting method.* Numerical solutions for first- and second-order reactions are plotted in Fig. 23-15.

The discontinuity of concentration at the inlet is commonly observed with CSTR operations, where $\text{Pe} = 0$. At other values of Pe, the effects are shown in Fig. 23-16.

Comparison of Models Only scattered and inconclusive results have been obtained by calculation of the relative performances of the different models as converters. Both the RTD and the dispersion coefficient require tracer tests for their accurate determination, so neither method can be said to be easier to apply. The exception is when one of the cited correlations of Peclet numbers in terms of other groups can be used, although they are rough. The tanks-in-series model, however, provides a mechanism that is readily visualized and is therefore popular.

The Erlang (or gamma) and dispersion models can be related by equating the variances of their respective $E(t_r)$ functions. The result for the "closed-ends" condition is

$$\sigma^2(t_r) = \frac{2[\text{Pe} - 1 + \exp(-\text{Pe})]}{\text{Pe}^2} \qquad (23\text{-}55)$$

$$= \frac{1}{n_{\text{erlang}}} \qquad (23\text{-}56)$$

For both large and small values of Pe,

$$n_{\text{erlang}} \Rightarrow \frac{\text{Pe}}{2} \qquad (23\text{-}57)$$

MULTIPLICITY AND STABILITY

Normally, when a small change is made in the condition of a reactor, only a comparatively small change in the response occurs. Such a system is uniquely stable. In some cases, a small positive perturbation can result in an abrupt change to one steady state, and a small negative perturbation to a different steady condition. Such multiplicities occur most commonly in variable temperature CSTRs. Also, there are cases where a process occurring in a porous catalyst may have more than one effectiveness at the same Thiele number and thermal balance. Some isothermal systems likewise can have multiplicities, for instance, CSTRs with rate equations that have a maximum, as in Example (*d*) following.

Conditions at steady state are determined by heat and material balances. Such balances for a CSTR can be put in the form,

Heat generated by reaction = Sensible heat pickup

or

$$-\Delta H_r V_r r_c = V'\rho C_p(T - T_f) \qquad (23\text{-}58)$$

Four examples of multiplicity and stability follow.

Example (a) For a first-order reaction in a CSTR, the rate of reaction is:

$$r_c = kC = \frac{kC_f}{1 + k\bar{t}} = \frac{C_f \exp(a + b/T)}{1 + \bar{t}\exp(a + b/T)}$$

When this is substituted into the previous equation, both sides become functions of T and may be plotted against each other. As Fig. 23-17 of a typical case shows, as many as three steady states are possible. When generation is greater than removal (as at points A– and B+), the temperature will rise to the next higher steady state; when generation is less than removal (as at points A+ and B–), it will fall to the next steady state. Point B is an unsteady state, while A and C are steady.

Example (b) In terms of fractional conversion, $f = 1 - C/C_f$, the material and energy balances for a first-order CSTR are:

$$f = \frac{k\bar{t}}{1 + k\bar{t}} = \frac{50k}{1 + 50k} = \frac{\rho C_p(T - T_f)}{-\Delta H_r C_f} = \frac{1.2(0.9)(T - T_f)}{46{,}000C_f}$$

The two equations are plotted for several combinations of C_f and T_f. The number of steady states can be one, two, or three if zero or complete conversion are considered possibilities.

Example (c) For the reactions $A \xrightarrow{1} B \xrightarrow{2} C$ the concentrations are:

$$A = \frac{A_f}{1 + k_1\bar{t}}, \qquad B = \frac{k_1\bar{t}A_f}{(1 + k_1\bar{t}(1 + k_2\bar{t})}$$

The heat balance is:

$$-\Delta H_a(A_f - A) - \Delta H_b(B - B_f) = \rho C_p(T - T_f)$$

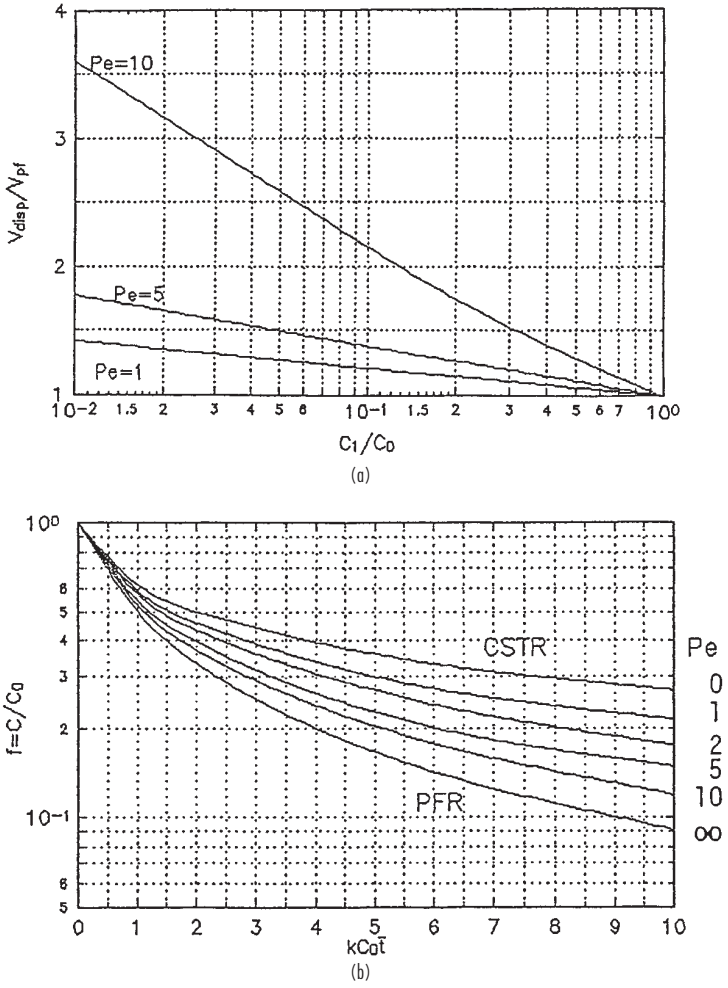

FIG. 23-15 Chemical conversion by the dispersion model. (*a*) First-order reaction, volume relative to plug flow against residual concentration ratio. (*b*) Second-order reaction, residual concentration ratio against $kC_0\bar{t}$.

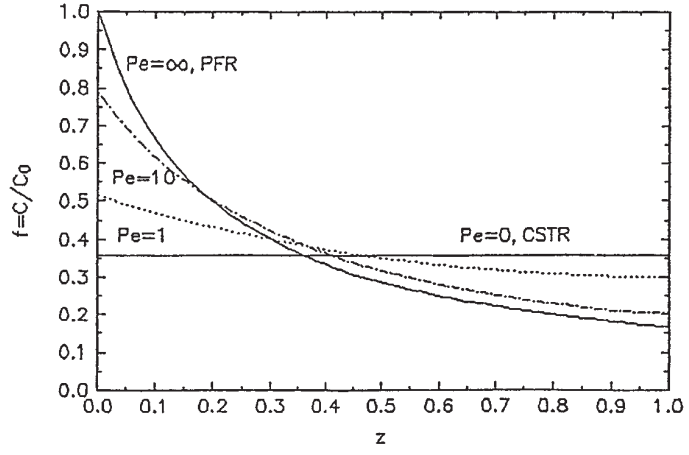

FIG. 23-16 Concentration jump at the inlet of a "closed ends" vessel with dispersion. Second-order reaction with $kC_0\bar{t} = 5$.

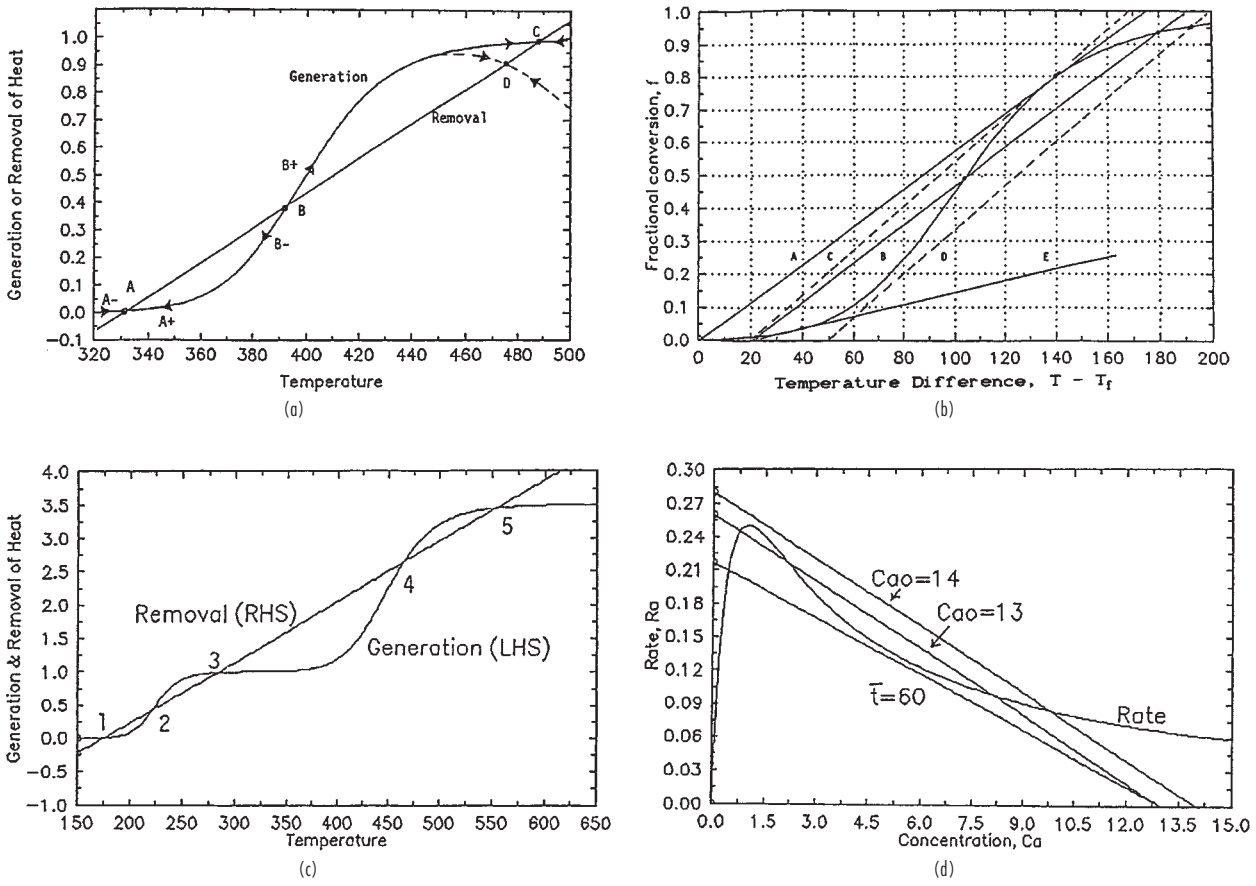

FIG. 23-17 Multiple steady states of CSTRs, stable and unstable, adiabatic except the last item. (*a*) First-order reaction, A and C stable, B unstable, A is no good for a reactor, the dashed line is of a reversible reaction. (*b*) One, two, or three steady states depending on the combination (C_f, T_f). (*c*) The reactions A ⇒ B ⇒ C, with five steady states, points 1, 3, and 5 stable. (*d*) Isothermal operation with the rate equation $r_a = C_a/(1 + C_a)^2 = (C_{a0} - C_a)/\bar{t}$.

In a specific case this becomes

$$110\left(\frac{k_1\bar{t}}{1+k_1\bar{t}}\right)\left(\frac{1+2.5k_2\bar{t}}{1+k_2\bar{t}}\right) = T - 175$$

with $k_1\bar{t}$ = exp (20 − 4,500/*T*) and $k_2\bar{t}$ = exp (20 − 9,000/*T*). The plot shows 5 steady states, of which 1, 3, and 5 are stable. *T* is in K.

Example (d) The rate equation and the CSTR material balance of this process are:

$$r_a = \frac{C_a}{(1+C_a)^2} = \frac{C_{a0} - C_a}{\bar{t}}$$

The plots of these equations with $C_{a0} = 13$ and $\bar{t} = 50$ show three intersections, and only one with $C_{a0} = 14$, but the conversion is poor. Keeping $C_{a0} = 13$ but making $\bar{t} = 60$ changes the stable operation to $C_a = 0.6$, or 95 percent conversion.

Instances of multiplicities in CSTR batteries and in PFRs also can be developed.

Only a very few experimental studies have been made for detection of multiplicities of steady states to check on theoretical predictions. The studies of multiplicities and of oscillations of concentrations have similar mathematical bases. Comprehensive reviews of these topics are by Schmitz (*Adv. Chem. Ser.*, **148**, 156, ACS [1975]), Razon and Schmitz (*Chem. Eng. Sci.*, **42**, 1,005–1,047 [1987]), Morbidelli, Varma, and Aris (in Carberry and Varma, eds., *Chemical Reaction and Reactor Engineering*, Dekker, 1987, pp. 975–1,054).

CATALYSIS

A catalyst is a substance that increases the rate of a reaction by participating chemically in intermediate stages of reaction and is ultimately liberated in a chemically unchanged form. Over a period of time, however, permanent changes in the catalyst—deactivation—may occur. *Inhibitors* are substances that slow down rates of reaction. The turnover ratio, the number of molecules converted per molecule of catalyst, can be in the millions. Many catalysts have specific actions in that they influence only one reaction or group of definite reactions. The outstanding example is the living cell in which there are several hundred catalysts, called *enzymes*, each one favoring a specific chemical process. When a reaction can proceed by more than one path, a particular catalyst may favor one path over another and thus lead to a product distribution different from an uncatalyzed reaction. A catalytic reaction requires a lower energy of activation, thus permitting a reduction of temperature at which the reaction can proceed favorably. The equilibrium condition is not changed since both forward and reverse rates are accelerated equally. For example, a good hydrogenation catalyst also is a suitable dehydrogenation accelerator but possibly with a different most-favorable temperature.

Catalytic processes may be homogeneous in the liquid or gas phase (for instance, nitrogen oxides in the Chamber process for sulfuric acid), but industrial examples are most often heterogeneous with a

solid catalyst and fluid reactants. Some large industrial reactors of this type are illustrated in Fig. 23-18.

HOMOGENEOUS CATALYSIS

The most numerous cases of homogeneous catalysis are by certain ions or metal coordination compounds in aqueous solution and in biochemistry, where enzymes function catalytically. Many ionic effects are known. The hydronium ion H_3O^+ and the hydroxyl ion OH^- catalyze hydrolyses such as those of esters; ferrous ion catalyzes the decomposition of hydrogen peroxide; decomposition of nitramide is catalyzed by acetate ion. Other instances are inversion of sucrose by HCl, halogenation of acetone by H^+ and OH^-, hydration of isobutene by acids, hydrolysis of esters by acids, and others.

The specific action of a particular metal complex can be altered by varying the ligands or coordination number of the complex or the oxidation state of the central metal atom.

Probable mechanisms often have been deduced: The reactant forms a short-lived intermediate with the catalyst that subsequently decomposes into the product and regenerated catalyst. In fluid phases such intermediates can be detected spectroscopically. This is in contrast to solid catalysis, where the detection of intermediates is much more difficult and is not often accomplished.

Significant characteristics of homogeneous catalysis are that they are highly specific and proceed under relatively mild conditions—again in contrast to solid catalysis, which is less discriminating as to reaction and may require extremes of temperature and pressure. A problem with homogeneous operation is the difficulty of separating product and catalyst.

A review of industrial processes that employ homogeneous catalysts is by Jennings, ed. (*Selected Developments in Catalysis,* Blackwell Scientific, 1985). Some of those processes are:

- Alkylation of isobutane with C_3-C_4 olefins in the presence of HF at 25 to 35°C or 90 to 98% sulfuric acid at 10°C (50°F).
- Alkylation of isobutane and ethylene with a complex of liquid hydrocarbon + $AlCl_3$ + HCl.
- The Wacker process for the oxidation of ethylene to acetaldehyde with $PdCl_2/CuCl_2$ at 100°C (212°F) with 95 percent yield and 95 to 99 percent conversion per pass.
- The OXO process for higher alcohols: $CO + H_2 + C_3H_6 \Rightarrow$ *n*-butanal $\Rightarrow$ further processing. Catalyst is rhodium triphenylphosphine coordination compound, 100°C (212°F), 30 atm (441 psi).
- Acetic acid from methanol by the Monsanto process, $CH_3OH + CO \Rightarrow CH_3COOH$, rhodium iodide catalyst, 3 atm (44 psi), 150°C (302°F), 99 percent selectivity of methanol.
- Ammonia is a cyclic reagent that is recovered by the end of the Solvay process for sodium carbonate from lime and salt. Although there is nothing obscure about the intermediate reactions, ammonia definitely participates in a catalytic sequence.

Immobilized or Polymer Bound, or Heterogenized Catalysts The specificity of homogeneous and separability of solid catalysts are realized by attaching the catalyst to a solid support. This is commonly done for enzymes. In use as carriers are organic polymers such as polystyrene and inorganic polymers such as zeolites, silica, or alumina. A catalyst metal atom, for instance, is anchored to the polymer through a group that is chemically bound to the polymer with a coordinating site such as $-P(C_6H_5)_2$ or $-C_5H_4$ (cyclopentadienyl). Immobilized catalysts have applications in hydrogenation, hydroformylation, and polymerization reactions (Lieto and Gates, *CHEMTECH,* 46–53 [Jan. 1983]).

Phase-Transfer Catalysis In phase-transfer catalysis (PTC), reactions between reactants located in different phases (typically organic and aqueous liquids) are brought about or accelerated by a catalyst that migrates between the phases. Ultimately, the reaction takes place in the organic phase. Although no one mechanism explains everything, the catalyst may combine with a reactant in one phase, migrate to the other phase in which it is also miscible, and react there. Ultimately, the reaction is homogeneous. The catalysts used most extensively are quaternary ammonium or phosphonium salts and crown ethers and cryptates, for instance benzyltriethylammonium chloride and the cheaper methyltrioctylammonium chloride. Reactions helped by PTC include making higher esters, ethers, and alkylates, polymerization of butyl acrylate, and oxidation of olefins with $KMnO_4$. In most of these instances the reaction rate is nil without the catalyst (Dehmlow, *Phase Transfer Catalysis,* Verlag Chemie, 1992).

Effect of Concentration All catalytic reactions appear to involve the formation of intermediate compounds with the catalyst. For a reactant A, product B, and catalyst the corresponding equation is

$$A + C \Rightarrow AC \Rightarrow B + C$$

When the first step is rate controling,

$$r_a = k[A][C]^\alpha$$

In some cases, the exponent is unity. In other cases, the simple power law is only an approximation for an actual sequence of reactions. For instance, the chlorination of toluene catalyzed by acids was found to have $\alpha = 1.15$ at 6°C (43°F) and 1.57 at 32°C (90°F), indicating some complex mechanism sensitive to temperature. A particular reaction may proceed in the absence of catalyst but at a reduced rate. Then the rate equation may be

$$r_a = (k_1 + k_2[C]^\alpha)[A]$$

An instance of *autocatalysis* is the hydrolysis of methyl acetate, which is catalyzed by product acetic acid, $A \Rightarrow C$. The rate equation may be

$$r_a = k[A][C] = k[A][A_0 - A]$$

which will have a maximum value that is characteristic of autocatalytic reactions in general.

CATALYSIS BY SOLIDS

Solid catalysts are widely employed because they are usually cheap, are easily separated from the reaction medium, and are adaptable to either flow or nonflow reactors. Their drawbacks are lack of specificity and possibly high temperatures and pressures.

Usually they are employed as porous pellets in a packed bed. Some exceptions are platinum for the oxidation of ammonia, which is in the form of several layers of fine-mesh wire gauze, and catalysts deposited on membranes. Pore surfaces can be several hundred m^2/g and pore diameters of the order of 100 Å. The entire structure may be of catalytic material (silica or alumina, for instance, sometimes exert catalytic properties) or an active ingredient may be deposited on a porous refractory carrier as a thin film. In such cases the mass of expensive catalytic material, such as Pt or Pd, may be only a fraction of 1 percent.

The principal components of most solid catalysts are three in number:

1. A catalytically active substance or mixture.
2. A carrier of more or less large specific surface, often refractory to withstand high temperatures. A carrier may have some promotion action; for example, silica carrier helps chromia catalyst.
3. Promoters, usually present in small amount, which enhance activity or retard degradation; for instance, rhenium slows coking of platinum reforming, and KCl retards vaporization of $CuCl_2$ in oxychlorination for vinyl chloride.

Selection of Catalysts A basic catalyst often can be selected by using general principles, but the subsequent fine tuning of a commercially attractive recipe must be done experimentally. A start for catalyst design usually is by analogy to what is known to be effective in chemically similar problems, although a scientific basis is being developed. This involves a study in detail of the main possible intermediate reactions that could occur and of the proton and electron receptivity of the catalyst and possible promoters, as well as reactant bond lengths and crystal lattice dimensions. Several designs are made from this point of view by Trimm (*Design of Industrial Catalysts,* Elsevier, 1980). Some of this scientific basis is treated by Hegedüs et al. (*Catalyst Design Progress and Perspectives,* Wiley, 1987). Preparation of specific catalysts is described by Stiles (*Catalyst Manufacture,* Dekker, 1983). A thorough coverage of catalytic reactions and catalysts arranged according to the periodic table is in a series by Roiter ed. (*Handbook of Catalytic Properties of Substances,* in Russian, 1968). Industrial catalyst practice is summarized by Thomas (*Cat-*

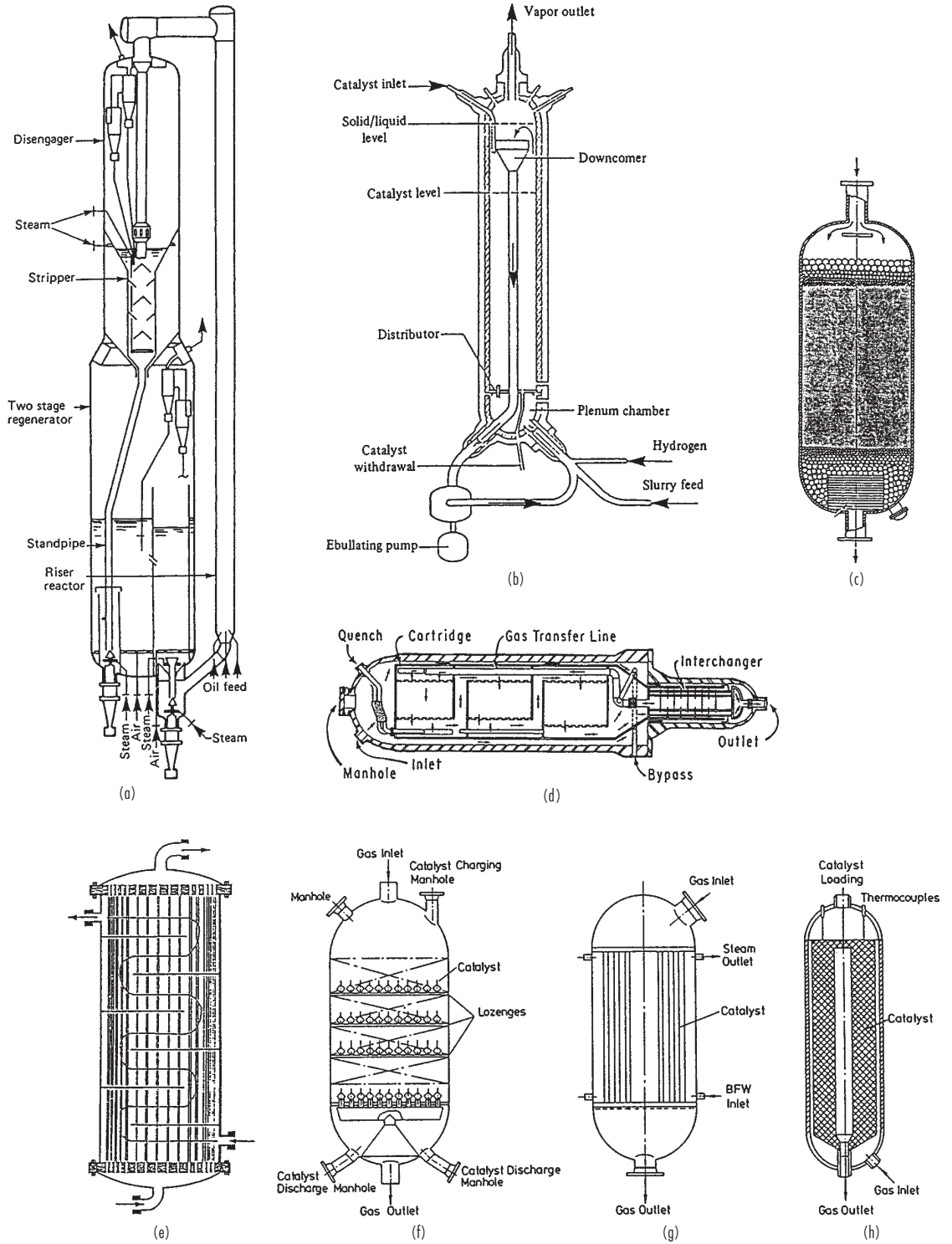

FIG. 23-18 Reactors with solid catalysts. (*a*) Riser cracker with fluidized zeolite catalyst, 540°C; circulation by density difference, 34 to 84 kg/m^3 in riser, 420 to 560 kg/m^2 in regenerator. (*b*) Ebullating fluidized bed for conversion of heavy stocks to gas and light oils. (*c*) Fixed bed unit with support and hold-down zones of larger spheres. (*d*) Horizontal ammonia synthesizer, 26 m long without the exchanger, 2,000 ton/d (*M W Kellogg Co.*). (*e*) Shell-and-tube vessel for hydrogenation of crotonaldehyde has 4,000 packed tubes, 30 mm ID, 10.7 m long, aldehyde feed 209 kg mol/h, hydrogen feed 2,090 kg mol/h. (*After Berty, in Leach,* ed., Applied Industrial Catalysis, *vol. 1, Academic Press, 1983, p. 51*). (*f*), (*g*), (*h*) Methanol synthesizers, 50 to 100 atm, 230 to 300°C, Cu catalyst; ICI quench type, Lurgi tubular, Haldor Topsoe radial flow (*Marschner and Moeller, in Leach, loc. cit.*). To convert ton/d to kg/h, multiply by 907; atm to kPa, multipy by 101.3.

alytic Processes and Proven Catalysts, Academic Press, 1970) who names manufacturers of catalysts for specific processes. Specific processes and general aspects of catalysts are covered by Leach, ed. (*Applied Industrial Catalysis,* 3 vols., Academic Press, 1983–1984). Many industrial processes are described by Gates et al. (*Chemistry of Catalytic Processes,* McGraw-Hill, 1979), Matar et al. (*Catalysis in Petrochemical Processes,* Kluwer Academic Publishers, 1989), Pines (*Chemistry of Catalytic Conversions of Hydrocarbons,* Academic Press, 1981) and Satterfield (*Heterogeneous Catalysis in Industrial Practice,* McGraw-Hill, 1991). Books and encyclopedia articles on particular chemicals and processes may be consulted for catalytic data. There are also eight journals devoted largely to catalytic kinetics.

Kinds of Catalysts To a certain extent it is known what kinds of reactions are speeded up by certain classes of catalysts, but individual members of the same class may differ greatly in activity, selectivity, resistance to deactivation, and cost. Since solid catalysts are not particularly selective, there is considerable crossing of lines in the classification of catalysts and the kinds of reactions they favor. Although some trade secrets are undoubtedly employed to obtain marginal improvements, the principal catalytic effects are known in many cases.

Strong acids are able to donate protons to a reactant and to take them back. Into this class fall the common acids, aluminum halides, and boron trifluoride. Also acid in nature are silica, alumina, aluminosilicates, metal sulfates and phosphates, and sulfonated ion exchange resins. They can transfer protons to hydrocarbons acting as weak bases. Zeolites are dehydrated aluminosilicates with small pores of narrow size distribution, to which is due their highly selective action since only molecules small enough to enter the pores can react.

Base catalysis is most effective with alkali metals dispersed on solid supports or, in the homogeneous form, as aldoxides, amides, and so on. Small amounts of promoters form organoalkali comnpounds that really contribute the catalytic power. Basic ion exchange resins also are useful. Base-catalyzed processes include isomerization and oligomerization of olefins, reactions of olefins with aromatics, and hydrogenation of polynuclear aromatics.

Metal oxides, sulfides, and hydrides form a transition between acid/base and metal catalysts. They catalyze hydrogenation/dehydrogenation as well as many of the reactions catalyzed by acids, such as cracking and isomerization. Their oxidation activity is related to the possibility of two valence states which allow oxygen to be released and reabsorbed alternately. Common examples are oxides of cobalt, iron, zinc, and chromium and hydrides of precious metals that can release hydrogen readily. Sulfide catalysts are more resistant than metals to the formation of coke deposits and to poisoning by sulfur compounds; their main application is in hydrodesulfurization.

Metals and alloys, the principal industrial metallic catalysts, are found in periodic group VIII, which are transition elements with almost-completed 3*d,* 4*d,* and 5*d* electronic orbits. According to theory, electrons from adsorbed molecules can fill the vacancies in the incomplete shells and thus make a chemical bond. What happens subsequently depends on the operating conditions. Platinum, palladium, and nickel form both hydrides and oxides; they are effective in hydrogenation (vegetable oils) and oxidation (ammonia or sulfur dioxide). Alloys do not always have catalytic properties intermediate between those of the component metals, since the surface condition may be different from the bulk and catalysis is a function of the surface condition. Addition of some rhenium to Pt/Al_2O_3 permits the use of lower temperatures and slows the deactivation rate. The mechanism of catalysis by alloys is still controversial in many instances.

Transition-metal organometallic catalysts in solution are more effective for hydrogenation than are metals such as platinum. They are used for reactions of carbon monoxide with olefins (hydroformylation) and for some oligomerizations. They are sometimes immobilized on polymer supports with phosphine groups.

Kinds of Catalyzed Organic Reactions A fundamental classification of organic reactions is possible on the basis of the kinds of bonds that are formed or destroyed and the natures of eliminations, substitutions, and additions of groups. Here a more pragmatic list of 20 commercially important kinds or classes of reactions will be discussed. In all instances of solid-catalyzed reactions, chemisorption is a primary step. Often molecules are dissociated on chemisorption into the more active atomic forms, for instance, of CO, H_2, N_2, and O_2 on platinum.

1. Alkylations—for example, of olefins with aromatics or isoparaffins—are catalyzed by sulfuric acid, hydrofluoric acid, BF_3 and $AlCl_3$.
2. Condensations of aldehydes and ketones are catalyzed homogeneously by acids and bases, but solid bases are preferred, such as anion exchange resins and alkali or alkaline earth hydroxides or phosphates.
3. Cracking, a rupturing of carbon-carbon bonds—for example, of gas oils to gasoline—is favored by silica-alumina, zeolites, and acid types generally. Zeolites have pores with small and narrow size distribution. They crack only molecules small enough to enter the pores. To restrain the undesirable formation of carbon and C_3-C_4 hydrocarbons, zeolite activity is reduced by dilution to 10 to 15 percent in silica-alumina.
4. Dehydration and dehydrogenation combined utilizes dehydration agents together with mild dehydrogenation agents. Included in this class are phosphoric acid, silica-magnesia, silica-alumina, alumina derived from aluminum chloride, and various metal oxides.
5. Esterification and etherification may be catalyzed by mineral acids or BF_3. The reaction of isobutylene with methanol to make MTBE is catalyzed by a sulfonated ion exchange resin.
6. Fischer-Tropsch oligomerization of $CO + H_2$ to make hydrocarbons and oxygenated compounds was originally catalyzed by cobalt, which forms the active carbonyl, but now iron promoted by potassium is favored. Dissociative chemisorption of CO has been observed in this process.
7. Halogenation and dehalogenation are catalyzed by substances that exist in more than one valence state and are able to donate and accept halogens freely. Silver and copper halides are used for gas-phase reactions, and ferric chloride commonly for liquid phase. Hydrochlorination (the absorption of HCl) is promoted by $BiCl_3$ or $SbCl_3$ and hydrofluorination by sodium fluoride or chromia catalysts that form fluorides under reaction conditions. Mercuric chloride promotes addition of HCl to acetylene to make vinyl chloride. Oxychlorination in the Stauffer process for vinyl chloride from ethylene is catalyzed by $CuCl_2$ with some KCl to retard its vaporization.
8. Hydration and dehydration employ catalysts that have a strong affinity for water. Alumina is the principal catalyst, but also used are aluminosilicates, metal salts and phosphoric acid or its metal salts on carriers, and cation exchange resins.
9. Hydrocracking is catalyzed by substances that promote cracking and hydrogenation together. In commercial use are Ni, Co, Cr, W, and V or their oxides, presulfided before use, on acid supports. Zeolites loaded with palladium also have been used.
10. Hydrodealkylation—for instance, of toluene to benzene—is catalyzed by supported oxides of Cr, Mo, and Co at 500 to 650°C and 50 atm.
11. Hydrodesulfurization. A commercial catalyst contains about 4 percent CoO and 12 percent MoO_3 on γ-alumina and is presulfided before use. Molybdena is a weak catalyst by itself and the cobalt has no catalytic action by itself.
12. Hydroformylation, or the OXO process, is the reaction of olefins with CO and H_2 to make aldehydes, which may subsequently be converted to higher alcohols. The catalyst base is cobalt naphthenate, which transforms to cobalt hydrocarbonyl in place. A rhodium complex that is more stable and functions at a lower temperature is also used.
13. Hydrogenation and dehydrogenation employ catalysts that form unstable surface hydrides. Raney nickel or cobalt are used for many reductions. In the hydrogenation of olefins, both olefin and hydrogen are chemisorbed, the latter with dissociation. Transition-group and bordering metals such as Fe, Ni, Co, and Pt are suitable, as well as transition-group oxides or sulfides. This class of reactions includes the important examples of ammonia and methanol syntheses, the Fischer-Tropsch, OXO, and SYNTHOL processes, and the production of alcohols, aldehydes, ketones, amines, and edible oils. In the sequence for making nylon, phenol is hydrogenated to cyclohexanol with nickel catalyst at 150°C (302°F) and 15 atm (221 psi); the product is hydrogenated to cyclohexanone at 400°C (752°F) using a zinc or copper catalyst; that product is hydrogenated to cyclohexane carboxylic acid at 150°C (302°F) and 15 atm (221 psi) with palladium on

charcoal; this last product is a precursor for ε-caprolactam, which goes on to make nylon.

14. Hydrolysis of esters is speeded up by both acids and bases. Soluble alkylaryl sulfonic acids or sulfonated ion exchange resins are suitable.

15. Isomerization is promoted by either acids or bases. Higher alkylbenzenes are isomerized in the presence of $AlCl_3$/HCl or BF_3/HF; olefins with most mineral acids, acid salts and silica-alumina; saturated hydrocarbons with $AlCl_3$ or $AlBr_3$ promoted by 0.1 percent of olefins.

16. Metathesis is the rupture and reformation of carbon-carbon bonds—for example, of propylene into ethylene plus butene. Catalysts are oxides, carbonyls, or sulfides of Mo, W, or Re.

17. Oxidation catalysts are either metals that chemisorb oxygen readily, such as platinum or silver, or transition metal oxides that are able to give and take oxygen by reason of their having several possible oxidation states. Ethylene oxide is formed with silver, ammonia is oxidized with platinum, and silver or copper in the form of metal screens catalyze the oxidation of methanol to formaldehyde. Cobalt catalysis is used in the following oxidations: butane to acetic acid and to butylhydroperoxide, cyclohexane to cyclohexylperoxide, acetaldehyde to acetic acid and toluene to benzoic acid. $PdCl_2$-$CuCl_2$ is used for many liquid-phase oxidations and V_2O_5 combinations for many vapor-phase oxidations.

18. Polymerization of olefins such as styrene is promoted by acid or base or sodium catalysts, and polyethylene is made with homogeneous peroxides. Condensation polymerization is catalyzed by acid-type catalysts such as metal oxides and sulfonic acids. Addition polymerization is used mainly for olefins, diolefins, and some carbonyl compounds. For these processes, initiators are coordination compounds such as Ziegler-type catalysts, of which halides of transition metals Ti, V, Mo, and W are important examples.

19. Reforming is the conversion primarily of naphthenes and alkanes to aromatics, but other reactions also occur under commercial conditions. Platinum or platinum/rhenium are the hydrogenation/dehydrogenation component of the catalyst and alumina is the acid component responsible for skeletal rearrangements.

20. Steam reforming is the reaction of steam with hydrocarbons to make town gas or hydrogen. The first stage is at 700 to 830°C (1,292 to 1,532°F) and 15–40 atm (221 to 588 psi). A representative catalyst composition contains 13 percent Ni supported on α-alumina with 0.3 percent potassium oxide to minimize carbon formation. The catalyst is poisoned by sulfur. A subsequent *shift reaction* converts CO to CO_2 and more H_2, at 190 to 260°C (374 to 500°F) with copper metal on a support of zinc oxide which protects the catalyst from poisoning by traces of sulfur.

Physical Characteristics With a few exceptions, solid catalysts are employed as porous pellets in a fixed or fluidized bed. Their physical characteristics of major importance are as follows.

• *Pellet size* is a major consideration. Shapes are primarily spherical, short cylindrical, or irregular. Special shapes like those used in mass-transfer equipment may be used to minimize pressure drop. In gas fluidized beds the diameters average less than 0.1 mm (0.0039 in); smaller sizes impose too severe loading on the entrainment recovery equipment. In slurry beds the diameters can be about 1.0 mm (0.039 in). In fixed beds the range is 2 to 5 mm (0.079 to 0.197 in). The competing factors are the pressure drop and accessibility of the internal surface, which vary in opposite directions with changes in diameter. With poor thermal conductivity, severe temperature gradients or peaks arise with large pellets that may lead to poor control of the reaction and undesirable side reactions like coking.

• *Specific surface* of solid spheres of 0.1 mm (0.0039 in) dia is 0.06 m^2/ml (18,300 ft^2/ft^3) and a porous activated alumina pellet has about 600 m^2/ml (1.83×10^8 ft^2/ft^3). Other considerations aside, a large surface is desirable because the rate of reaction is proportional to the accessible surface. On the other hand, large specific surface means pores of small diameter.

• *Pore diameter and distribution* are important factors. Small pores limit the accessibility of internal surface because of increased resistance to diffusion of reactants inwards. Diffusion of products outwards also is slowed, and degradation of those products may result. When the catalyst is expensive, the inaccessible internal surface is a liability, and in every case it makes for a larger reactor size. A more or less uniform pore diameter is desirable, but this is practically realizable only with molecular sieves. Those pellets that are extrudates of compacted masses of smaller particles have bimodal pore size distributions, between the particles and inside them. Micropores have diameters of 10 to 100 Å, macropores of 1,000 to 10,000 Å. The macropores provide rapid mass transfer into the interstices that lead to the micropores where the reaction takes place.

• *Diffusivity and tortuosity* affect resistance to diffusion caused by collision with other molecules (bulk diffusion) or by collision with the walls of the pore (Knudsen diffusion). Actual diffusivity in common porous catalysts is intermediate between the two types. Measurements and correlations of diffusivities of both types are known. Diffusion is expressed per unit cross section and unit thickness of the pellet. Diffusion rate through the pellet then depends on the porosity ϑ and a tortuosity factor τ that accounts for increased resistance of crooked and varied-diameter pores. Effective diffusion coefficient is $D_{\text{eff}} = D_{\text{theo}}\vartheta/\tau$. Empirical porosities range from 0.3 to 0.7, tortuosities from 2 to 7. In the absence of other information, Satterfield (*Heterogeneous Catalysis in Practice,* McGraw-Hill, 1991) recommends taking $\vartheta = 0.5$ and $\tau = 4$. In this area, clearly, precision is not a feature.

Rate of Reaction Rate equations of fluid reactions catalyzed by solids are of two main types:

1. Power law type, based directly on the law of mass action, say,

$$r_a = kP_a^{\alpha}P_b^{\beta}P_c^{\gamma}P_d^{\delta} \ldots \tag{23-59}$$

with a term for every reactant or product. The exponents are empirical and may be positive or negative, integral or fractional.

2. Hyperbolic, based on the Langmuir adsorption principle; for instance,

$$r_a = \frac{k(P_aP_b - P_cP_d/K_e)}{(1 + k_aP_a + K_bP_b + K_cP_c + K_dP_d)^2} \tag{23-60}$$

The latter kind of formulation is described at length in Sec. 7. The assumed mechanism is comprised of adsorption and desorption rates of the several participants and of the reaction rates of adsorbed species. In order to minimize the complexity of the resulting rate equation, one of the several rates in series may be assumed controlling. With several controlling steps the rate equation usually is not explicit but can be used with some extra effort.

Two quite successful rate equations of catalytic industrial processes are cited by Rase (*Chemical Reactor Design for Process Plants,* vol. 2, Wiley, 1977):

1. For the synthesis of ammonia,

$$r_{NH_3} = k(P_{N_2}P_{H_2}P_{NH_3}^{-1.5} P_{NH_3}P_{H_2}^{-1.5}) \tag{23-61}$$

2. For the oxidation of sulfur dioxide,

$$r_{SO_2} = \frac{k_1P_{SO_2}}{(P_{SO_3}^{0.5} + k_2P_{SO_2})^2}\left(P_{O_2} - \frac{P_{SO_3}}{K_eP_{SO_2}}\right)^2 \tag{23-62}$$

The first is a power law type modified for reversibility, and the second is a modified hyperbolic.

The partial pressures in the rate equations are those in the vicinity of the catalyst surface. In the presence of diffusional resistance, in the steady state the rate of diffusion through the stagnant film equals the rate of chemical reaction. For the reaction $A + B \Rightarrow C + \ldots$, with rate of diffusion of A limited,

$$r = r_d = r_s = k_1(P_{ag} - P_{as}) = \frac{k_2P_{as}P_b}{(1 + K_aP_{as} + P_b + K_cP_c + \cdots)^2} \tag{23-63}$$

The unknown partial pressure at the external surface can be eliminated as $P_{as} = P_{ag} - r/k_1$), which results in a cubic equation for r.

Another complication arises when not all of the internal surface of a porous catalyst is accessed. Then a factor called the effectiveness η is applied, making the power law equation, for instance,

$$r = k\eta P_a^{\alpha}P_b^{\beta}P_c^{\gamma}P_d^{\delta} \tag{23-64}$$

The effectiveness is known from experiment for important industrial catalysts and is correlated, in general, in terms of pore characteristics, concentrations, and specific rate equations.

From a statistical viewpoint, there is often little to choose between power law and hyperbolic equations as representations of data over an experimental range. The fact, however, that a particular hyperbolic equation is based on some kind of possible mechanism may lead to a belief that such an equation may be extrapolated more safely outside the experimental range, although there may be no guarantee that the controlling mechanism will remain the same in the extrapolated region.

Effectiveness As a reactant diffuses into a pore, it undergoes a falling concentration gradient and a falling rate of reaction. The concentration depends on the radial position in the pores of a spherical pellet according to

$$\frac{d^2C}{dr^2} + \frac{2}{r}\frac{dC}{dr} = \frac{R_c}{D} \tag{23-65}$$

where R_C is the rate of reaction per unit volume; for a reaction of order n, $R_c = kC^n$. In terms of the normalized variables $f = C/C_s$ and $\rho = r/R$, and the Thiele modulus for a sphere,

$$\phi_s = R\sqrt{\frac{kC_s^{n-1}}{D}} \tag{23-66}$$

this becomes

$$\frac{d^2f}{d\rho^2} + \frac{2}{\rho}\frac{df}{d\rho} = \phi_s^2 f^n \tag{23-67}$$

At the inlet to the pore, $\rho = 1$ and $f = f_s$. At the center, $\rho = 0$ and $df/d\rho = 0$.

Although the point values of the rate diminish with ρ, in the steady state the rate of reaction equals the rate of diffusion at the mouth of the pores. The effectiveness of the catalyst is a ratio

$$\eta = \frac{r_{\text{actual}}}{r_{\text{ideal}}} = \frac{D(dC/dr)_{r=R}}{\frac{4\pi R^3}{3}kC_s^n} \tag{23-68}$$

where r_{actual} = rate of diffusion at the mouth of the pore
r_{ideal} = rate on the assumption that all of the pore surface is exposed to the concentration at the external surface
C_s = concentration at the external surface

Numerical and some analytical solutions of the diffusion/reaction equations are represented closely by an empirical curve/fit,

$$\eta = \frac{1.0357 + 0.3173\phi_m + 0.000427\phi_m^2}{1 + 0.4172\phi_m + 0.1390\phi_m^2} \tag{23-69}$$

where the modified Thiele modulus for an nth order reaction, $R_c = kC^n$ per unit volume, is

$$\phi_m = 3\left(\frac{V_p}{A_p}\right)\left(\frac{3}{n+1}\right)^{1/2}\left(\frac{kC_s^{n-1}}{D_{\text{eff}}}\right)^{1/2} \tag{23-70}$$

where V_p/A_p = (volume of pellet)/(external surface of pellet)
= $R/3$ for spheres of radius R
= L for a slab with one permeable face
= $R/2$ for a cylinder with sealed flat ends

The analytical result for a first-order reaction in a spherical pellet is:

$$\eta = \frac{3}{\phi^2}\left(\frac{\phi}{\tanh\phi} - 1\right), \qquad \phi = R\sqrt{\frac{k}{D_{\text{eff}}}} \tag{23-71}$$

The effectiveness of a given size of pellet can be found experimentally by running tests of reaction conversion with a series of diminishing sizes of pellets until a limiting rate is found. Then η will be the ratio of the rate with the pellet size in question to the limiting value.

Since theoretical calculation of effectiveness is based on a hardly realistic model of a system of equal-sized cylindrical pores and a shaky assumption for the tortuosity factor, in some industrially important cases the effectiveness has been measured directly. For ammonia synthesis by Dyson and Simon (*Ind. Eng. Chem. Fundam.*, **7,** 605 [1968]) and for SO_2 oxidation by Kadlec et al. (*Coll. Czech. Chem. Commun.*, **33,** 2388, 2526 [1968]).

When account is taken of the effectiveness, the rate of reaction becomes

$$R_c = k\eta C_s^n$$

where η depends on C_s except for first-order reactions.

Example 5: Application of Effectiveness For a second-order reaction in a plug flow reactor the Thiele modulus is $\phi = 8\sqrt{C_s}$, and inlet concentration is $C_{s0} = 1.0$. The equation will be integrated for 80 percent conversion with Simpson's rule. Values of η are

$$(C_s, \eta) = (1.0, 0.272), (0.6, 0.338), (0.2, 0.510)$$

The material balance and the integral become

$$-V'dC_s = k\eta C_s^2 dV_r$$

$$kV_r/V' = \int_{0.2}^{1.0}\left(\frac{1}{\eta C_s^2}\right)dC = \left(\frac{0.4}{3}\right)[3.68 + 4\,(8.22) + 49.02] = 11.4$$

Adiabatic Reactions Aside from the Thiele modulus, two other parameters are necessary in this case:

$$\beta = -\frac{\Delta H_r D C_s}{\lambda T_s}$$

$$\gamma = \frac{E}{RT_s}$$

where ΔH_r = heat of reaction
λ = thermal conductivity
E = energy of activation
R = gas constant, 1.987 cal/g mol

Figure 23-19 is one of several by Weisz and Hicks (*Chem. Eng. Sci.*, **17,** 263 [1962]). Although this predicts some very large values of η in some ranges of the parameters, these values are mostly not realized in practice, as Table 23-5 shows. The modified Lewis number is $Lw' = \lambda_s/\rho_s C_{ps} D_{\text{eff}}$.

Deactivation in Process The active surface of a catalyst can be degraded by chemical, thermal, or mechanical factors. Poisons and

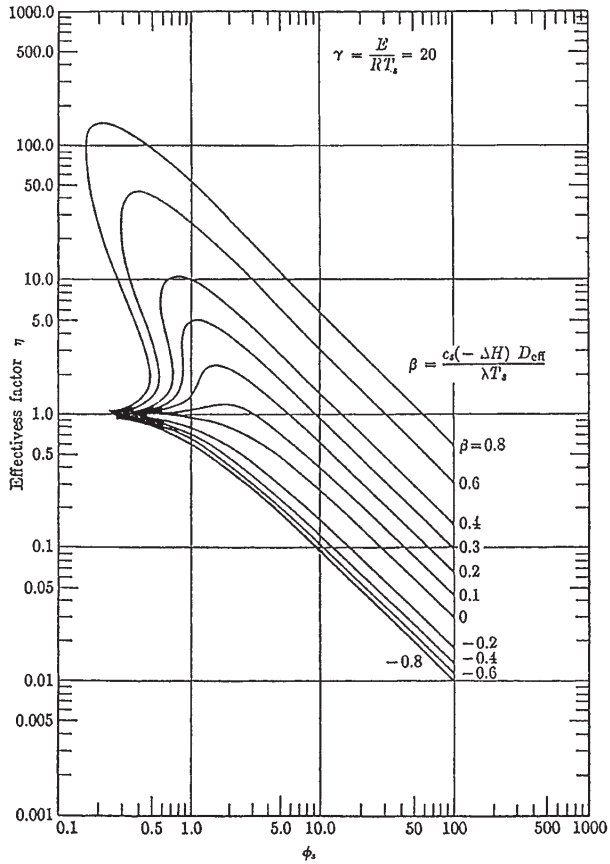

FIG. 23-19 Effectiveness of first-order reactions in spheres under adiabatic conditions (*Weisz and Hicks,* Chem. Eng. Sci., ***17,*** *265* [1962]).

TABLE 23-5 Parameters of Some Exothermic Catalytic Reactions

Reaction	β	γ	γβ	Lw'	ϕ
NH_3 synthesis	0.000061	29.4	0.0018	0.00026	1.2
Synthesis of higher alcohols from CO and H_2	0.00085	28.4	0.024	0.00020	—
Oxidation of CH_3OH to CH_2O	0.0109	16.0	0.175	0.0015	1.1
Synthesis of vinyl chloride from acetylene and HCl	0.25	6.5	1.65	0.1	0.27
Hydrogenation of ethylene	0.066	23–27	2.7–1	0.11	0.2–2.8
Oxidation of H_2	0.10	6.75–7.52	0.21–2.3	0.036	0.8–2.0
Oxidation of ethylene to ethylenoxide	0.13	13.4	1.76	0.065	0.08
Dissociation of N_2O	0.64	22.0	1.0–2.0	—	1–5
Hydrogenation of benzene	0.12	14–16	1.7–2.0	0.006	0.05–1.9
Oxidation of SO_2	0.012	14.8	0.175	0.0415	0.9

SOURCE: After Hlavacek, Kubicek, and Marek, *J. Catal.*, **15,** 17, 31 (1969).

inhibitors are known in specific cases. For instance, Thomas (*Catalytic Processes and Proven Catalysts,* Academic Press, 1970) often cites the poisons for the processes he describes. Potent poisons are compounds of P, S, As, Te, and Bi that have free electron pairs. In some cases a reduced life is simply accepted, as in the case of slow accumulation of trace metals from feed to catalytic cracking, but in other cases the deactivation is too rapid. Sulfur and water are removed from feed to ammonia synthesis, sulfur from the feed to platinum reforming, and arsenic from feed to SO_2 oxidation with platinum but not necessarily with vanadium. The catalyst also can be modified by additives; for instance, chromia to nickel to prevent sintering, rhenium to platinum to reduce coking, and so on. Reactivation sometimes is done in place; for instance, coke is burned off cracking catalyst or off nickel and nickel-molybdenum catalysts in a fluidized reactor/regenerator system. Platinum-alumina catalyst is regenerated in place by chlorine treatment. Much work has been done in this general field (Butt and Petersen, *Activation, Deactivation and Poisoning of Catalysts,* Academic Press, 1988). A list of 18 important industrial processes with catalyst lives and factors influencing them is in Delmon and Froment (*Catalyst Deactivation,* Elsevier, 1980). The lives range from a few days to several years.

Dependence of activity α may be simply on time onstream. One index is the ratio of the rate at time t to the rate with fresh catalyst,

$$\alpha = \frac{r_c \,@\, t}{r_c \,@\, t = 0} \tag{23-72}$$

The rate of destruction of active sites and pore structure can be expressed as a mass-transfer relation; for instance, as a second-order reaction

$$-\frac{d\alpha}{dt} = k_d \alpha^2 \tag{23-73}$$

and the corresponding integral

$$\alpha = \frac{1}{1 + k_d t} \tag{23-74}$$

The specific rate is expected to have an Arrhenius dependence on temperature. Deactivation by coke deposition in cracking processes apparently has this kind of correlation.

Assumption of a first-order rate law gives rise to

$$\alpha = \exp\,(k_1 - k_2 t) \tag{23-75}$$

Another relation that is sometimes successful is

$$\alpha = \frac{1}{1 + k_1 t^{k_2}} \tag{23-76}$$

When the feedstock contains constant proportions of reactive impurities, the rate of decline also may depend on the concentration of the main reactant, thus:

$$-\frac{d\alpha}{dt} = k_d\, \alpha^p\, C^q \tag{23-77}$$

Such a differential equation together with a rate equation for the main reactant constitutes a pair that must be solved simultaneously. Take the example of a CSTR for which the unsteady material balance is

$$C_0 = C + k\bar{t}\alpha C^q + \bar{t}\,\frac{dC}{dt} \tag{23-78}$$

With most values of the constants of these two equations a numerical solution will be needed.

The constants of the various time dependencies of activity are found by methods like those for finding constants of any rate equation, given suitable (α,t) data.

Uniform deactivation is one of the two limiting cases of the behavior of catalyst poisoning that are recognized. In one, the poison is distributed uniformly throughout the pellet and degrades it gradually. In the other, the poison is so effective that it kills completely as it enters the pore and is simultaneously removed from the stream. Complete deactivation begins at the mouth and moves gradually inward.

When uniform poisoning occurs the specific rate declines by a factor 1 − β where β is the fractional poisoning. Then a power law rate equation becomes

$$r_c = k_v(1 - \beta)\, \eta C_s^q \tag{23-79}$$

The effectiveness also depends on β through the Thiele modulus,

$$\phi = L\sqrt{\frac{k_v(1 - \beta)C_s^{q-1}}{D}} \tag{23-80}$$

To find the effectiveness under poisoned conditions, this form of the modulus is substituted into the appropriate relation for effectiveness. For first-order reaction in slab geometry, for instance,

$$\eta = \frac{1}{L}\sqrt{\frac{D}{k_v(1 - \beta)}}\,\tanh\left[L\sqrt{\frac{k_v(1 - \beta)}{D}}\right] \tag{23-81}$$

Pore mouth (*or shell*) *poisoning* occurs when the poisoning of a pore surface begins at the mouth and moves gradually inward. In this case the reactant must diffuse through the dead zone before it starts to react. β is the fraction of the pore that is deactivated, C_1 is the concentration at the end of the inactive region, and $x = (1 - \beta)L$ is the coordinate there.

The rate of diffusion into the pore equals the rate of diffusion through the dead zone,

$$D\left(\frac{dC}{dx}\right)_{x=(1-\beta)L} = D\,\frac{\Delta C}{\Delta x} = d\,\frac{C_s - C_1}{\beta L} \tag{23-82}$$

The concentration profile in a porous slab is represented by

$$\frac{d^2C}{dx^2} = \frac{k}{D}\,C^q \tag{23-83}$$

At a sealed face or at the center of a slab with two permeable faces, the condition is:

$$\left(\frac{dC}{dx}\right)_{x=0} = 0 \tag{23-84}$$

The three preceding equations may be solved simultaneously by the shooting method. A result for a first-order reaction is shown in Fig. 23-20, together with the case of uniform poisoning.

Distribution of Catalyst in Pores Because of the practical requirements of manufacturing, commercial impregnated catalysts usually have a higher concentration of active ingredient near the outside than near the tip of the pores. This may not be harmful, because it seems that effectiveness sometimes is better with some kind of nonuniform distribution of a given mass of catalyst. Such effects may be present in cases where the rate exhibits a maximum as a function of

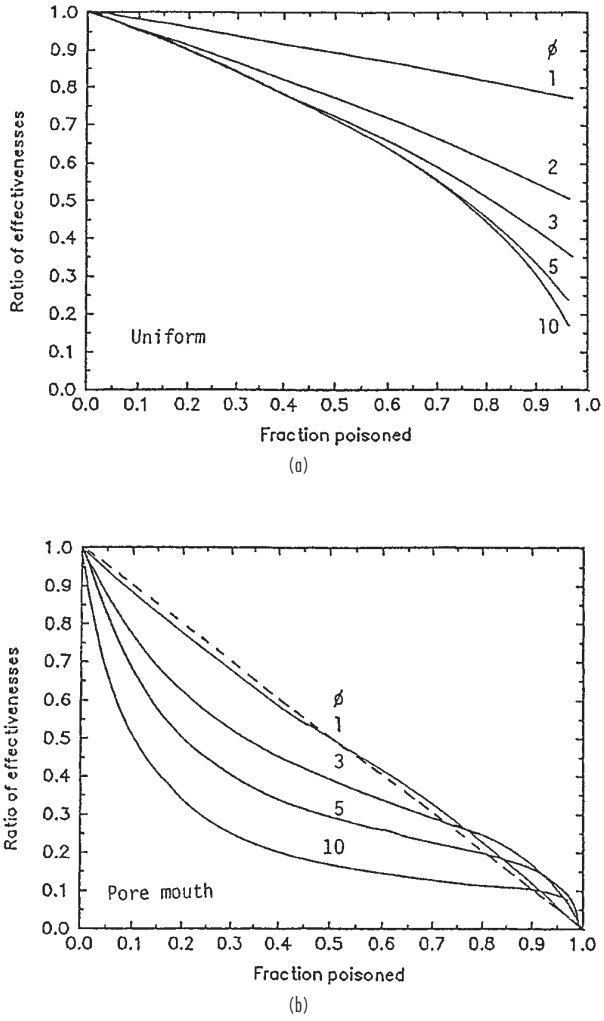

FIG. 23-20 Poisoning of a first-order reaction: (*a*) uniform poisoning, (*b*) pore mouth poisoning.

concentration of reactant, which is the case, for instance, with bimolecular Langmuir-Hinshelwood kinetics. Even under isothermal conditions, a catalyst's effectiveness can be several times unity at an optimum location of catalyst in the pore. Theoretical studies have recognized three zones: inner, middle, and outer (or egg yolk, egg white, and eggshell). Rather more theoretical studies have been made than experimental ones.

When a carrier is impregnated with a solution, where the catalyst deposits will depend on the rate of diffusion and the rate of adsorption on the carrier. Many studies have been made of Pt deposition from chloroplatinic acid (H_2PtCl_6) with a variety of acids and salts as coimpregnants. HCl results in uniform deposition of Pt. Citric or oxalic acid drive the Pt to the interior. HF coimpregnant produces an egg white profile. Photographs show such varied distributions in a single pellet.

Some studies of potential commercial significance have been made. For instance, deposition of catalyst some distance away from the pore mouth extends the catalyst's life when pore mouth deactivation occurs. Oxidation of CO in automobile exhausts is sensitive to the catalyst profile. For oxidation of propane the activity is eggshell > uniform > egg white. Nonuniform distributions have been found superior for hydrodemetallation of petroleum and hydrodesulfurization with molybdenum and cobalt sulfides. Whether any commercial processes with programmed pore distribution of catalysts are actually in use is not mentioned in the recent extensive review of Gavrillidis et al. (in Becker and Pereira, eds., *Computer-Aided Design of Catalysts,* Dekker, 1993, pp. 137–198), with the exception of monolithic automobile exhaust cleanup where the catalyst may be deposited some distance from the mouth of the pore and where perhaps a 25-percent longer life thereby may be attained.

Catalytic Membrane Reactors Membrane reactors combine reaction and separation in a single vessel. By removing one of the products of reaction, the membrane reactor can make conversion beyond thermodynamic equilibrium in the absence of separation.

For these studies, laboratory reactors have been of two main types: (1) a bed of catalyst pellets in series with a membrane, and (2) a membrane with catalyst deposited on the pore surface. Industrial membranes must be sturdy, temperature resistant, and affordable. Palladium alloys have high hydrogen permselectivity but are not commercially feasible because of their high cost. Microporous ceramic membranes in use thus far are able to separate gases only in accordance with the Knudsen diffusion law; that is, permeability is inversely proportional to the square root of the molecular weight. Efforts are being made for the development of membranes with molecular sieving properties, including zeolite, carbon, and polyphosphazene membranes.

Dehydrogenation processes in particular have been studied, with conversions in most cases well beyond thermodynamic equilibrium: Ethane to ethylene, propane to propylene, water-gas shift reaction $CO + H_2O \Leftrightarrow CO_2 + H_2$, ethylbenzene to styrene, cyclohexane to benzene, and others. Some hydrogenations and oxidations also show improvement in yields in the presence of catalytic membranes, although it is not obvious why the yields should be better since no separation is involved: hydrogenation of nitrobenzene to aniline, of cyclopentadiene to cyclopentene, of furfural to furfuryl alcohol, and so on; oxidation of ethylene to acetaldehyde, of methanol to formaldehyde, and so on.

At present, according to the review of Tsotsis et al. (in Becker and Pereira, eds., *Computer-Aided Design of Catalysts,* Dekker, 1993, pp. 471–551), there is no record of industrial implementation of reactors with catalytic membranes.

HOMOGENEOUS REACTIONS

Much of the basic theory of reaction kinetics presented in Sec. 7 of this Handbook deals with homogeneous reactions in batch and continuous equipment, and that material will not be repeated here. Material and energy balances and sizing procedures are developed for batch operations in ideal stirred tanks—during startup, continuation, and shutdown—and for continuous operation in ideal stirred tank batteries and plug flow tubulars and towers.

LIQUID PHASE

Batch reactions of single or miscible liquids are almost invariably done in stirred or pumparound tanks. The agitation is needed to mix multiple feeds at the start and to enhance heat exchange with cooling or heating media during the process.

Topics that acquire special importance on the industrial scale are the quality of mixing in tanks and the residence time distribution in vessels where plug flow may be the goal. The information about agitation in tanks described for gas/liquid and slurry reactions is largely applicable here. The relation between heat transfer and agitation also is discussed elsewhere in this Handbook. Residence time distribution is covered at length under "Reactor Efficiency." A special case is that of laminar and related flow distributions characteristic of non-Newtonian fluids, which often occurs in polymerization reactors.

Laminar Flow A mathematically simple deviation from uniform flow across a cross section is that of power law fluids whose linear velocity in a tube depends on the radial position $\beta = r/R$, according to the equation

$$u = \bar{u}\left(\frac{2n+1}{n+1}\right)(1-\beta^{(n+1)/n}) \tag{23-85}$$

where $\bar{u}$ is the average velocity. For normal fluids $n = 0$, for laminar ones $n = 1$, and other values apply to pseudoplastic and dilatant fluids. Along any particular radius, all molecules have the same residence time; that is, plug flow is achieved on that streamline. The average over the cross section is the value of primary interest.

For laminar flow, the velocity at the centerline is $u_0 = 2\bar{u}$. For a power law rate equation $r_c = kC^q$, the differential material balance on a streamline is

$$-u_0(1-\beta^2)dC = kC^q dL \tag{23-86}$$

when $q = 1$,

$$\frac{C}{C_0} = \exp(-kt) = \exp\left[\frac{kL}{u_0(1-\beta^2)}\right] \tag{23-87}$$

and when $q = 2$,

$$\frac{1}{C} - \frac{1}{C_0} = kt = \frac{kL}{u_0(1-\beta^2)} \tag{23-88}$$

The average concentration is found by integration over the cross section. After some algebraic manipulation, the result is

$$\frac{\bar{C}}{C_0} = 2t_0^2\int_{t_0}^{\infty} C\,\frac{dt}{t^3} \tag{23-89}$$

where $t_0 = 0.5\bar{t}$ is the residence time along the centerline and C is to be substituted from the previous equations. Figure 23-21 compares the performances of plug flow and laminar reactors of first- and second-order processes.

When it is deleterious, laminar flow can be avoided by mixing over the cross section. For this purpose static mixers in line can be provided. For very viscous materials and pastes, screws of the type used for pumping and extrusion are used as reactors.

Nonisothermal Operation Some degree of temperature control of a reaction may be necessary. Figures 23-1 and 23-2 show some of the ways that may be applicable to homogeneous liquids. More complex modes of temperature control employ internal surfaces, recycles, split flows, cold shots, and so on. Each of these, of course, requires an individual design effort.

Heat transfer through a vessel wall is often satisfactory:

1. In tubular reactors of only a few cm in diameter, the temperature is substantially uniform over the cross section so only an axial gradient occurs in the heat balance.
2. In towers with inert packing, both radial and axial gradients occur, although conduction in the axial direction often is neglected in view of the preponderant transfer of sensible enthalpy in a flow system.

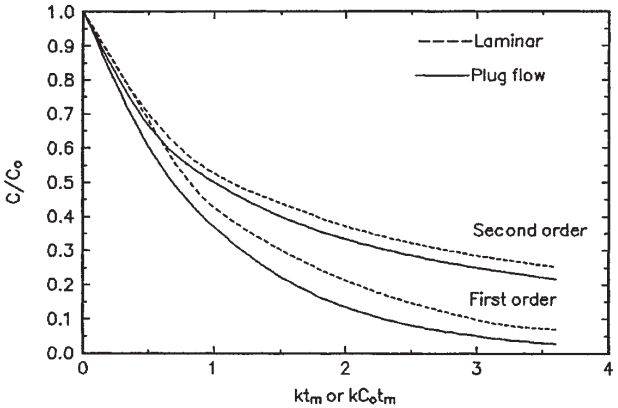

FIG. 23-21 Laminar compared with plug flow of first- and second-order reactions.

3. In an ideal CSTR, there are no gradients of temperature or composition, only the overall changes.

The simultaneous equations of heat and material balance and rate equations for these three cases are stated in several tables of Sec. 7.

The profiles of temperature and composition shown in Fig. 23-3 are not of homogeneous liquid reactions, but are perhaps representative of all kinds of reactions. Only in stirred tanks and some fluidized beds are nearly isothermal conditions practically attainable.

GAS PHASE

Although they are termed homogeneous, most industrial gas-phase reactions take place in contact with solids, either the vessel wall or particles as heat carriers or catalysts. With catalysts, mass diffusional resistances are present; with inert solids, the only complication is with heat transfer. A few of the reactions in Table 23-1 are gas-phase type, mostly catalytic. Usually a system of industrial interest is liquefied to take advantage of the higher rates of liquid reactions, or to utilize liquid homogeneous catalysts, or simply to keep equipment size down. In this section, some important noncatalytic gas reactions are described.

Mixing of feed gases and temperature control are major process requirements. Gases are usually mixed by injecting one of the streams from a high-speed nozzle into the rest of the gases, as in the flame reactor shown in Fig. 23-22*d*. Different modes of heat transfer are described, along with some processes that utilize each particular mode, following.

1. Heat is supplied from combustion gases through tubes in fired heaters. Olefins are made this way from light hydrocarbons and naphthas at 800°C (1472°F) and enough above atmospheric pressure to overcome friction. Superheated steam is injected to bring the final temperature up quickly and to retard carbon deposits. Contact times are 0.5 to 3.0 s, followed by rapid quenching. The total tube length of an industrial furnace may be more than 1,000 m. Other important gas-phase cracking processes are: Toluene ⇒ benzene, diphenyl ⇒ benzene, dicyclopentadiene ⇒ CPD, and butene-1 ⇒ butadiene. Figure 23-22*a* shows a cracking furnace.
2. Heat is transferred by direct contact with solids that have been preheated by combustion gases. The process is a cycle of alternate heating and reacting periods. The Wulf process for acetylene by pyrolysis of natural gas utilizes a heated brick checkerwork on a 4-min cycle of heating and reacting. The temperature play is 15°C (59°F), peak temperature is 1,200°C (2,192°F), residence time is 0.1 s of which 0.03 s is near the peak (Faith, Keyes, and Clark, *Industrial Chemicals*, vol. 27, Wiley, 1975).
3. The pebble heater recirculates refractory pebbles continuously through heating and reaction zones. The Wisconsin process for the fixation of nitrogen from air operates at 2,200°C (3,992°F), followed by extremely rapid quenching to freeze the small equilibrium content of nitrogen oxide that is made (Ermenc, *Chem. Eng. Prog.*, **52,** 149 [1956]). Such moving-bed units have been proposed for cracking to olefins but have been obsolesced like most moving-bed reactors.
4. The heat-carrying solids are particles of fluidized sand that circulate between the heating and reaction zones. The reaction section for light hydrocarbons is at 720 to 850°C (1,328 to 1,562°F), the regenerated sand returns at 50 to 100°C (122 to 212°F) above the reactor temperature. The heat comes mostly from the burning of carbon deposited on the sand. This equipment is perhaps competitively suited to cracking heavy stocks that coke readily.
5. Inert combustion gases are injected directly into the reacting stream in flame reactors. Figures 23-22*a* and 23-22*d* show two such devices used for making acetylene from light hydrocarbons and naphthas; Fig. 23-22*e* shows a temperature profile, reaction times in ms.
6. Burning a portion of a combustible reactant with a small additive of air or oxygen. Such oxidative pyrolysis of light hydrocarbons to acetylene is done in a special burner, at 0.001 to 0.01 s reaction time, peak at 1,400°C (2,552°F), followed by rapid quenching with oil or water.
7. Exothermic processes, with cooling through heat transfer surfaces or cold shots. In use are shell-and-tube reactors with small-diameter tubes, or towers with internal recirculation of gases, or multiple stages with intercooling. Chlorination of methane and other hydrocarbons results in a mixture of products whose relative amounts

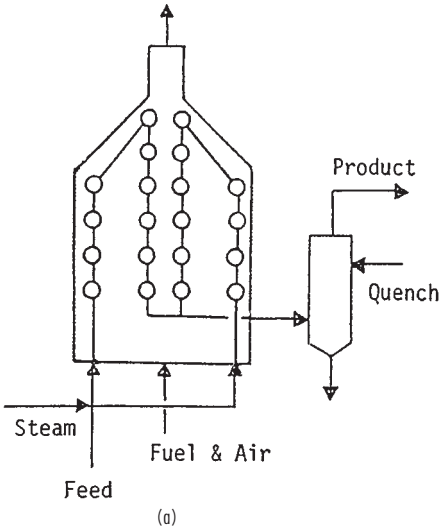

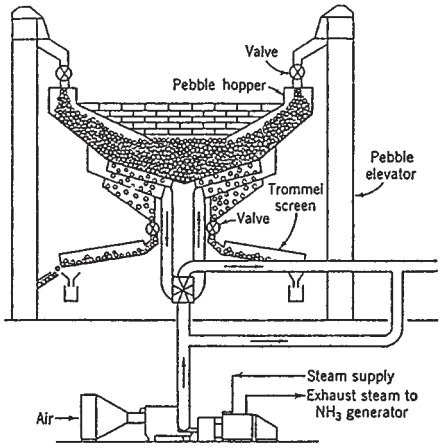

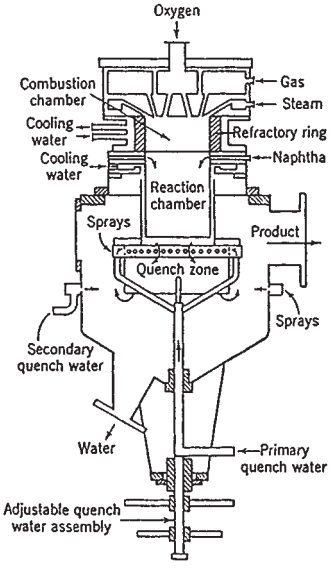

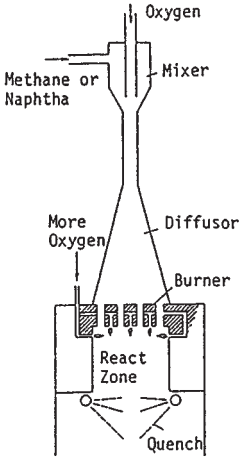

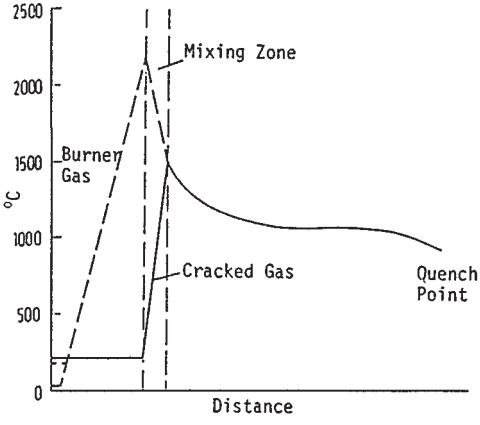

FIG. 23-22 Noncatalytic gas phase reactions. (*a*) Steam cracking of light hydrocarbons in a tubular fired heater. (*b*) Pebble heater for the fixation of nitrogen from air. (*c*) Flame reactor for the production of acetylene from hydrocarbon gases or naphthas (*Patton, Grubb, and Stephenson,* Pet. Ref. **37**(*11*), *180* [*1958*]). (*d*) Flame reactor for acetylene from light hydrocarbons (*BASF*). (*e*) Temperature profiles in a flame reactor for acetylene (Ullmann Encyclopadie der Technischen Chemie, *vol. 3, Verlag Chemie, 1973, p. 335*).

can be controlled by varying the Cl/HC ratio and recycling unwanted derivatives; for instance, recycling the mono and di derivatives when only the tri and tetra derivatives are of value, or keeping the chlorine ratio low when emphasizing the lower derivatives. Chlorination temperatures are normally kept in the range 230 to 400°C (446 to 752°F) to limit carbon formation, but may be raised to 500°C (932°F) when favoring CCl_4.

SUPERCRITICAL CONDITIONS

The critical properties of water are 374°C (705°F) and 218 atm (3,205 psi). Above this condition a heterogeneous mixture of water, organic compounds, and oxygen may become homogeneous. Then the rate of oxidation may be considerably accelerated because of (1) elimination of diffusional resistances, (2) increase of oxygen concentration by reason of greater density of the mixture, (3) enhanced solubility of oxygen and the organic compound, and (4) increase of the specific rate of reaction by pressure.

That the specific rate is affected by extremes of pressure—sometimes upward, sometimes downward—is well known. A review of this subject is by Kohnstam ("The Kinetic Effects of Pressure," in *Progress in Reaction Kinetics,* Pergamon, 1970). Three examples follow:

1. Thermal decomposition of Di-*t*-butyl peroxide in toluene at 120°C (248°F): 10^6k, 1/s, = 13.4 @ 1 atm (14.7 psi), = 5.7 @ 53 atm (779 psi)
2. Isomerization of cyclopropane at 491°C (916°F): 10^4k, 1/s, = 0.303 @ 0.067 atm (0.98 psi), = 1.30 @ 1.37 atm (20.1 psi), = 2.98 @ 84.1 atm (1,236 psi)
3. Fading of bromphenol blue at 25°C (77°F), 10^4k, L/m·s, = 9.3 @ 1 atm (14.7 psi), = 17.9 @ 1088 atm (16,000 psi)

Solubilities also may be changed greatly in the supercritical region. For naphthalene in ethylene at 35°C (95°F), the mol fraction of naphthalene goes from 0.004 @ 20 atm (294 psi) to 0.02 at 100 atm (1,470 psi) and 0.05 at 300 atm (4,410 psi).

High destructive efficiencies (above 99.99 percent) of complex organic compounds in water can be achieved with residence times under 5 min. Although there are some disagreements, the rate appears to be first order in the organic compound and first or zero order in oxygen.

Recent reviews of research in this area are: Bruno and Ely, eds., *Supercritical Fluid Technology,* CRC Press, 1991; Kiran and Brennecke, eds., *Supercritical Engineering Science,* ACS, 1992.

There is no mention in these reviews of any industrial implementation of supercritical kinetics. Two areas of interest are wastewater treatment—for instance, removal of phenol—and reduction of coking on catalysts by keeping heavy oil decomposition products in solution.

POLYMERIZATION

Polymers that form from the liquid phase may remain dissolved in the remaining monomer or solvent, or they may precipitate. Sometimes beads are formed and remain in suspension; sometimes emulsions form. In some processes solid polymers precipitate from a fluidized gas phase.

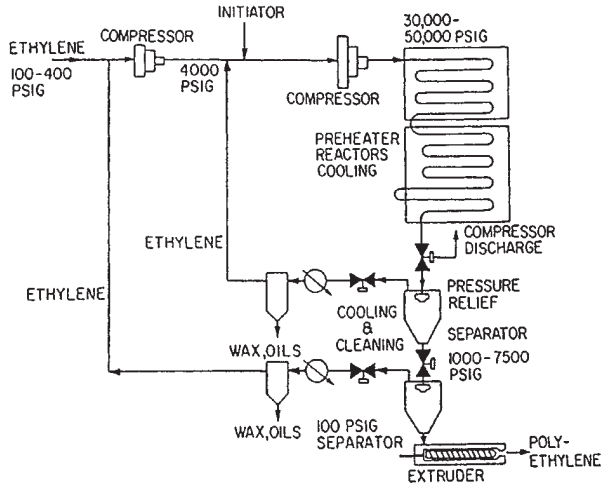

(a)

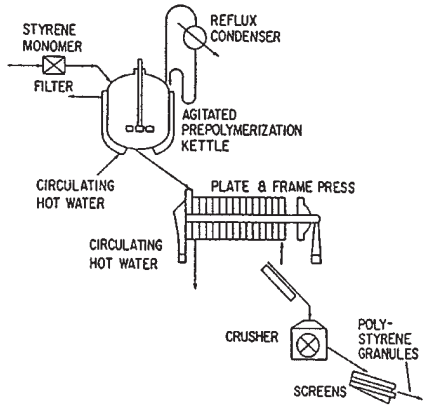

(b)

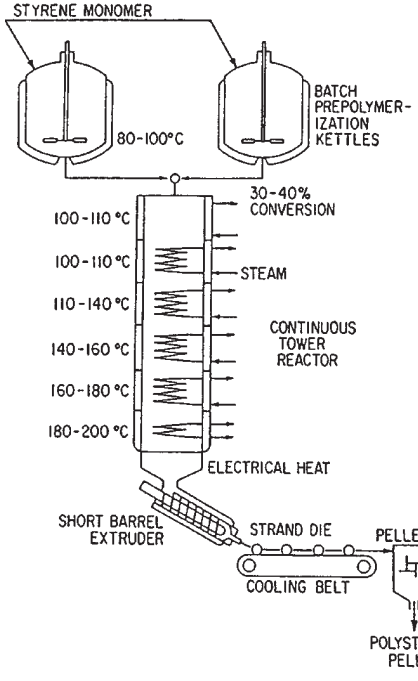

(c)

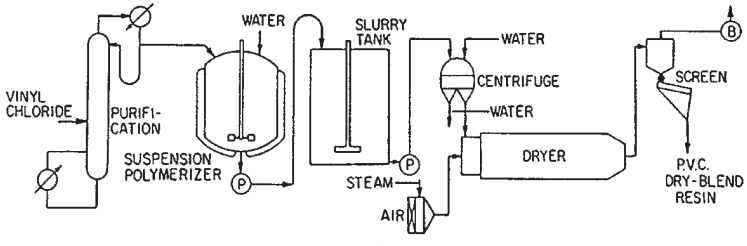

(d)

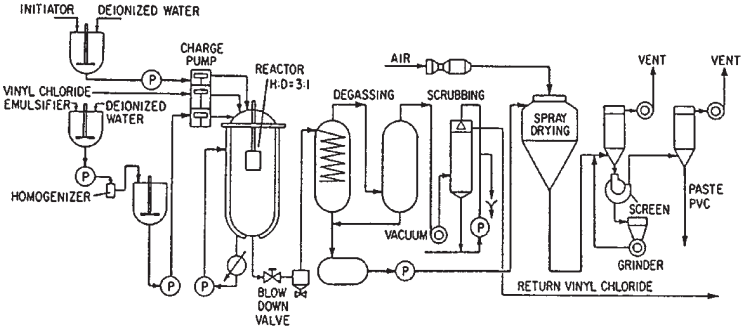

(e)

FIG. 23-23 Batch and continuous polymerizations. (*a*) Polyethylene in a tubular flow reactor, up to 2 km long by 6.4 cm ID. (*b*) Batch process for polystyrene. (*c*) Batch-continuous process for polystyrene. (*d*) Suspension (bead) process for polyvinylchloride. (*e*) Emulsion process for polyvinylchloride. (*Ray and Laurence, in Lapidus and Amundson,* eds., Chemical Reactor Theory Review, *Prentice-Hall, 1977.*)

Stirred batch and continuous reactors are widely used because of their flexibility, but a variety of reactor configurations are in use for particular cases. A selection may be made on rational grounds, or for historical reasons, or due simply to individual taste or a sense of proprietorship. For this complex area, in a given space, it is hardly possible to improve on the guide to selection of polymerization reactors by Gerrens (*German Chemical Engineering,* **4,** 1–13 [1981]; *ChemTech,* 380–383, 434–443 [1982]). Interested parties should go there. A general reference is Rodriguez (*Principles of Polymer Systems,* McGraw-Hill, 1989).

Polymerization processes are characterized by extremes. Industrial products are mixtures with molecular weights of 10^4 to 10^7. In a particular polymerization of styrene the viscosity increased by a factor of 10^6 as conversion went from 0 to 60 percent. The adiabatic reaction temperature for complete polymerization of ethylene is 1,800 K (3,240 R). Heat transfer coefficients in stirred tanks with high viscosities can be as low as 25 W/(m^2·°C) (16.2 Btu/[h·ft^2·°F]). Reaction times for butadiene-styrene rubbers are 8 to 12 h; polyethylene molecules continue to grow for 30 min; whereas ethyl acrylate in 20% emulsion reacts in less than 1 min, so monomer must be added gradually to keep the temperature within limits. Initiators of the chain reactions have concentration of 10^{-8} g mol/L so they are highly sensitive to poisons and impurities.

The physical properties of polymers depend largely on the molecular weight distribution, which can cover a wide range. Since it is impractical to fractionate the products and reformulate them into desirable ranges of molecular weights, immediate attainment of desired properties must be achieved through the correct choice of reactor type and operating conditions, notably of distributions of residence time and temperature. Those factors are influenced by high viscosities. In tubular reactors there are strong gradients in the radial direction. In stirred tanks ideal mixing is not attainable; wide variations in temperatures may result, and stagnant zones and bypassing may exist. Devices that counteract these unfavorable characteristics include inserts that cause radial mixing, scraping impellers, screw feeders, hollow-shaft impellers with coolant flow through them, recirculation through draft tubes, and so on. High viscosities of bulk and melt polymerizations are avoided with solution, bead, or emulsion operations. Then more nearly normal RTDs exist in CSTR batteries and tubular flow vessels.

KINDS OF POLYMERIZATION PROCESSES

Bulk Polymerization The monomer and initiators are reacted without or with mixing; without mixing to make useful shapes directly, like bakelite products. Because of viscosity limitations, stirred bulk polymerization is not carried to completion but only to 30 to 60 percent or so, with the remaining monomer stripped out and recycled. A variety of processes is in use for polystyrene, two of which are represented in Figs. 23-23*b* and 23-23*c*. A twin-screw extruder is used for polymerization of trioxane and of polyamide.

Bead Polymerization Bulk reaction proceeds in independent droplets of 10 to 1,000 μm diameter suspended in water or other medium and insulated from each other by some colloid. A typical suspending agent is polyvinyl alcohol dissolved in water. The polymerization can be done to high conversion. Temperature control is easy because of the moderating thermal effect of the water and its low viscosity. The suspensions sometimes are unstable and agitation may be critical. Only batch reactors appear to be in industrial use: polyvinyl acetate in methanol, copolymers of acrylates and methacrylates, polyacrylonitrile in aqueous $ZnCl_2$ solution, and others. Bead polymerization of styrene takes 8 to 12 h.

Emulsions Emulsions have particles of 0.05 to 5.0 μm diameter. The product is a stable latex, rather than a filterable suspension. Some latexes are usable directly, as in paints, or they may be coagulated by various means to produce massive polymers. Figures 23-23*d* and 23-23*e* show bead and emulsion processes for vinyl chloride. Continuous emulsion polymerization of butadiene-styrene rubber is done in a CSTR battery with a residence time of 8 to 12 h. Batch treating of emulsions also is widely used.

Solution Polymerization These processes may retain the polymer in solution or precipitate it. Polyethylene is made in a tubular flow reactor at supercritical conditions so the polymer stays in solution. In the Phillips process, however, after about 22 percent conversion when the desirable properties have been attained, the polymer is recovered and the monomer is flashed off and recyled (Fig. 23-23*a*). In another process, a solution of ethylene in a saturated hydrocarbon is passed over a chromia-alumina catalyst, then the solvent is separated and recyled. Another example of precipitation polymerization is the copolymerization of styrene and acrylonitrile in methanol. Also, an aqueous solution of acrylonitrile makes a precipitate of polyacrylonitrile on heating to 80°C (176°F).

A factor in addition to the RTD and temperature distribution that affects the molecular weight distribution (MWD) is the nature of the chemical reaction. If the period during which the molecule is growing is short compared with the residence time in the reactor, the MWD in a batch reactor is broader than in a CSTR. This situation holds for many free radical and ionic polymerization processes where the reaction intermediates are very short lived. In cases where the growth period is the same as the residence time in the reactor, the MWD is narrower in batch than in CSTR. Polymerizations that have no termination step—for instance, polycondensations—are of this type. This topic is treated by Denbigh (*J. Applied Chem.,* **1,** 227 [1951]).

FLUIDS AND SOLID CATALYSTS

In the design of reactors for fluids in the presence of granular catalysts, account must be taken of heat transfer, pressure drop and contacting of the phases, and, in many cases, of provision for periodic or continuous regeneration of deteriorated catalyst. Several different kinds of vessel configurations for continuous processing are in commercial use. Some reactors with solid catalysts are represented in Figs. 23-18 and 23-24.

Most solid catalytic processes employ fixed beds. Although fluidized beds have the merit of nearly uniform temperature and can be designed for continuous regeneration, they cost more and are more difficult to operate, require extensive provisions for dust recovery, and suffer from backmixing. Accordingly, they have been adopted on a large scale for only a few processes. Ways have been found in some instances to avoid the need for continuous regeneration. In the case of platinum reforming with fixed beds, for instance, a large recycle of hydrogen prevents coke deposition while a high temperature compensates for the retarding effect of hydrogen on this essentially dehydrogenating process.

SINGLE FIXED BEDS

These are used for adiabatic processing or when it is practical to embed heat-transfer surface in the bed. Usually, heat transfer is more effective with the catalyst inside small tubes than outside them. Hydrodesulfurization of petroleum fractions is one large-scale application of single-bed reactors.

During filling, the catalyst is distributed uniformly to avoid the possibility of channeling that could lead to poor heat transfer, poor conversion, and harm to the catalyst because of hot spots. During startup, sudden surges of flow may disturb the bed and are to be avoided. For instance, in a study of a hydrodesulfurizer by Murphree et al. (*Ind. Eng. Chem. Proc. Des. & Dev.,* **3,** 381 [1964]) the efficiency of conversion in a commercial size unit varied between 47 and 80 percent with different modes of loading and startup.

MULTIPLE FIXED BEDS

These enable temperature control with built-in exchangers between the beds or with pumparound exchangers. Converters for ammonia, SO_3, cumene, and other processes may employ as many as five or six beds in series. The Sohio process for vapor-phase oxidation of propylene to acrylic acid uses two beds of bismuth molybdate at 20 to 30 atm (294 to 441 psi) and 290 to 400°C (554 to 752°F). Oxidation of ethylene to ethylene oxide also is done in two stages with supported

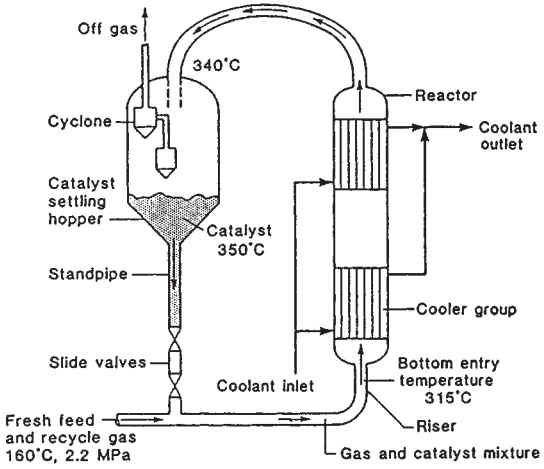

(a)

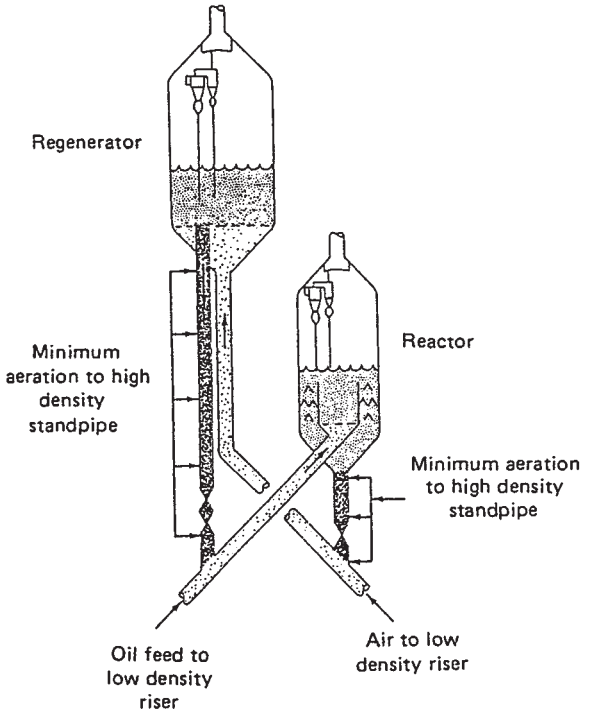

(b)

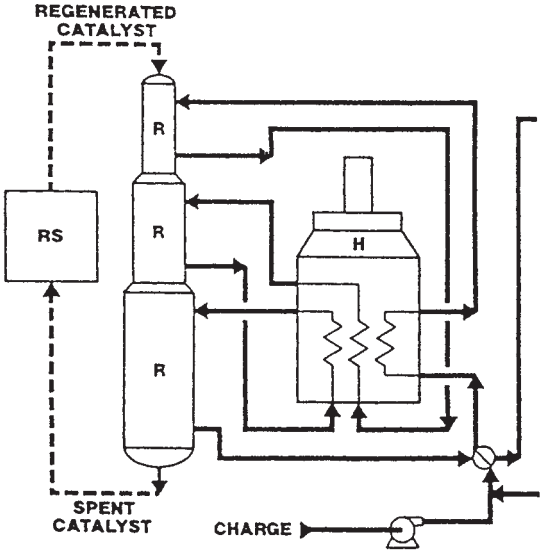

(c)

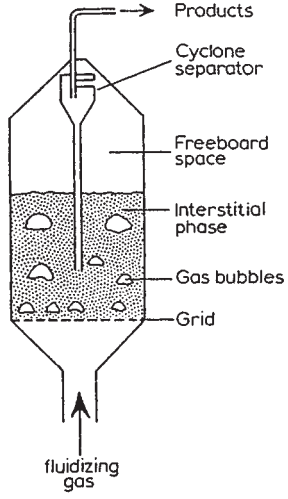

(d)

FIG. 23-24 Reactors with moving catalysts. (*a*) Transport fluidized type for the Sasol Fischer-Tropsch process, nonregenerating. (*b*) Esso type of stable fluidized bed reactor/regenerator for cracking petroleum oils. (*c*) UOP reformer with moving bed of platinum catalyst and continuous regeneration of a controlled quantity of catalyst. (*d*) Flow distribution in a fluidized bed; the catalyst rains through the bubbles.

silver catalyst, the first stage to 30 percent conversion, the second to 76 percent, with a total of 1.0 s contact time.

MULTITUBULAR REACTORS

These reactors are of shell-and-tube configuration and mostly have the catalyst in the tubes, although some ammonia converters have the catalyst on the shell side. Hundreds of tubes of a few cm diameter may be required. Their diameters may be approximately 8 times the diameters of the pellets and lengths limited by allowable pressure drop. Catalyst pellet sizes usually are in the range of 0.3 to 0.5 cm (0.76 to 1.27 in). Uniform loading is ensured by using special equipment that charges the same amount of catalyst to each tube at a definite rate. After filling, each tube is checked for pressure drop.

Maleic anhydride is made by oxidation of benzene with air above 350°C (662°F) with V-Mo catalyst in a multitubular reactor with 2-cm tubes. The heat-transfer medium is a eutectic of molten salt at 375°C (707°F). Even with small tubes, the heat transfer is so limited that a peak temperature 100°C (212°F) above the shell side is developed and moves along the tubes.

Butanol by the hydrogenation of crotonaldehyde is made in a reactor with 4,000 tubes, 28 mm (0.029 ft) ID by 10.7 m (35.1 ft) long (Berty, in Leach, ed., *Applied Industrial Catalysis,* vol. 1, Academic Press, 1983, p. 51).

Vinyl acetate is made from ethylene, oxygen, and acetic acid in the vapor phase at 150 to 175°C (302 to 347°F) with supported Pd catalyst in packed tubes, 25 mm (0.082 ft) ID.

Vinyl chloride is made from ethylene and chlorine with Cu and K chlorides. The Stauffer process employs 3 multitubular reactors in series with 25 mm (0.082 ft) ID tubes (Naworski and Velez, in Leach, ed., *Applied Industrial Catalysis,* vol. 1, Academic Press, 1983, p. 251).

SLURRY REACTORS

These reactors for liquids and liquids plus gases employ small particles in the range of 0.05 to 1.0 mm (0.0020 to 0.039 in), the minimum size limited by filterability. Small diameters are used to provide as large an interface as possible since the internal surface of porous pellets is poorly accessible to the liquid phase. Solids concentrations up to 10 percent by volume can be handled. In hydrogenation of oils with Ni catalyst, however, the solids content is about 0.5 percent, and in the manufacture of hydroxylamine phosphate with Pd-C it is 0.05 percent. Fischer-Tropsch slurry reactors have been tested with concentrations of 10 to 950 g catalyst/L (0.624 to 59.3 lbm/ft^3) (Satterfield and Huff, *Chem. Eng. Sci.,* **35,** 195 [1980]).

Advantages of slurry reactors are high heat capacity, which makes for good temperature stability, and good heat transfer. Catalyst activity can be maintained by partial removal of degraded material and replenishment during operation. Disadvantages are a lower conversion for a given size because of essentially complete backmixing, power for agitation to keep the catalyst in suspension and to enhance heat transfer, and separation of entrained catalyst from the product.

Most industrial processes with slurry reactors are used for gases with liquids, such as chlorination, hydrogenation, and oxidation.

Liquid benzene is chlorinated in the presence of metallic iron turnings or Raschig rings at 40 to 60°C (104 to 140°F). Carbon tetrachloride is made from CS_2 by bubbling chlorine into it in the presence of iron powder at 30°C (86°F).

Substances that have been hydrogenated in slurry reactors include: nitrobenzene with Pd-C, butynediol with Pd-$CaCO_3$, chlorobenzene with Pt-C, toluene with Raney Ni, and acetone with Raney Ni.

Some oxidations in slurry reactors include: cumene with metal oxides, cyclohexene with metal oxides, phenol with CuO, and *n*-propanol with Pt.

TRANSPORT (OR ENTRAINMENT) REACTORS

The fluid and catalyst travel through the vessel in essentially plug flow and are separated downstream by settling and with cyclones and filters. The main publicized applications are for cracking to gasoline-range hydrocarbons with highly active zeolite catalysts and in the Sasol Fischer-Tropsch process. A considerable body of experience with transport of solids by entrainment with gases (pneumatic conveying) and with pneumatic drying has been accumulated; nevertheless, five years elapsed before the Sasol reactor was made to function satisfactorily. A principal advantage of transport reactors is that they approach plug flow, whereas stable fluidized beds have much backmixing. Figure 23-24*a* shows an in-line heat exchanger in the Sasol unit. The catalyst is promoted iron. It circulates through the 1.0-m (3.28-ft) ID riser at 72,600 kg/h (160,000 lbm/h) at 340°C (644°F) and 23 atm (338 psi) and has a life of about 50 days.

FLUIDIZED BEDS

Particle sizes in fluidized bed applications average below 0.1 mm, but very small particles impose severe restrictions on the recovery of entrained material. The original reactor of this type was the Winkler coal gasifier (patented 1922), followed in 1940 by the Esso cracker, several hundred of which have been operated; they are now being replaced by riser reactors with zeolite catalysts. The other large application is combustion of solid fuels, for which some 30 installations are listed in *Encyclopedia of Chemical Technology,* vol. 10, Wiley, 1980, p. 550). A list of 55 other applications with references is in the same source. It is not clear how many of these are successful because many processes were tried with enthusiasm for the new technology and found wanting.

Advantages of fluidized beds are temperature uniformity, good heat transfer, and transportability of rapidly decaying catalyst between reacting and regenerating sections. Disadvantages are attrition, recovery of fines, and backmixing. Baffles have been used to reduce backmixing.

Phthalic anhydride is made by oxidation of naphthalene at temperatures of 340 to 380°C (644 to 716°F) controlled by heat exchangers immersed in the bed. At these temperatures the catalyst is stable and need not be regenerated. The excellence of temperature control was a major factor for the adoption of this process, but it was obsolesced by 1972.

Acrylonitrile, on the other hand, is still being made from propylene, ammonia, and oxygen at 400 to 510°C (752 to 950°F) in this kind of equipment. The good temperature control with embedded heat exchangers permits catalyst life of several years.

Another process where good temperature control is essential is the synthesis of vinyl chloride by chlorination of ethylene at 200 to 300°C (392 to 572°F), 2 to 10 atm (29.4 to 147 psi), with supported cupric chloride, but a process with multitubular fixed beds is a strong competitor.

Although it is not a catalytic process, the roasting of iron sulfide in fluidized beds at 650 to 1,100°C (1,202 to 2,012°F) is analogous. The pellets are 10-mm (0.39-in) diameter. There are numerous plants, but they are threatened with obsolescence because cheaper sources of sulfur are available for making sulfuric acid.

MOVING BEDS

The catalyst, in the form of large granules, circulates by gravity and gas lift between reaction and regeneration zones. The first successful operation was the Houdry cracker that replaced a plant with fixed beds that operated on a 10-min cycle between reaction and regeneration. It was soon obsolesced by FCC units. The only currently publicized moving bed process is a UOP platinum reformer (Fig. 23-24*c*) that regenerates a controlled quantity of catalyst on a continuous basis. It is not known how competitive this process is with units having multiple reactors that regenerate in place or operate at such low severity that catalyst life of several years is obtained.

THIN BEDS AND WIRE GAUZES

Fast catalytic reactions that must be quenched rapidly are done in contact with wire screens or thin layers of fine granules. Ammonia in a 10% concentration in air is oxidized by flow through a fine gauze catalyst made of 2 to 10% Rh in Pt, 10 to 30 layers, 0.075-mm (0.0030-in) diameter wire. Contact time is 0.0003 s at 750°C (1,382°F) and 7 atm (103 psi) followed by rapid quenching. Methanol is oxidized to formaldehyde in a thin layer of finely divided silver or a multilayer screen, with a contact time of 0.01 s at 450 to 600°C (842 to 1,112°F).

GAS/LIQUID REACTIONS

Industrial gas/liquid reaction processes are of four main categories:

1. Gas purification or the removal of relatively small amounts of impurities such as CO_2, CO, COS, SO_2, H_2S, NO, and others from air, natural gas, hydrogen for ammonia synthesis, and others
2. Liquid phase processes, such as hydrogenation, halogenation, oxidation, nitration, alkylation, and so on
3. Manufacture of pure products, such as sulfuric acid, nitric acid, nitrates, phosphates, adipic acid, and so on
4. Biochemical processes, such as fermentation, oxidation of sludges, production of proteins, biochemical oxidations, and so on

Reaction between an absorbed solute and a reagent reduces the equilibrium partial pressure of the solute, thus increasing the rate of mass transfer. The mass-transfer coefficient likewise is enhanced, which contributes further to increased absorption rates. Extensive theoretical analyses of these effects have been made, but rather less experimental work and design guidelines.

For reaction between a gas and a liquid, three modes of contacting are possible: (1) the gas is dispersed as bubbles in the liquid, (2) the liquid is dispersed as droplets in the gas, and (3) the liquid and gas are brought together as thin films over a packing or wall. The choice between these modes is an important problem. Some considerations are the magnitude and distribution of the residence times of the phases, the power requirements, the scale of the operation, the opportunity for heat transfer, and so on. Industrial equipment featuring particular factors is available. The main types of apparatus appear in Fig. 23-25, but many variations are practiced. Specific liquid/gas processes are represented in Fig. 23-26. Equipment is selected and designed by a combination of theory, pilot plant work, and experience, with rather less reliance on theory than in some other areas of reactor design.

MASS TRANSFER COEFFICIENTS

The resistance to transfer of mass between a gas and a liquid is assumed confined to that of fluid films between the phases. Let

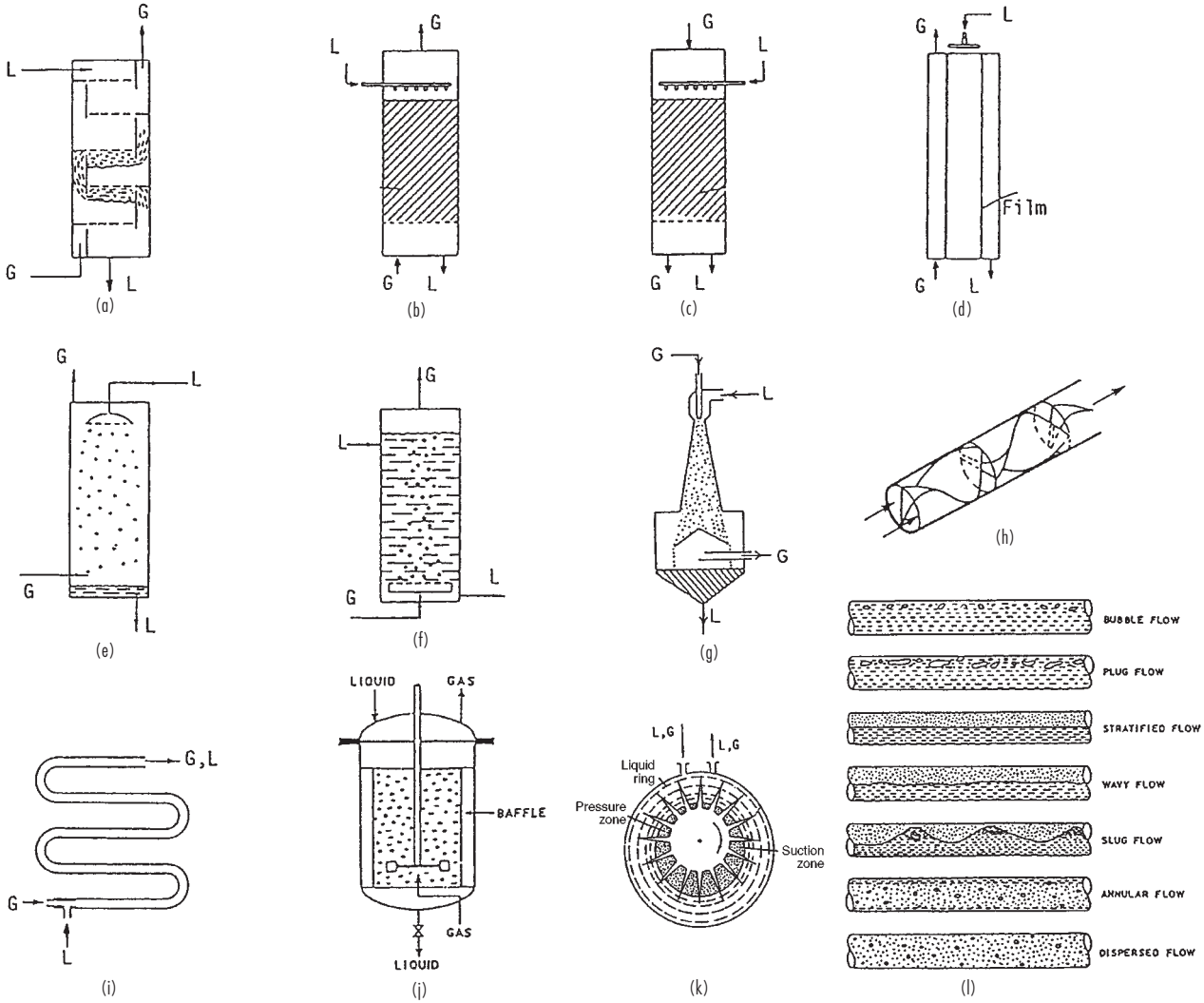

FIG. 23-25 Types of industrial gas/liquid reactors. (*a*) Tray tower. (*b*) Packed, counter current. (*c*) Packed, parallel current. (*d*) Falling liquid film. (*e*) Spray tower. (*f*) Bubble tower. (*g*) Venturi mixer. (*h*) Static in line mixer. (*i*) Tubular flow. (*j*) Stirred tank. (*k*) Centrifugal pump. (*l*) Two-phase flow in horizontal tubes.

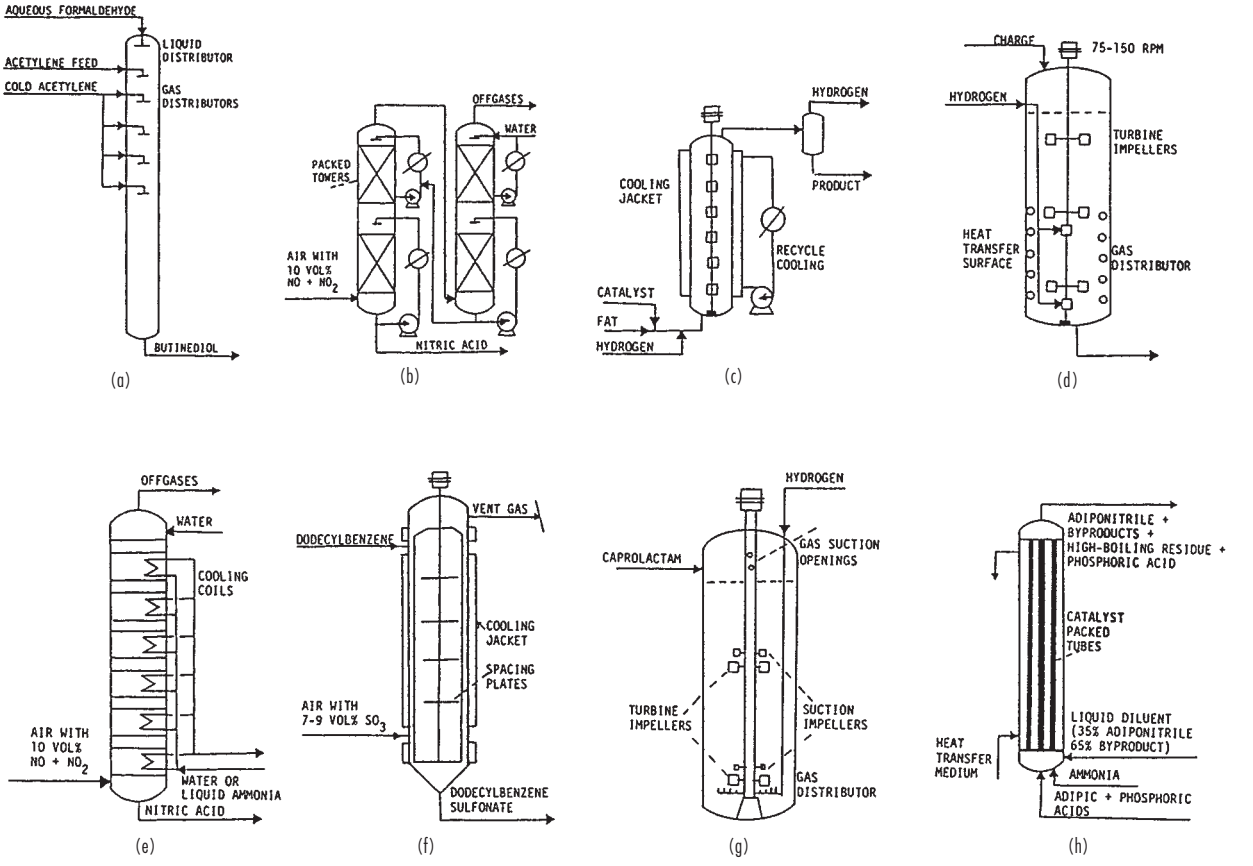

FIG. 23-26 Examples of reactors for specific liquid/gas processes. (*a*) Trickle reactor for synthesis of butinediol, 1.5 m diameter by 18 m high. (*b*) Nitrogen oxide absorption in packed columns. (*c*) Continuous hydrogenation of fats. (*d*) Stirred tank reactor for batch hydrogenation of fats. (*e*) Nitrogen oxide absorption in a plate column. (*f*) A thin-film reactor for making dodecylbenzene sulfonate with SO_3. (*g*) Stirred tank reactor for the hydrogenation of caprolactam. (*h*) Tubular reactor for making adiponitrile from adipic acid in the presence of phosphoric acid.

D = diffusivity

$p_i = f(C_i)$ or $p_i = HC_i$, equilibrium relation at the interface

a = interfacial area/unit volume

z_g, z_L = film thicknesses

The steady rates of solute transfer are

$$r = k_g a(p_g - p_i)$$
$$= k_L a(C_i - C_L)$$

where

$$k_g = \frac{D}{z_g}$$

$$k_L = \frac{D}{z_L}$$

are the mass-transfer coefficients of the individual films. Overall coefficients are defined by

$$r = K_g a(p_g - p_L) = K_L a(C_g - C_L)$$

Upon introducing the equilibrium relation $p = HC$, the relation between the various mass-transfer coefficients is

$$\frac{1}{K_g a} = \frac{H}{K_L a} = \frac{1}{k_g a} + \frac{H}{k_L a} \qquad (23\text{-}90)$$

When the solubility is low, H is large and $k_L \Rightarrow K_L$; when the solubility is high, H is small and $k_g \Rightarrow K_g$.

For purely physical absorption, the mass-transfer coefficients depend on the hydrodynamics and the physical properties of the phases. Many correlations exist; for example, that of Dwivedi and Upadhyay (*Ind. Eng. Chem. Proc. Des. & Dev.*, **16,** 157 [1977]),

$$k = \frac{u'}{\mathrm{Sc}^{2/3}}\left(\frac{0.765}{\mathrm{Re}^{0.82}} + \frac{0.365}{\mathrm{Re}^{0.386}}\right) \qquad (23\text{-}91)$$

where $\mathrm{Re} = \rho u' d_p/\mu$.

With a reactive solvent, the mass-transfer coefficient may be enhanced by a factor E so that, for instance, K_g is replaced by EK_g. Like specific rates of ordinary chemical reactions, such enhancements must be found experimentally. There are no generalized correlations. Some calculations have been made for idealized situations, such as complete reaction in the liquid film. Tables 23-6 and 23-7 show a few spot data. On that basis, a tower for absorption of SO_2 with NaOH is smaller than that with pure water by a factor of roughly 0.317/7.0 = 0.045. Table 23-8 lists the main factors that are needed for mathematical representation of $K_g a$ in a typical case of the absorption of CO_2 by aqueous monethanolamine. Figure 23-27 shows some of the complex behaviors of equilibria and mass-transfer coefficients for the absorption of CO_2 in solutions of potassium carbonate. Other than Henry's law, $p = HC$, which holds for some fairly dilute solutions, there is no general form of equilibrium relation. A typically complex equation is that for CO_2 in contact with sodium carbonate solutions (Harte, Baker, and Purcell, *Ind. Eng. Chem.*, **25,** 528 [1933]), which is

$$p_{CO_2} = \frac{137 f^2 N^{1.29}}{S(1-f)(365 - T)}, \qquad \text{Torr} \qquad (23\text{-}92)$$

TABLE 23-6 Typical Values of K_Ga for Absorption in Towers Packed with 1.5-in Intalox Saddles at 25% Completion of Reaction*

Absorbed gas	Absorbent	K_Ga, lb mol/(h·ft³·atm)
Cl_2	H_2O·NaOH	20.0
HCl	H_2O	16.0
NH_3	H_2O	13.0
H_2S	H_2O·MEA	8.0
SO_2	H_2O·NaOH	7.0
H_2S	H_2O·DEA	5.0
CO_2	H_2O·KOH	3.10
CO_2	H_2O·MEA	2.50
CO_2	H_2O·NaOH	2.25
H_2S	H_2O	0.400
SO_2	H_2O	0.317
Cl_2	H_2O	0.138
CO_2	H_2O	0.072
O_2	H_2O	0.0072

*To convert in to cm, multiply by 2.54; lb mol/(h·ft³·atm) to kg mol/(h·m³·kPa), multiply by 0.1581.

SOURCE: From Eckert, et al., *Ind. Eng. Chem.*, **59**, 41 (1967).

TABLE 23-7 Selected Absorption Coefficients for CO_2 in Various Solvents in Towers Packed with Raschig Rings*

Solvent	K_ga, lb mol/(h·ft³·atm)
Water	0.05
1-*N* sodium carbonate, 20% Na as bicarbonate	0.03
3-*N* diethanolamine, 50% converted to carbonate	0.4
2-*N* sodium hydroxide, 15% Na as carbonate	2.3
2-*N* potassium hydroxide, 15% K as carbonate	3.8
Hypothetical perfect solvent having no liquid-phase resistance and having infinite chemical reactivity	24.0

*Basis: L = 2,500 lb/(h·ft²); G = 300 lb/(h·ft²); T = 77°F; pressure, 1.0 atm. To convert lb mol/(h·ft³·atm) to kg mol/(h·m³·kPa) multiply by 0.1581.

SOURCE: From Sherwood, Pigford, and Wilke, *Mass Transfer*, McGraw-Hill, 1975, p. 305.

TABLE 23-8 Correlation of K_Ga for Absorption of CO_2 by Aqueous Solutions of Monoethanolamine in Packed Towers*

$$K_Ga = F\left(\frac{L}{\mu}\right)^{2/3}[1 + 5.7(C_e - C)M\, e^{0.0067T - 3.4p}]$$

where K_Ga = overall gas-film coefficient, lb mol/(h·ft³·atm)
μ = viscosity, centipoises
C = concentration of CO_2 in the solution, mol/mol monoethanolamine
M = amine concentration of solution (molarity, g mol/L)
T = temperature, °F
p = partial pressure, atm
L = liquid-flow rate, lb/(h·ft²)
C_e = equilibrium concentration of CO_2 in solution, mol/mol monoethanolamine
F = factor to correct for size and type of packing

Packing	F	Basis for calculation of F
5- to 6-mm glass rings	7.1×10^{-3}	Shneerson and Leibush data, 1-in column, atmospheric pressure
⅜-in ceramic rings	3.0×10^{-3}	Unpublished data for 4-in column, atmospheric pressure
¾- by 2-in polyethylene Tellerettes	3.0×10^{-3}	Teller and Ford data, 8-in column, atmospheric pressure
1-in steel rings		
1-in ceramic saddles	2.1×10^{-3}	
1½- and 2-in ceramic rings	$0.4–0.6 \times 10^{-3}$	Gregory and Scharmann and unpublished data for two commercial plants, pressures 30 to 300 psig

*To convert in to cm multiply by 2.54.

SOURCE: From Kohl and Riesenfeld, *Gas Purification*, Gulf, 1985.

where f = fraction of total base present as bicarbonate
N = normality, 0.5 to 2.0
S = solubility of CO_2 in pure water at 1 atm, g mol/L
T = temperature, 65 to 150°F

COUNTERCURRENT ABSORPTION TOWERS

Consider mass transfer in a countercurrent tower, packed or spray or bubble. Let

$$G_m = \frac{\text{mol inert gas}}{(\text{unit time})(\text{unit cross section})}$$

$$L_m = \frac{\text{mol solute-free liquid}}{(\text{unit time})(\text{unit cross section})}$$

$$Y = \frac{y}{(1-y)} = \frac{\text{mol solute, gas phase}}{\text{mol inert gas, vapor phase}}$$

$$X = \frac{x}{(1-x)} = \frac{\text{mol solute in the liquid}}{\text{mol inert solvent in the liquid}}$$

Z = height of active tower section.

The material balance over a differential height is

$$G_m dY = L_m dX$$

In terms of gas film conditions,

$$G_m dY = k_g a(p_g - p_i)dZ$$

The partial pressure of the gas is related to the total pressure π by

$$p_g = y\pi = \frac{Y}{1+Y}\pi, \qquad p_i = \frac{Y_i}{1+Y_i}\pi$$

Substitution and rearrangement leads to the equation for the tower height,

$$Z = \frac{G_m}{\pi}\int_{Y_2}^{Y_1} \frac{(1+Y)(1+Y_i)}{k_g a(Y - Y_i)}\, dY \qquad (23\text{-}93)$$

Similarly, in terms of the liquid-phase condition,

$$C = \frac{X}{1+X}C_t$$

$$C_t = \frac{\text{mol (solute + solvent)}}{\text{volume of liquid}}$$

$$L_m dX = k_L a(C_i - C)dZ$$

$$Z = \frac{L_m}{C_t}\int_{x_2}^{x_1} \frac{(1+X)(1+X_i)}{k_L a(X_i - X)}\, dX \qquad (23\text{-}94)$$

The balance around one end of the tower can be written:

$$X = X_1 + \frac{G_m}{L_m}(Y - Y_1) \qquad (23\text{-}95)$$

If the equilibrium relation is

$$y_i = mx \qquad \text{or} \qquad \frac{Y_i}{1+Y_i} = m\frac{X}{1+X} \qquad (23\text{-}96)$$

or any other functional form, substitution of Eqs. (23-95) and (23-96) into (23-93) will enable the last equation to be solved numerically. Graphical methods of solution are explained in the chapter on physical absorption.

For physical absorption, values of the mass-transfer coefficients may not vary greatly, so a mean value could be adequate and could be taken outside the integral sign, but for reactive absorption the variation usually is too great.

Note that the tower height is inversely proportional to the enhanced mass-transfer coefficient, or to the enhancement factor itself.

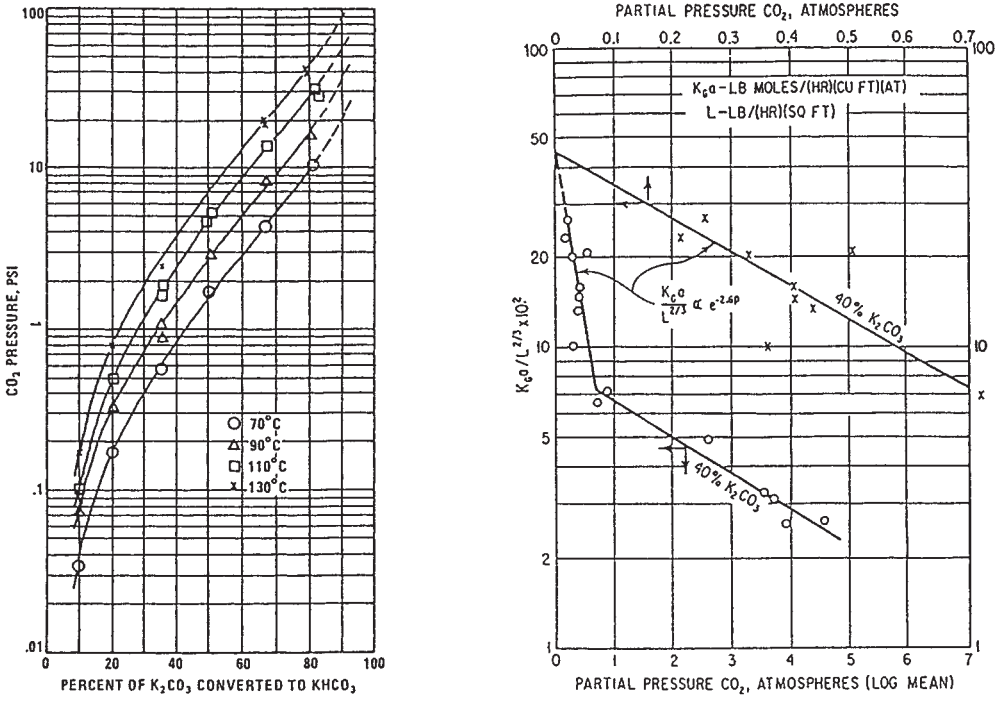

FIG. 23-27 CO_2 in potassium carbonate solutions: (*a*) equilibrium in 20% solution, (*b*) mass-transfer coefficients in 40% solutions. (*Data cited by Kohl and Riesenfeld,* Gas Purification, *Gulf Publishing, 1985.*)

FIRST-ORDER OR PSEUDO-FIRST-ORDER REACTION IN A LIQUID FILM

A reactant A diffuses into a stagnant liquid film where the concentration of excess reactant B remains essentially constant at C_{b0}. At the inlet face the concentration is C_{ai}. Making the material balance over a differential dz of the distance leads to the second-order diffusional equation,

$$\frac{d^2C_a}{dz^2} = \frac{k_c C_{b0}}{D} C_a = \alpha^2 C_a$$

The boundary conditions are $C_a = C_{ai}$ where $z = 0$, and $C_a = C_{aL}$ where $z = z_L$. The integral is

$$C_a = \frac{C_{aL} \sinh(\alpha z) + C_{ai} \sinh[\alpha(z_L - z)]}{\sinh(\alpha z_L)}$$

Since this is a steady condition, the rate of reaction in the film equals the rate of input to the film,

$$r = -D\left(\frac{dC_a}{dz}\right)_{C_a = C_{ai}} = \frac{\alpha D[\cosh(\alpha z_L) + C_{aL}]}{\sinh(\alpha z_L)} \qquad (23\text{-}97)$$

An important special case is that of complete reaction in the film; that is, for $C_{aL} = 0$ where $z = z_L$. Then,

$$r = \alpha D \coth(\alpha z_L)(C_{ai} - 0)$$
$$= \alpha z_L \left(\frac{D}{z_L}\right) \coth(\alpha z_L)(C_{ai} - 0)$$
$$= k_L \beta \coth(\beta)\, \Delta C_a = k_L E\, \Delta C_a \qquad (23\text{-}98)$$

where the enhancement factor is

$$E = \beta \coth(\beta)$$

and a parameter called the *Hatta number* is

$$\beta = \alpha z_L = z_L \sqrt{\frac{k_c C_{b0}}{D}} = \frac{\sqrt{k_c D C_{b0}}}{k_L} \qquad (23\text{-}99)$$

Note that this parameter has the same form as the Thiele number which occurs in the theory of diffusion/reaction in catalyst pores.

SECOND-ORDER REACTION IN A LIQUID FILM

A pure gas A diffuses into a liquid film where it reacts with B from the liquid phase. Material balances on the two participants are:

$$D_a \frac{d^2C_a}{dz^2} = k_c C_a C_b \qquad (23\text{-}100)$$

$$D_b \frac{d^2C_b}{dz^2} = k_c C_a C_b \qquad (23\text{-}101)$$

At the gas/liquid interface, $z = 0$, $C_a = C_{ai}$, $dC_b/dz = 0$. On the liquid side of the film, $z = z_L$, $C_b = C_{bL}$. The volume of the bulk liquid per unit of interfacial area

$$V_L = \text{total volume} - \text{film volume}$$
$$= \frac{\varepsilon}{a - z_L} \qquad (23\text{-}102)$$

where ε is fractional holdup of liquid and a is interfacial area per unit volume of liquid. The remaining boundary condition at z_L is

$$-D_a\left(\frac{dC_a}{dz}\right) = k_c C_{aL} C_{bL}\left(\frac{\varepsilon}{a - z_L}\right) \qquad (23\text{-}103)$$

The numerical solution of these equations is shown in Fig. 23-28. This is a plot of the enhancement factor E against the Hatta number, with several other parameters. The factor E represents an enhancement of the rate of transfer of A caused by the reaction compared with physical absorption with zero concentration of A in the liquid. The uppermost line on the upper right represents the pseudo-first-order reaction, for which $E = \beta \coth \beta$.

Three regions are identified with different requirements of ε and a, and for which particular kinds of contacting equipment may be best:

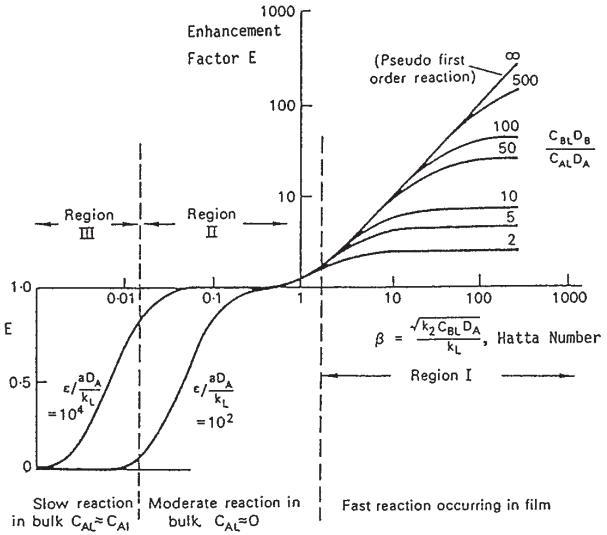

FIG. 23-28 Enhancement factor E and Hatta number of first- and second-order gas/liquid reactions, numerical solutions by several hands.

$$\text{Hatta number} = \beta = \frac{\sqrt{k_2 C_{B2} D_A}}{k_L}$$

(*Coulson and Richardson,* Chemical Engineering, *vol. 3, Pergamon, 1971, p. 80.*)

Region I, $\beta > 2$. Reaction is fast and occurs mainly in the liquid film so $C_{aL} \Rightarrow 0$. The rate of reaction $r_a = k_L a E C_{ai}$ will be large when a is large, but liquid holdup is not important. Packed towers or stirred tanks will be suitable.

Region II, $0.02 < \beta < 2$. Most of the reaction occurs in the bulk of the liquid. Both interfacial area and holdup of liquid should be high. Stirred tanks or bubble columns will be suitable.

Region III, $\beta < 0.02$. Reaction is slow and occurs in the bulk liquid. Interfacial area and liquid holdup should be high, especially the latter. Bubble columns will be suitable.

SCALE-UP FROM LABORATORY DATA

Three criteria for scale-up are that the laboratory and industrial units have the same mass-transfer coefficients k_g and Ek_L and the same ratio of the specific interfacial surface and liquid holdup a/ε_L. Tables 23-9 and 23-10 give order-of-magnitude values of some parameters that may be expected in common types of liquid/gas contactors.

Auxiliary data are the sizes of bubbles and droplets. These data and the holdups of the two phases are measured by a variety of standard techniques. Interfacial area measurements utilize techniques of transmission or reflection of light. Data on and methods for finding solubilities of gases or the relation between partial pressure and concentration in liquid are also well established.

Hatta Number A film-conversion parameter is defined as

$$M = \frac{\text{maximum possible conversion in the film}}{\text{maximum diffusional transport through the film}} = \frac{k_c C_a C_{b0} z_L}{Da(C_a - 0)/z_L} = \frac{k_c C_{b0} z_L^2}{D_a} = \frac{D_a k_c C_{b0}}{k_L^2} = \text{Ha}^2 \qquad (23\text{-}104)$$

When $\text{Ha}^2 >> 1$, all of the reaction occurs in the film and the amount of interfacial area is controlling, necessitating equipment that has a large interfacial area. When $\text{Ha} << 1$, no reaction occurs in the film and the bulk volume controls. The Hatta criteria are often applied in the following form.

$\text{Ha} < 0.3$	Reaction needs large bulk liquid volume
$0.3 < \text{Ha} < 3.0$	Reaction needs large interfacial area and large bulk liquid volume
$\text{Ha} > 3.0$	Reaction needs large interfacial area

Of the parameters making up the Hatta number, liquid diffusivity data and measurement methods are well reviewed in the literature.

Specific Rate k_c For the liquid-phase reaction without the complications of diffusional resistances, the specific rate can be determined after dissolving the gas solute and liquid reactant separately in the same solvent, mixing the two liquids quickly and thoroughly and following the progress of the liquid-phase reaction at the elevated pressure. Unless the reaction is very fast, the mixing time may be ignored. There may be an advantage in employing supercritical conditions at which gas solubility may be appreciably enhanced.

A number of successful devices have been in use for finding mass-transfer coefficients, some of which are sketched in Fig. 23-29, and all of which have known or adjustable interfacial areas. Such laboratory testing is reviewed, for example, by Danckwerts (*Gas-Liquid Reactions,* McGraw-Hill, 1970) and Charpentier (in Ginetto and Silveston, eds., *Multiphase Chemical Reactor Theory, Design, Scaleup,* Hemisphere, 1986).

Gas-Film Coefficient k_g Since the gas film is not affected by the liquid-phase reaction, one of the many available correlations for physical absorption may be applicable. The coefficient also may be found directly after elimination of the liquid-film coefficient by employing a solution that reacts instantaneously and irreversibly with the dissolved gas, thus canceling out any backpressure. Examples of such systems are SO_2 in NaOH and NH_3 in H_2SO_4.

Liquid-Film Coefficients k_L (Physical) and Ek_L (Reactive) The gas-side resistance can be eliminated by employing a pure gas, thus leaving the liquid film as the only resistance. Alternatively, after the gas-film resistance has been found experimentally or from corre-

TABLE 23-9 Mass-Transfer Coefficients, Interfacial Areas and Liquid Holdup in Gas/Liquid Reactions

Type of reactor	ε_L, %	k_G, gm mol/(cm²·s·atm) s·atm) × 10⁴	k_L cm/s × 10²	a, cm²/cm³ reactor	$k_L a$, s⁻¹ × 10²
Packed columns					
Countercurrent	2–25	0.03–2	0.4–2	0.1–3.5	0.04–7
Cocurrent	2–95	0.1–3	0.4–6	0.1–17	0.04–102
Plate columns					
Bubble cap	10–95	0.5–2	1–5	1–4	1–20
Sieve plates	10–95	0.5–6	1–20	1–2	1–40
Bubble columns	60–98	0.5–2	1–4	0.5–6	0.5–24
Packed bubble columns	60–98	0.5–2	1–4	0.5–3	0.5–12
Tube reactors					
Horizontal and coiled	5–95	0.5–4	1–10	0.5–7	0.5–70
Vertical	5–95	0.5–8	2–5	1–20	2–100
Spray columns	2–20	0.5–2	0.7–1.5	0.1–1	0.07–1.5
Mechanically agitated bubble reactors	20–95	—	0.3–4	1–20	0.3–80
Submerged and plunging jet	94–99	—	0.15–0.5	0.2–1.2	0.03–0.6
Hydrocyclone	70–93	—	10–30	0.2–0.5	2–15
Ejector reactor	—	—	—	1–20	—
Venturi	5–30	2–10	5–10	1.6–25	8–25

SOURCE: From Charpentier, *Advances In Chemical Engineering,* vol. 11, Academic Press, 1981, pp. 2–135).

TABLE 23-10 Order-of-Magnitude Data of Equipment for Contacting Gases and Liquids

Device	k_La, s^{-1}	V, m^3	k_LaV, m^3/s (duty)	a, m^{-1}	ε_L	Liquid mixing	Gas mixing	Power per unit volume, kW/m^3
Baffled agitated tank	0.02–0.2	0.002–100	10^{-4}–20	~200	0.9	~Backmixed	Intermediate	0.5–10
Bubble column	0.05–0.01	0.002–300	10^{-5}–3	~20	0.95	~Plug	Plug	0.01–1
Packed tower	0.005–0.02	0.005–300	10^{-5}–6	~200	0.05	Plug	~Plug	0.01–0.2
Plate tower	0.01–0.05	0.005–300	10^{-5}–15	~150	0.15	Intermediate	~Plug	0.01–0.2
Static mixer (bubble flow)	0.1–2	Up to 10	1–20	~1000	0.5	~Plug	Plug	10–500

SOURCE: From J. C. Middleton, in Harnby, Edwards, and Nienow, *Mixing in the Process Industries,* Butterworth, 1985.

lations, the liquid-film coefficient can be calculated from a measured overall liquid-film coefficient with the relation

$$\frac{1}{K_L} = \frac{1}{Hk_g} + \frac{1}{k_L} \tag{23-105}$$

In order to allow integration of countercurrent relations like Eq. (23-93), point values of the mass-transfer coefficients and equilibrium data are needed, over ranges of partial pressure and liquid-phase compositions. The same data are needed for the design of stirred tank performance. Then the conditions vary with time instead of position. Because of limited solubility, gas/liquid reactions in stirred tanks usually are operated in semibatch fashion, with the liquid phase charged at once, then the gas phase introduced gradually over a period of time. CSTR operation rarely is feasible with such systems.

INDUSTRIAL GAS/LIQUID REACTION PROCESSES

Two lists of gas/liquid reactions of industrial importance have been compiled recently. The literature survey by Danckwerts (*Gas-Liquid Reactions,* McGraw-Hill, 1970) cites 40 different systems. A supplementary list by Doraiswamy and Sharma (*Heterogeneous Reactions: Fluid-Fluid-Solid Reactions,* Wiley, 1984) cites another 50 items, and indicates the most suitable kind of reactor to be used for each. Estimates of values of parameters that may be expected of some types of gas/liquid reactors are in Tables 23-9 and 23-10.

Examples are given of common operations such as absorption of ammonia to make fertilizers and of carbon dioxide to make soda ash. Also of recovery of phosphine from offgases of phosphorous plants; recovery of HF; oxidation, halogenation, and hydrogenation of various organics; hydration of olefins to alcohols; oxo reaction for higher aldehydes and alcohols; ozonolysis of oleic acid; absorption of carbon monoxide to make sodium formate; alkylation of acetic acid with isobutylene to make *tert*-butyl acetate, absorption of olefins to make various products; HCl and HBr plus higher alcohols to make alkyl halides; and so on.

By far the greatest number of installations is for the removal or recovery of mostly small concentrations of acidic and other components from air, hydrocarbons, and hydrogen. Hundreds of such plants are in operation, many of them of great size. They mostly employ either packed or tray towers. Power requirements for such equipment are small. When the presence of solid impurities could clog the equipment or when the pressure drop must be low, spray towers are used in spite of their much larger size for a given capacity and scrubbing efficiency.

Removal of CO_2 and H_2S from Inert Gases, Packed and Tray Towers The principal reactive solvents for the removal of acidic constituents from gas streams are aqueous solutions of monethanolamine (MEA), diethanolamine (DEA) and K_2CO_3. These are all regenerable. Absorption proceeds at a lower temperature or higher pressure and regeneration in a subsequent vessel at higher temperature or lower pressure, usually with some assistance from stripping steam. CO_2 is discharged to the atmosphere or recovered to make dry ice. H_2S is treated for recovery of the sulfur. Any COS in the offgases is destroyed by catalytic hydrogenation.

Some performance data of plants with DEA are shown in Table 23-11. Both the absorbers and strippers have trays or packing. Vessel diameters and allowable gas and liquid flow rates are established by the same correlations as for physical absorptions. The calculation of tower heights utilizes data of equilibria and enhanced mass-transfer coefficients like those of Fig. 23-27 but for DEA solutions. Such calculations are complex enough to warrant the use of the professional methods of tower design that are available from a number of service companies.

Partly because of their low cost, aqueous solutions of sodium or potassium carbonate also are used for CO_2 and H_2S. Potassium bicarbonate has the higher solubility so the potassium salt is preferred. In view of the many competitive amine and carbonate plants that are in operation, fairly close figuring apparently is required to find an economic superiority, but other intangibles may be involved.

Both the equilibria and the enhancement of the coefficients can be improved by additives, of which sodium arsenite is the major one in use, but sodium hypochlorite and small amounts of amines also are effective. *Sterically hindered amines* as promoters are claimed by Say et al. (*Chem. Eng. Prog.,* **80**(10), 72–77 [1984]) to result in 50 percent more capacity than ordinary amine promoters of carbonate solutions.

Many operating data for carbonate plants are cited by Kohl and Riesenfeld (*Gas Purification,* Gulf, 1985) but not including tower heights. Pilot plant tests, however, are reported on 0.10- and 0.15-m (4- and 6-in) columns packed to depths of 9.14 m (30 ft) of Raschig rings by Benson et al. (*Chem. Eng. Prog.,* **50,** 356 [1954]).

Sulfur Dioxide, Spray Towers Flue gases and offgases from sulfuric acid plants contain less than 0.5 percent SO_2; smelter gases like those from ore processing plants may contain 8 percent. The high-concentration streams are suitable for the manufacture of sulfuric acid. The low concentrations usually are regarded as contaminants to be destroyed or recovered as elemental sulfur by, for example, the Claus process.

Of the removal processes that have attained commercial status, the current favorite employs a slurry of lime or limestone. The activity of the reagent is promoted by the addition of small amounts of carboxylic acids such as adipic acid. The gas and the slurry are contacted in a spray tower. The calcium salt is discarded. A process that employs aqueous sodium citrate, however, is suited for the recovery of elemental sulfur. The citrate solution is regenerated and recycled. (Kohl and Riesenfeld, *Gas Purification,* Gulf, 1985, p. 356.)

Limestone is pulverized to 80 to 90 percent through 200 mesh. Slurry concentrations of 5 to 40% have been checked in pilot plants. Liquid to gas ratios are 0.2 to 0.3 gal/MSCF. Flue gas enters at 149°C (300°F) at a velocity of 2.44 m/s (8 ft/s). Utilization of 80 percent of the solid reagent may be approached. Flow is in parallel downward. Residence times are 10 to 12 s. At the outlet the particles are made just dry enough to keep from sticking to the wall, and the gas is within 11 to 28°C (20 to 50°F) of saturation. The fine powder is recovered with fabric filters.

Rotary wheel atomizers require 0.8 to 1.0 kWh/1,000 L. The lateral throw of a spray wheel requires a large diameter to prevent accumulation on the wall; length to diameter ratios of 0.5 to 1.0 are in use in such cases. The downward throw of spray nozzles permits smaller diameters but greater depths; L/D ratios of 4 to 5 or more are used. Spray vessel diameters of 15 m (50 ft) or more are known. The technology of spray drying is applicable.

In one test facility, a gas with 4,000 ppm SO_2 had 95 percent removal with lime and 75 percent removal with limestone.

Stirred Vessels Gases may be dispersed in liquids by spargers or nozzles and redispersed by packing or trays. More intensive dispersion and redispersion is obtained by mechanical agitation. At the same time, the agitation will improve heat transfer and will keep catalyst particles in suspension if necessary. Power inputs of 0.6 to 2.0 kW/m^3 (3.05 to 10.15 hp/1,000 gal) are suitable.

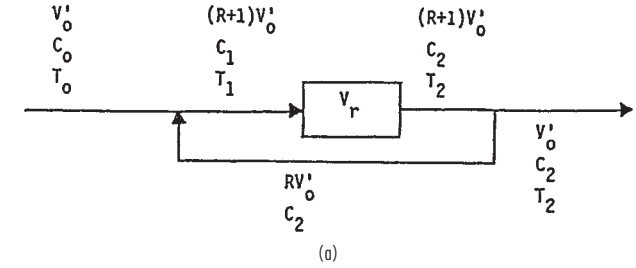

(a)

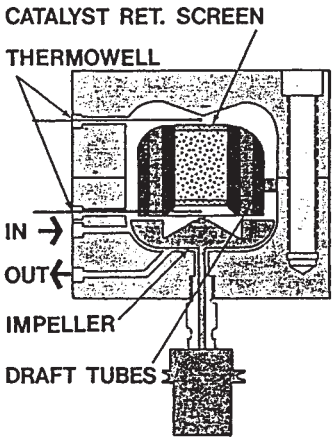

(b)

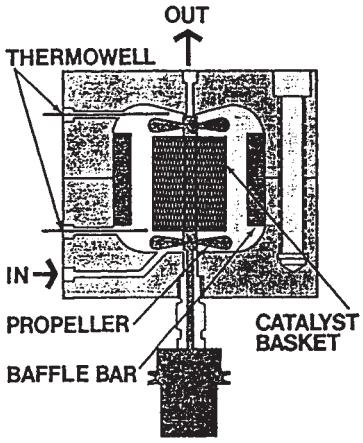

(c)

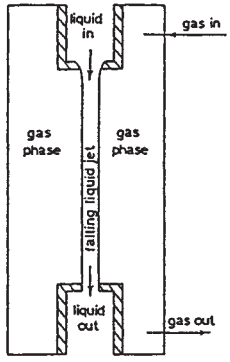

(d)

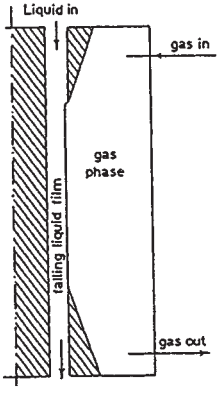

(e)

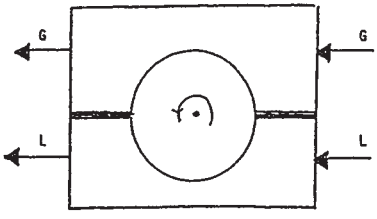

(f)

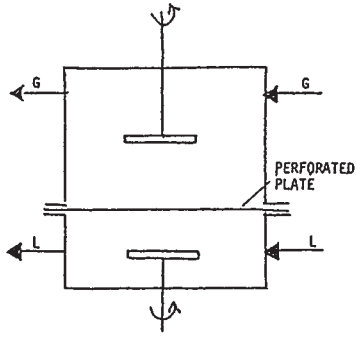

(g)

FIG. 23-29 Laboratory reactors for gas/liquid and fluid/solid processes. (*a*) Plug flow with external recycle, isothermal approach, $T_1 - T_2 = (T_0 - T_2)/(R + 1) \Rightarrow 0$. (*b*) Internal recycle, fixed basket. (*Berty, Autoclave Engineers Inc.*) (*c*) Rotating basket. (*Carberry, Autoclave Engineers Inc.*) (*d*) Falling liquid jet, known interfacial area, $t = 0.001–0.1$ s. (*e*) Falling film, $t = 0.1–0.25$ s. (*f*) Rotating drum, $t = 0.01–0.25$ s. (*Danckwerts,* Gas-Liquid Reactions, *McGraw-Hill, 1970.*) (*g*) L and G stirred, gradientless, $t = 1–10$ s. (*Levenspiel and Godfrey,* Chem. Eng. Sci., **29,** *1723* [*1974*].)

Bubble sizes tend to a minimum regardless of power input because coalescence eventually sets in. Pure liquids are coalescing type; solutions with electrolytes are noncoalescing but their bubbles also tend to a minimum. Agitated bubble size in air/water is about 0.5 mm (0.020 in), holdup fractions are about 0.10 coalescing and 0.25 noncoalescing, but more elaborate correlations have been made.

Mass-transfer coefficients seem to vary as the 0.7 exponent on the power input per unit volume, with the dimensions of the vessel and impeller and the superficial gas velocity as additional factors. A survey of such correlations is made by van't Riet (*Ind. Eng. Chem. Proc. Des. Dev.,* **18,** 357 [1979]). Table 23-12 shows some of the results.

A basic stirred tank design is shown in Fig. 23-30. Height to diameter ratio is $H/D = 2$ to 3. Heat transfer may be provided through a jacket or internal coils. Baffles prevent movement of the mass as a whole. A draft tube enhances vertical circulation. The vapor space is about 20 percent of the total volume. A hollow shaft and impeller increase gas circulation (as in Fig. 23-31). A splasher can be attached to the shaft at the liquid surface to improve entrainment of gas. A variety of impellers is in use. The pitched propeller moves the liquid axially, the flat blade moves it radially, and inclined blades move it both axially and radially. The anchor and some other designs are suited to viscous liquids.

TABLE 23-11 Hydrocarbon Gas Treatments with Aqueous DEA*

Item	A	B	C	D	E
Absorber					
P, atm	68	14	7	15	12
T, °C			19	60	52
Trays	30	23	16		
Packing				26 ft, 3 in	30 ft, ¾
Stripper					
P, atm	2	2			
T, °C	133	118			
Trays	20	20			
Input					
CO_2	10%	0.35%			
H_2S gr/100 scf	15%	170	3,196	1,490	2,500
COS	300 ppm				
CS_2	600 ppm				
Output					
CO_2 gr/100 scf	1.6				
H_2S gr/100 scf	0.28	0.3	15	26	15
COS gr/100 scf	0				

*1 gr/100 scf = 0.0229 g/std m^3

TABLE 23-12 Correlations of Mass-Transfer Coefficients in Stirred Tanks

Correlations of Koetsier, et al. (*Chem. Eng. Journal,* **5,** 61, 71 [1973])

For coalescing liquids:

$$k_L a = 0.05\left(\frac{N^2 D_i^2}{D_t^{1.5}}\right)^{1.95} = 0.05\, E^{0.65}\left(\frac{D_i}{D_t}\right)^{0.65} D_t^{-0.33}, \qquad 1/s$$

$$k_L = 0.002\left(\frac{N D_i^2}{D_t^{1.6}} - 0.45\right), \qquad m/s$$

For noncoalescing liquids (electrolytes):

$$k_L a = 0.11\, E^{0.7}\left(\frac{D_i}{D_t}\right)^{0.7} D_t^{-0.35}$$

$$k_L = 0.000325\, E^{0.3}\left(\frac{D_i}{D_t}\right)^{0.7} D_t^{-0.35}$$

where N = revolutions/s
D_i = impeller diameter, m, 6-blade turbine
D_t = tank diameter, m
E = power input, kW/m^3

Correlation cited by Middleton (in Harnby, et al., *Mixing in the Process Industries,* Butterworth, 1985)

Coalescing:

$$k_L a = 1.2\, E^{0.7} u_s^{0.6}, \qquad 1/s$$

Noncoalescing:

$$k_L a = 2.3\, E^{0.7} u_s^{0.6}, \qquad 1/s$$

where u_s = superficial gas velocity, m/sec

For gas dispersion the six-bladed turbine is preferred. When the ratio of liquid height to diameter is $H/D \le 1$ a single impeller suffices, and in the range $1 \le H/D \le 1.8$ two are needed. The oil hydrogenator of Fig. 23-32, which is to scale, uses three impellers. The greater depth there will give longer contact time, which is desirable for slow reactions. The best position for inlet of gas is below and at the center of the impeller, or at the bottom of the draft tube. An open pipe is in common use, but a sparger may be helpful. A two-speed motor is desirable to prevent overloading, the lower speed to cut in when the gas supply is cut off but agitation is to continue, since gassed power requirement is significantly less than ungassed.

In tanks of 5.7 to 18.9 m^3 (1,500 to 5,000 gal) rotation speeds are from 50 to 200 rpm and power requirements are 2 to 75 hp; both depend on superficial velocities of gas and liquid (Hicks and Gates, *Chem. Eng.,* 141–148 [July 1976]). As a rough guide, power requirements and impeller tip speeds are as follows.

Operation	hp/1,000 gal*	Tip speed, ft/s
Homogeneous reaction	0.5–1.5	7.5–10
With heat transfer	1.5–5	10–15
Liquid/liquid mixing	5	15–20
Gas/liquid mixing	5–10	15–20

*1 hp/1,000 gal = 0.197 kw/m^3.

Hydrogenation of Oils in Stirred Tanks Large-scale uses of stirred tanks include the gas/liquid reactions of hydrogenation and fermentation. For hydrogenation of vegetable and animal oils, semibatch operations often are preferred to continuous ones because of the variety of feedstocks or product specifications or long reaction times or small production rates. Sketches of batch and continuous hydrogenators are shown in Figs. 23-32 and 23-33.

The composition of an oil and the progress of its hydrogenation is expressed in terms of its iodine value (IV). Edible oils are mixtures of unsaturated compounds with molecular weights in the vicinity of 300. The IV is a measure of this unsaturation. It is found by a standardized procedure. A solution of ICl in a mixture of acetic acid and carbon tetrachloride is mixed in with the oil and allowed to react to completion, usually for less than 1 h. Halogen addition takes place at the double bond, after which the amount of unreacted iodine is determined by analysis. The reaction is

$$ICl + RCH{=}CHR_1 \Rightarrow RCHI{-}CHClR_1$$

and the definition is

$$IV = \frac{I \text{ absorbed}}{100 \text{ g oil}}$$

To start a hydrogenation process, the oil and catalyst are charged first, then the vessel is evacuated for safety and hydrogen is supplied continuously from storage and kept at some fixed pressure, usually in the range of 1 to 10 atm (14.7 to 147 psi). Internal circulation of

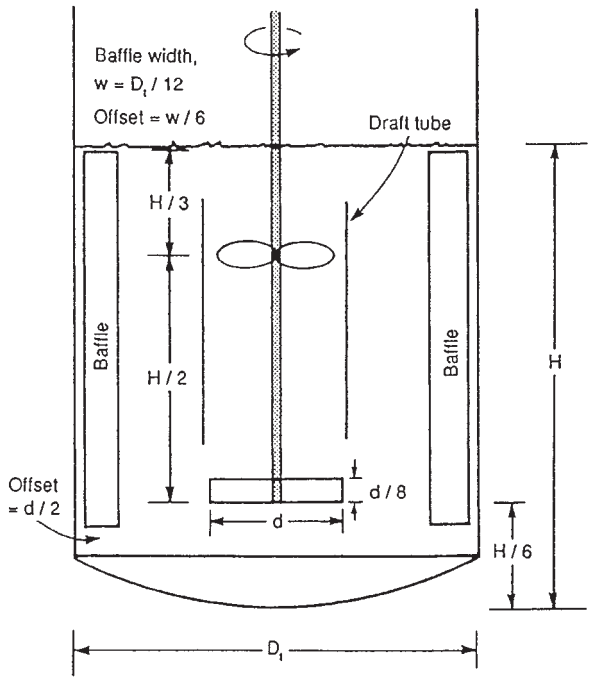

FIG. 23-30a A basic stirred tank design, not to scale, showing a lower radial impeller and an upper axial impeller housed in a draft tube. Four equally spaced baffles are standard. H = height of liquid level, D_t = tank diameter, d = impeller diameter. For radial impellers, $0.3 \le d/D_t \le 0.6$.

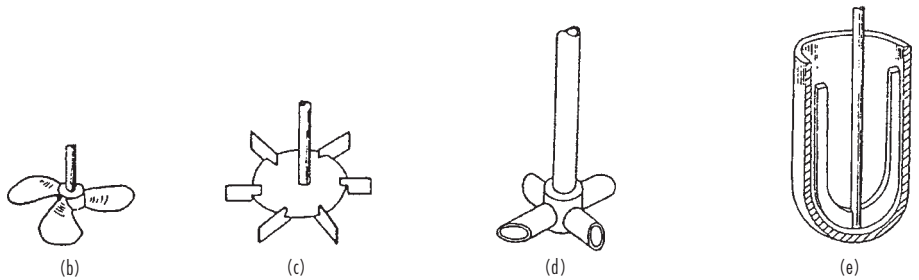

FIG. 23-30 Basic stirred tank design and selected kinds of impellers. (*b*) Propeller. (*c*) Turbine. (*d*) Hollow. (*e*) Anchor.

hydrogen is provided by axial and radial impellers or with a hollow impeller that throws the gas out centrifugally and sucks gas in from the vapor space through the hollow shaft. Some plants have external gas circulators. Reaction times are 1 to 4 h.

For edible oils the temperature is kept at about 180°C (356°F). Consumption of hydrogen per unit change of IV is

$$\frac{0.0795 \text{ kg } H_2}{1{,}000 \text{ kg oil}}$$

$$\frac{883.3 \text{ L STP } H_2}{1{,}000 \text{ kg oil}}$$

Solubility of hydrogen depends on the temperature and pressure but only slightly on the natures of the oils that are usually processed.

$$S = (0.04704 + 0.000294T)P, \quad \frac{\text{L STP}}{\text{kg oil}} \qquad (23\text{-}106)$$

with T in °C and P in atm.

Heat evolution is 0.94 to 1.10 kcal/(kg oil)(unit drop of IV) (1.69 to 1.98 Btu/[lbm oil][unit drop of IV]). Because space for heat-transfer coils in the vessel is limited, the process is organized to give a maximum IV drop of about 2.0/min. The rate of reaction, of course, drops off rapidly as the reaction proceeds, so a process may take several hours. The end point of a hydrogenation is a specified IV of the product, but the progress of a reaction before the end can be followed by measuring hardness or refractive index.

Saturation of the oil with hydrogen is maintained by agitation. The rate of reaction depends on agitation and catalyst concentration. Beyond a certain agitation rate, resistance to mass transfer is eliminated and the rate becomes independent of pressure. The effect of catalyst concentration also reaches limiting values. The effects of pressure and temperature on the rate are indicated by Fig. 23-34 and of catalyst concentration by Fig. 23-35. Reaction time is related to temperature, catalyst concentration, and IV in Table 23-13.

Nickel is the most used catalyst, 20 to 25 percent Ni on a porous siliceous support in the form of flakes that are readily filterable. The pores allow access of the reactants to the extended pore surface, which is in the range of 200 to 600 m^2/g (977×10^3 to $2{,}931 \times 10^3$ ft^2/lbm) of

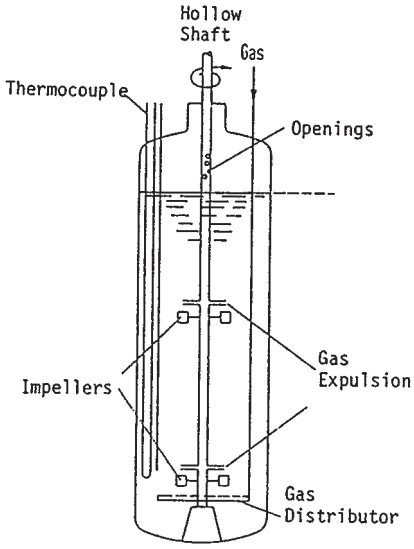

FIG. 23-31 Stirred tank with hollow shaft for hydrogenation of nitrocaprolactam. (*Dierendonk et al.*, 5th European Symp. Chem. React. Eng., *Pergamon, 1972, pp. B6–45.*)

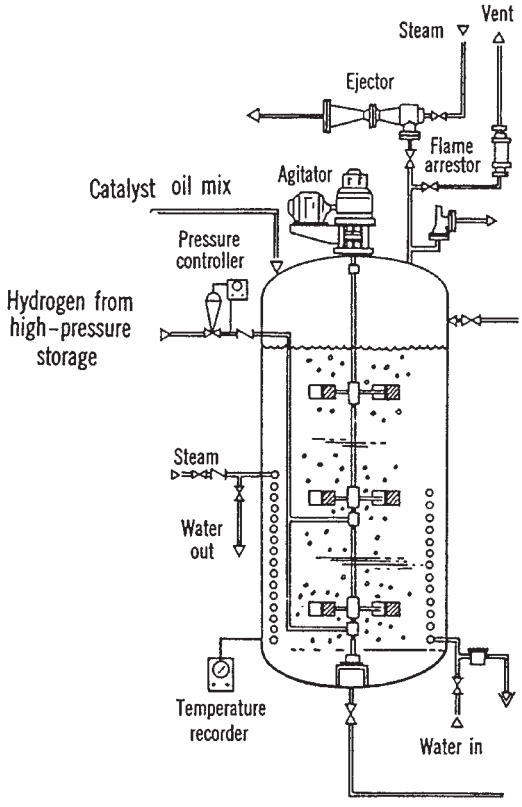

FIG. 23-32 Stirred tank hydrogenator for edible oils. (*Votator Division, Chemetron Corporation.*)

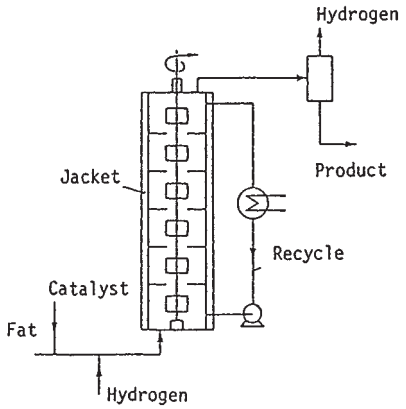

FIG. 23-33 Continuous hydrogenation of fats (*Albright,* Chem. Eng., ***74,*** *249* [*9 Oct. 1967*].)

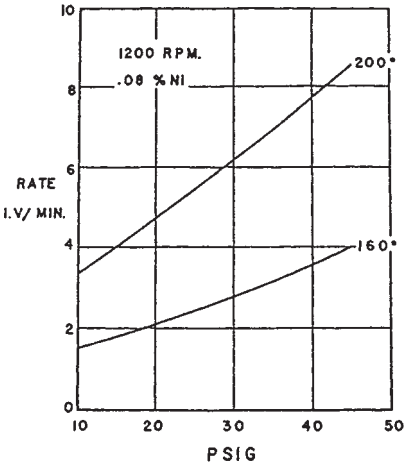

FIG. 23-34 Effect of reaction pressure and temperature on the rate of hydrogenation of soybean oil. (*Swern, ed.,* Bailey's Industrial Oil and Fat Products, *vol. 2, Wiley, 1979.*)

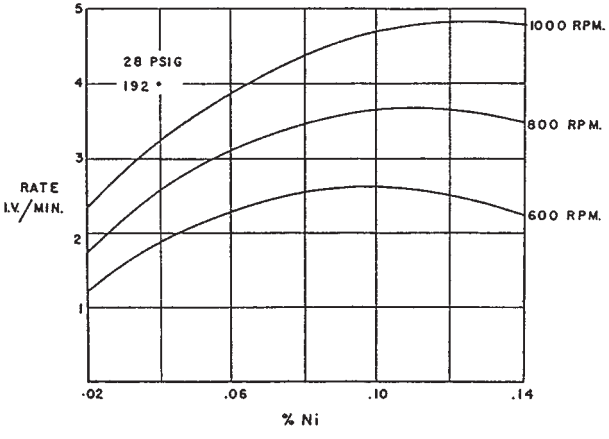

FIG. 23-35 Effect of catalyst concentration and stirring rate on hydrogenation of soybean oil. (*Swern, ed.,* Bailey's Industrial Fat and Oil Products, *vol. 2, Wiley, 1979.*)

TABLE 23-13 Time, Temperature, and Iodine Value of Tallow Hydrogenation*

	0.03% Ni, $P = 20$ atm		0.04% Ni, $P = 25$ atm		0.08% Ni, $P = 3$ atm	
t, min	T, °C	IV	T, °C	IV	T, °C	IV
0	140	42.3	140	44.1	160	42.3
5	145	39.7			165	35.0
10	150	37.3	147	38.0	170	27.8
30	160	27.1	160	26.6	180	8.4
60	180	14.5	180	13.4	200	1.7
90	190	5.4	180	5.6	200	0.3
120	200	1.0	180	0.5	200	0.25
180	200	0.3			200	0.1

*To convert atm to kPa, multiply by 101.3.
SOURCE: From Patterson, *Hydrogenation of Fats and Oils,* Applied Science Publishers, 1983.

which 20 to 30 percent is catalytically active. The concentration of catalyst in the slurry can vary over a wide range but is usually under 0.1% Ni. Catalysts are subject to degradation and poisoning, particularly by sulfur compounds. Accordingly, about 10 to 20 percent of the recovered catalyst is replaced by fresh before recycling. Other catalysts are applied in special cases. Expensive palladium has about 100 times the activity of nickel and is effective at lower temperatures.

While the liquid is saturated with hydrogen the reaction is pseudo-first-order. One sequence of reactions of acids that has been investigated (Swern, ed., *Bailey's Industrial Oil and Fat Products,* vol. 2, Wiley, 1979, p. 12) is

$$\text{Linolenic} \overset{1}{\Rightarrow} \text{Linoleic} \overset{2}{\Rightarrow} \text{Oleic} \overset{3}{\Rightarrow} \text{Stearic}$$

At 175°C (347°F), 0.02% Ni, 1 atm, 600 rpm the specific rates are: $k_1 = 0.367$, $k_2 = 0.159$, $k_3 = 0.013$/min.

Figure 23-36 shows a computer calculation with these specific rates, but which does not agree quantitatively with the figure shown by Swern. The time scales appear to be different, but both predict a peak in the amount of oleic acid and rapid disappearance of the first two acids.

A case study of the hydrogenation of cottonseed oil is made by Rase (*Chemical Reactor Design for Process Plants,* vol. 2, Wiley, 1977, pp. 161–178).

Semibatch hydrogenation of edible oils has a long history and a well-established body of practice by manufacturers and catalyst suppliers. Problems of new oils, new specifications, new catalyst poisons,

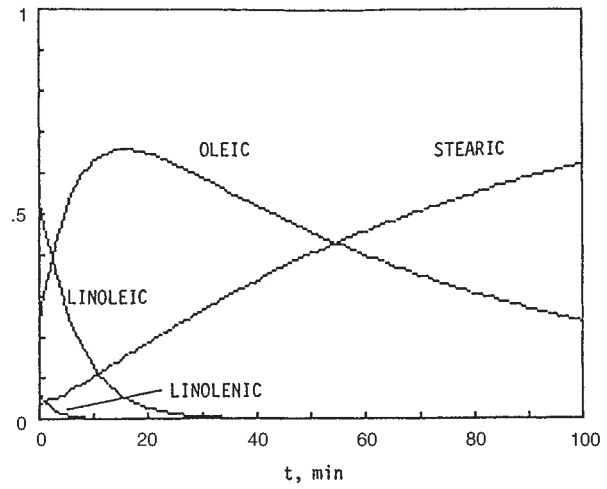

FIG. 23-36 Product compositions of the first-order sequence of fatty acids: Linolenic ⇒ Linoleic ⇒ Oleic ⇒ Stearic.

and even new scales of operation can probably be handled with a minimum amount of laboratory or pilot plant work.

Aerobic Fermentation The classic example of large-scale aerobic fermentation is the production of penicillin by the growth of a specific mold. Commercial vessel sizes are 40,000 to 200,000 L (1,400 to 7,000 ft^3). The operation is semibatch in that the lactose or glucose nutrient and air are charged at controlled rates to a precharged batch of liquid nutrients and cell mass. Reaction time is 5 to 6 days.

The broth is limited to 7 to 8 percent sugars, which is all the mold will tolerate. Solubility of oxygen is so limited that air must be supplied over a long period as it is used up. The pH is controlled at about 6.5 and the temperature at 24°C (75°F). The air is essential to the growth. Dissolved oxygen must be kept at a high level for the organism to survive. Air also serves to agitate the mixture and to sweep out the CO_2 and any noxious byproducts that are formed. Air supply is in the range of 0.5 to 1.5 volumes/(volume of liquid)(min). For organisms grown on glucose the oxygen requirement is 0.4 g/g dry weight; on methanol it is 1.2 g/g.

The heat of reaction requires cooling water at the rate of 10 to 40 L/(1,000 L holdup)(h). Vessels under about 500 L (17.6 ft^3) are provided with jackets, larger ones with coils. For a 55,000-L vessel, 50 to 70 m^2 may be taken as average.

Mechanical agitation is needed to break up the gas bubbles but must avoid rupturing the cells. The disk turbine with radial action is most suitable. It can tolerate a superficial gas velocity up to 120 m/h (394 ft/h) without flooding, whereas the propeller is limited to about 20 m/h (66 ft/h). When flooding occurs, the impeller is working in a gas phase and cannot assist the transfer of gas to the liquid phase. Power input by agitation and air sparger is 1 to 4 W/L (97 to 387 Btu/[ft^3·h]) of liquid.

Bubble Reactors In bubble columns the gas is dispersed by nozzles or spargers without mechanical agitation. In order to improve the operation, redispersion at intervals may be effected by static mixers, such as perforated plates. The liquid may be clear or be a slurry.

Because of their large volume fraction of liquid, bubble reactors are suited to slow reactions; that is, those whose rate of reaction is smaller than their rate of diffusion. Major advantages are the absence of moving parts, the ability to handle solid particles without erosion or plugging, good heat transfer at the wall or coils, high interfacial area, and high mass-transfer coefficients. A disadvantage is the occurrence of backmixing of the liquid phase and some of the gas phase, which may result in poor selectivity with some complex reactions. High pressure drop because of the static head of the liquid also is harmful. At high height/diameter ratios (>15), the effective interfacial area decreases rapidly. Generally, the tower height is greater than for tray or packed towers.

Two complementary reviews of this subject are by Shah et al. (*AIChE Journal,* **28,** 353–379 [1982]) and Deckwer (in de Lasa, ed., *Chemical Reactor Design and Technology,* Martinus Nijhoff, 1985, pp. 411–461). Useful comments are made by Doraiswamy and Sharma (*Heterogeneous Reactions,* Wiley, 1984). Charpentier (in Gianetto and Silveston, eds., *Multiphase Chemical Reactors,* Hemisphere, 1986, pp. 104–151) emphasizes parameters of trickle bed and stirred tank reactors. Recommendations based on the literature are made for several design parameters: namely, bubble diameter and velocity of rise, gas holdup, interfacial area, mass-transfer coefficients k_La and k_L but not k_g, axial liquid-phase dispersion coefficient, and heat-transfer coefficient to the wall. The effect of vessel diameter on these parameters is insignificant when $D \geq 0.15$ m (0.49 ft), except for the dispersion coefficient. Application of these correlations is to: (1) chlorination of toluene in the presence of $FeCl_3$ catalyst, (2) absorption of SO_2 in aqueous potassium carbonate with arsenite catalyst, and (3) reaction of butene with sulfuric acid to butanol.

Some qualitative observations can be made. Increase of the superficial gas velocity increases the holdup of gas, the interfacial area, and the overall mass-transfer coefficient. The ratio of height to diameter is not important in the range of 4 to 10. Increase of viscosity and decrease of surface tension increase the interfacial area. Electrolyte solutions have smaller bubbles, higher gas holdup, and higher interfacial area. Sparger design is unimportant for superficial gas velocities > 5 to 10 cm/s (0.16 to 0.32 ft/s). Gas conversion falls off at higher superficial velocities, so values under 10 cm/s (0.32 ft/s) are advisable.

The gas approximates plug flow except in wide columns, but the liquid undergoes considerable backmixing. The latter effect can be reduced with packing or perforated plates. The effect on selectivity may become important. In the oxidation of liquid *n*-butane, for instance, the ratio of methyl ethyl ketone to acetic acid is much higher in plug flow than in mixed. Similarly, in the air oxidation of isobutane to *tert*-butyl hydroperoxide, where *tert*-butanol also is obtained, plug flow is more desirable.

Bubble action provides agitation about equivalent to that of mechanical stirrers, and thus about the same heat-transfer coefficients.

In cases of high liquid velocities (>30 cm/s [0.98 ft/s]) and low gas velocities (1 to 3 cm/s [0.033 to 0.098 ft/s]) it is advantageous to have concurrent downward flow.

Pulsations can improve performance. According to Baird and Garstang (*Chem. Eng. Sci.,* **22,** 1663 [1967]; **27,** 823 [1972]) at low gas velocity (0.8 to 2.4 cm/s [0.026 to 0.079 ft/s]) the value of k_La can be increased by as much as three-fold by pulsations.

Packed bubble columns operate with flooded packing, in contrast with normal packed columns which usually operate below 70 percent of the flooding point. With packing, liquid backmixing is reduced and interfacial area is increased 15 to 80 percent, but the true mass-transfer coefficient remains the same. The installation of perforated plates or grids at intervals also reduces liquid backmixing. At relatively high superficial gas velocities (10 to 15 cm/s [0.33 to 0.49 ft/s]) mixing between zones is small so the vessel performs as a CSTR battery. Radial baffles (also called disk-and-doughnut baffles) are also helpful. One set of rules is that the hole should be about 0.7 times the vessel diameter and the spacing should be 0.8 times the diameter.

Liquid Dispersion Spray columns are used with slurries or when the reaction product is a solid. The absorption of SO_2 by a lime slurry is an example. In the treatment of phosphate rock with sulfuric acid, offgases contain HF and SiF_4. In a spray column with water, solid particles of fluorosilic acid are formed but do not harm the spray operation. The coefficient k_L in spray columns is about the same as in packed columns, but the spray interfacial area is much lower. Considerable backmixing of the gas also takes place, which helps to make the spray volumetrically inefficient. Deentrainment at the outlet usually is needed.

In Venturi scrubbers the gas is the motive fluid. This equipment is of simple design and is able to handle slurries and large volumes of gas, but the gas pressure drop may be high. When the reaction is slow, further holdup in a spray chamber is necessary.

In liquid ejectors or aspirators, the liquid is the motive fluid, so the gas pressure drop is low. Flow of slurries in the nozzle may be erosive. Otherwise, the design is as simple as that of the Venturi.

The application of liquid dispersion reactors to the absorption of fluorine gases is described by Kohl and Riesenfeld (*Gas Purification,* Gulf, 1985, pp. 268–288).

Tubular Reactors In a tubular reactor with concurrent flow of gas and liquid, the variety of flow patterns ranges from a small quantity of bubbles in the liquid to small quantities of droplets in the gas, depending on the rates of the two streams. Figure 23-25 shows the patterns in horizontal flow; those in vertical flow are a little different. This equipment has good heat transfer, accommodates wide ranges of T and P, and is primarily in plug flow, and the high velocities prevent settling of slurries or accumulations on the walls. Mixing of the phases can be improved by helical static mixing inserts like those made by Kenics Corporation and others.

The reasons why a tubular reactor was selected for the production of adipic acid nitrile from adipic acid and ammonia are discussed by Weikard (in Ullmann, *Enzyklopaedie,* 4th ed., vol. 3, Verlag Chemie, 1973, p. 381).

1. The process has a large Hatta number; that is, the rate of reaction is much greater than the rate of diffusion, so a large interfacial area is desirable for carrying out the reaction in the film.
2. With normal excess ammonia the gas/liquid ratio is about 3,500 m^3/m^3. At this high ratio there is danger of fouling the surface with tarry reaction products. The ratio is brought down to a more satisfactory value of 1,000 to 1,500 by recycle of some of the effluent.
3. High selectivity of the nitrile is favored by short contact time.
4. The reaction is highly endothermic so heat input must be at a high rate.

Points 2 and 4 are the main ones governing the choice of reactor type. The high gas/liquid ratio restricts the choice to types *d, e, i,* and *k* of Fig. 23-25, but because of the high rate of heat transfer that is needed the choice falls to the falling film or tubular types.

The final selection was a tubular reactor with upward concurrent flow, with liquid holdup of 20 to 30 percent, and with residence times of 1.0 s for gas and 3 to 5 min for liquid.

Reaction in a Centrifugal Pump In the reaction between acetic acid and gaseous ketene to make acetic anhydride, the pressure must be kept low (0.2 atm) to prevent polymerization of ketene. A packed tower with low pressure drop could be used but the required volume is very large because of the low pressure. Spes (*Chem. Ing. Tech.,* **38,** 963–966 [1966]) selected a centrifugal pump reactor where compression to atmospheric pressure does take place but the contact time is too short for polymerization yet long enough for the reaction to occur. The reaction product is cooled in an external unit and partly recycled for temperature control.

Falling Film Reactor Dodecylbenzene sulfonic acid is made by reacting 5 to 10% SO_3 in air with dodecylbenzene. The gas/liquid ratio is about 1,000 m^3/m^3, and the product is highly viscous. Process requirements are a short contact time, a high rate of heat removal (170 kJ/g mol) and minimum backmixing of the liquid phase to avoid byproducts. To satisfy these requirements, a falling film reactor was selected by Ujidhy, Babos, and Farady (*Chemische Technik,* **18,** 652–654 [1966]). The gas velocity was made 12 to 15 m/s (39 to 49 ft/s) through a narrowed passage counter to the liquid flow.

LIQUID/LIQUID REACTIONS

Liquid/liquid reactions of industrial importance are fairly numerous. A list of 26 classes of reactions with 61 references has been compiled by Doraiswamy and Sharma (*Heterogeneous Reactions,* Wiley, 1984). They also indicate the kind of reactor normally used in each case. The reactions range from such prosaic examples as making soap with alkali, nitration of aromatics to make explosives, and alkylation of C_4s with sulfuric acid to make improved gasoline, to some much less familiar operations.

EQUIPMENT

Equipment suitable for reactions between liquids is represented in Fig. 23-37. Almost invariably, one of the phases is aqueous with reactants distributed between phases; for instance, NaOH in water at the start and an ester in the organic phase. Such reactions can be carried out in any kind of equipment that is suitable for physical extraction, including mixer-settlers and towers of various kinds: empty or packed, still or agitated, either phase dispersed, provided that adequate heat transfer can be incorporated. Mechanically agitated tanks are favored because the interfacial area can be made large, as much as 100 times that of spray towers, for instance. Power requirements for L/L mixing are normally about 5 hp/1,000 gal and tip speeds of turbine-type impellers are 4.6 to 6.1 m/s (15 to 20 ft/s).

Table 23-14 gives data for common types of L/L contactors. Since the given range of k_La is more than 100/1, this information is not of direct value for sizing of equipment. The efficiencies of various kinds of small liquid/liquid contactors are summarized in Fig. 23-38. Larger units may have efficiencies of less than half these values.

MECHANISMS

Few mechanisms of liquid/liquid reactions have been established, although some related work such as on droplet sizes and power input has been done. Small contents of surface-active and other impurities in reactants of commercial quality can distort a reactor's predicted performance. Diffusivities in liquids are comparatively low, a factor of 10^5 less than in gases, so it is probable in most industrial examples that they are diffusion controlled. One consequence is that L/L reactions may not be as temperature sensitive as ordinary chemical reactions, although the effect of temperature rise on viscosity and droplet size can result in substantial rate increases. L/L reactions will exhibit behavior of homogeneous reactions only when they are very slow, nonionic reactions being the most likely ones. On the whole, in the present state of the art, the design of L/L reactors must depend on scale-up from laboratory or pilot plant work.

Particular reactions can occur in either or both phases or near the interface. Nitration of aromatics with HNO_3-H_2SO_4 occurs in the aqueous phase (Albright and Hanson, eds., *Industrial and Laboratory Nitrations,* ACS Symposium Series **22** [1975]). An industrial example of reaction in both phases is the oximation of cyclohexanone, a step in the manufacture of caprolactam for nylon (Rod, *Proc. 4th International/6th European Symposium on Chemical Reactions,* Heidelberg, Pergamon, 1976, p. 275). The reaction between butene and isobutane to form isooctane in the presence of sulfuric acid is judged to occur at the acid/hydrocarbon interface, although side reactions to form higher hydrocarbons may occur primarily in the acid phase (Albright, in Albright and Goldsby, eds., *Industrial and Laboratory Nitrations,* ACS Symposium Series **55,** 145 [1977]). The formation of dioxane from isobutene in a hydrocarbon phase and aqueous formaldehyde occurs preponderantly in the aqueous phase where the rate equation is first-order in formaldehyde, although the specific rate is also proportional to the concentration of isobutene in the organic phase (Hellin et al., *Genie. Chim.,* **91,** 101 [1964]).

Reactions involving ions can be favored to occur in the organic phase by use of phase-transfer catalysts. Thus the conversion of 1-chlorooctane to 1-cyanooctane with aqueous NaCN is vastly accelerated in the organic phase by 1.3 percent of tributyl (hexadecyl) phosphonium bromide in the aqueous phase. (Starks and Owens, *J. Am. Chem. Soc.,* **95,** 3613 [1973]). A large class of such promotions is known.

There are instances where an extractive solvent is employed to force completion of a reversible homogeneous reaction by removing the reaction product. In the production of KNO_3 from KCl and HNO_3, for instance, the HCl can be removed continuously from the aqueous phase by contact with amyl alcohol, thus forcing completion (Baniel and Blumberg, *Chim. Ind.,* **4,** 27 [1957]).

OPERATING DATA

Not many operating data of large-scale liquid/liquid reactions are published. One study was made of the hydrolysis of fats with water at 230 to 260°C (446 to 500°F) and 41 to 48 atm (600 to 705 psi) in a continuous commercial spray tower. A small amount of water dissolved in the fat and reacted to form an acid and glycerine. Then most of the glycerine migrated to the water phase. The tower was operated at about 18 percent of flooding, at which condition the HETS was found to be about 9 m (30 ft) compared with an expected 6 m (20 ft) for purely physical extraction (Jeffreys, Jenson, and Miles, *Trans. Inst. Chem. Eng.,* **39,** 389–396 [1961]). A similar mathematical treatment of a batch hydrolysis is made by Jenson and Jeffreys (*Inst. Chem. Engrs. Symp. Ser.,* No. 23 [1967]).

LABORATORY STUDIES

For many laboratory studies, a suitable reactor is a cell with independent agitation of each phase and an undisturbed interface of known area, like the item shown in Fig. 23-29*d.* Whether a rate process is controlled by a mass-transfer rate or a chemical reaction rate sometimes can be identified by simple parameters. When agitation is sufficient to produce a homogeneous dispersion and the rate varies with further increases of agitation, mass-transfer rates are likely to be significant. The effect of change in temperature is a major criterion: a rise of 10°C (18°F) normally raises the rate of a chemical reaction by a factor of 2 to 3, but the mass-transfer rate by much less. There may be instances, however, where the combined effect on chemical equilibrium, diffusivity, viscosity, and surface tension also may give a comparable enhancement.

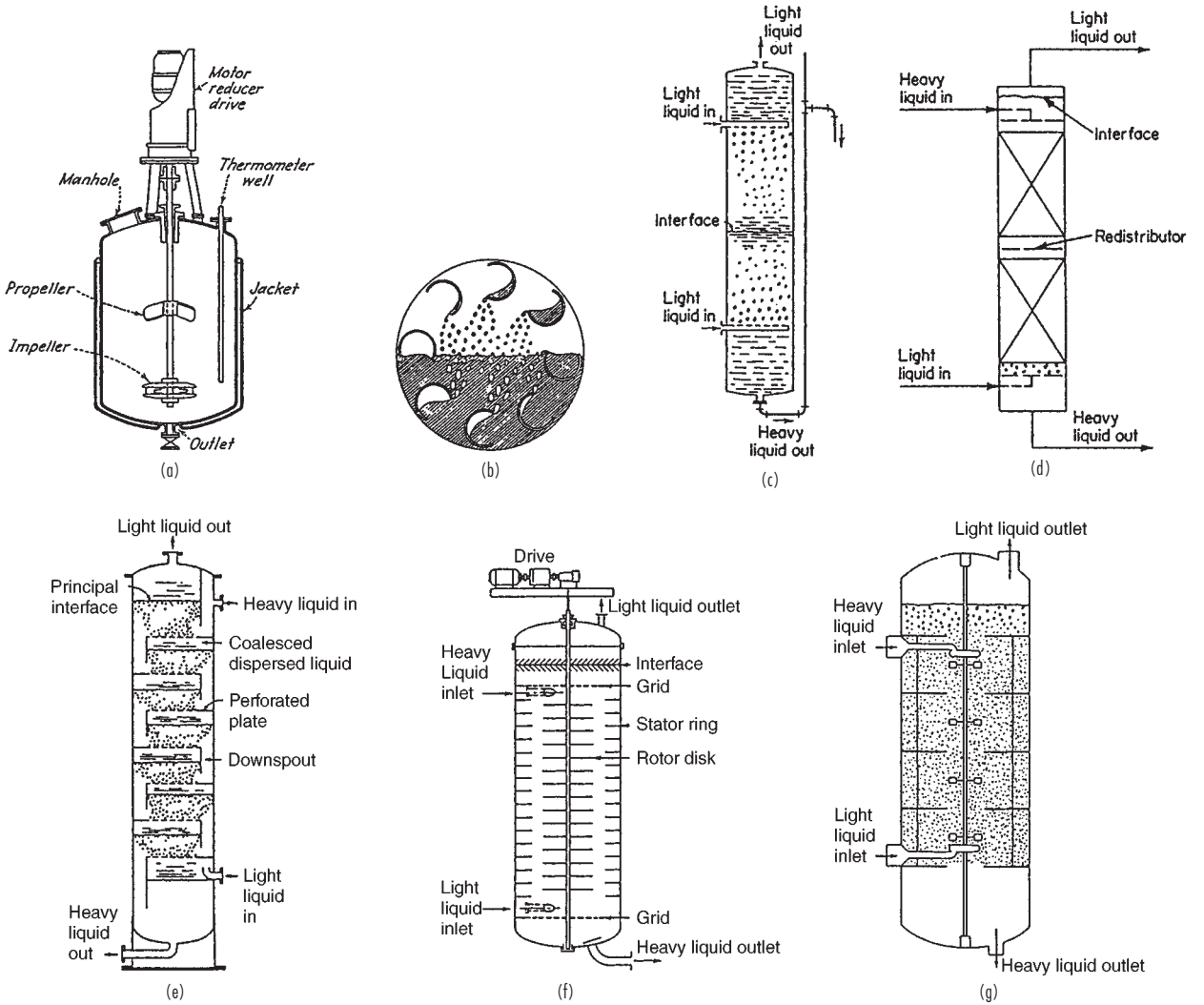

FIG. 23-37 Equipment for liquid/liquid reactions. (*a*) Batch stirred sulfonator. (*b*) Raining bucket (*RTL S A, London*). (*c*) Spray tower with both phases dispersed. (*d*) Two-section packed tower with light phase dispersed. (*e*) Sieve tray tower with light phase dispersed. (*f*) Rotating disk contactor (RDC) (*Escher B V, Holland*). (*g*) Oldshue-Rushton extractor (*Mixing Equipment Co.*).

For a chemically controlled process, conversion depends only on the residence time and not on which phase is dispersed, whereas the interfacial area and, consequently, the rate of mass transfer will change when the relative volumes of the phases are changed. If a reaction is known to occur in a particular phase, and the conversion is found to depend on the residence time in that phase, chemical reaction is controlling.

Laboratory investigations may possibly establish reaction mechanisms, but quantitative data for design purposes require pilot plant work with equipment of the type expected to be used in the plant.

TABLE 23-14 Continuous-Phase Mass-Transfer Coefficients and Interfacial Areas in Liquid/Liquid Contactors*

Type of equipment	Dispersed phase	Continuous phase	ε_D	τ_D	$k_L \times 10^2$, cm/s	a, cm^2/cm^3	$k_L a \times 10^2$, s^{-1}
Spray columns	P	M	0.05–0.1	Limited	0.1–1	1–10	0.1–10
Packed columns	P	P	0.05–0.1	Limited	0.3–1	1–10	0.3–10
Mechanically agitated contactors	PM	M	0.05–0.4	Can be varied over a wide range	0.3–1	1–800	0.3–800
Air-agitated liquid/liquid contactors	PM	M	0.05–0.3	Can be varied over a wide range	0.1–0.3	10–100	1.0–30
Two-phase cocurrent (horizontal) contactors	P	P	0.05–0.2	Limited	0.1–1.0	1–25	0.1–25

*P = plug flow, M = mixed flow, ε_D = fractional dispersed phase holdup, τ_D = residence time of the dispersed phase.
SOURCE: From Doraiswamy and Sharma, *Heterogeneous Reactions*, Wiley, 1984.

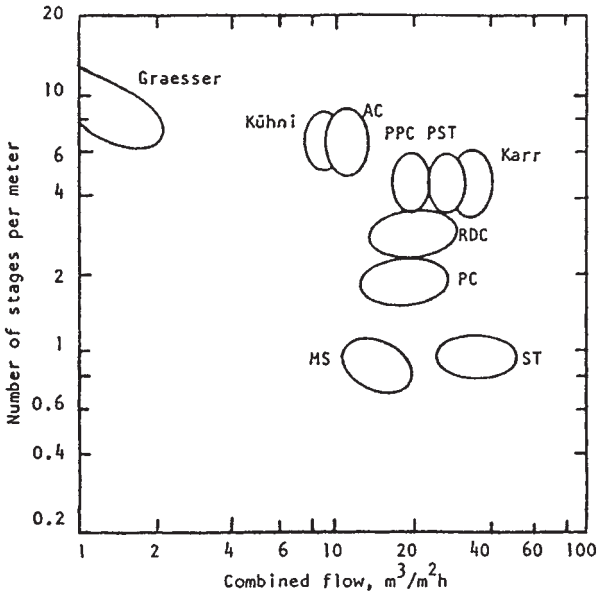

FIG. 23-38 Efficiency and capacity range of small-diameter extractors, 50 to 150 mm diameter. Acetone extracted from water with toluene as the disperse phase, $V_d/V_c = 1.5$. Code: AC = agitated cell; PPC = pulsed packed column; PST = pulsed sieve tray; RDC = rotating disk contactor; PC = packed column; MS = mixer-settler; ST = sieve tray. (*Stichlmair,* Chem. Ing. Tech. **52**(*3*), *253–255* [*1980*]).

MASS-TRANSFER COEFFICIENTS

When liquid/liquid contactors are used as reactors, values of their mass-transfer coefficients may be enhanced by reaction, analogously to those of gas/liquid processes, but there do not seem to be any published data of this nature.

Mass-transfer coefficients and other characteristics of some types of liquid/liquid contactors are summarized in Table 23-14, which may be compared with Tables 23-9 and 23-10 for gas-liquid contactors. Efficiencies of several kinds of small-scale extractors are shown in Fig. 23-38. Larger-diameter equipment may have less than one-half these efficiencies. Spray columns are inefficient and are used only when other kinds of equipment could become clogged. Packed columns as liquid/liquid reactors are operated at 20 percent of flooding. Their HETS range from 0.6 to 1.2 m (1.99 to 3.94 ft). Sieve trays minimize backmixing and provide repeated coalescence and redispersion. Mixer-settlers provide approximately one theoretical stage, but several stages can be incorporated in a single shell, although with some loss of operating flexibility. The HETS of rotating disk contactor (RDC) is 1 to 2 m (3.2 to 6.4 ft). More elaborate staged extractors bring this down to 0.35 to 1.0 m (1.1 to 3.3 ft).

CHOICE OF DISPERSED PHASE

It is difficult to disperse a liquid when it occupies more than 75 percent of the volume. Otherwise, either liquid can be made continuous in a stirred tank by charging that liquid first, starting the agitator, and introducing the liquid to be dispersed. Customarily, the phase with the higher volumetric rate is dispersed since a larger interfacial area results in this way with a given droplet size. When a reactant diffuses away from a phase, that phase should be dispersed since the travel path then will be lower. In equipment that is subject to backmixing, such as spray or packed towers but not tray towers, the dispersed phase is the one with the smaller volumetric rate. When a substantial difference is known to exist for the two phases, the high phase resistance should be compensated for with increased surface by dispersion. The continuous phase should be the one that wets the material of construction. Usually, it is best to disperse a highly viscous phase. Since the holdup of continuous phase is greater, the phase that is less hazardous or less expensive should be continuous.

Experimentally, both modes probably should be tried. In the alkylation of C_4s with sulfuric acid, for instance, the continuous emulsion of acid produces a much better product and consumes less acid.

REFERENCES FOR LIQUID/LIQUID REACTORS

Hanson, C., ed., *Recent Advances in Liquid-Liquid Extraction,* Pergamon, 1971, pp. 429–453. Lo, T. C., M. H. I. Baird, and C. Hanson, eds., *Handbook of Solvent Extraction,* Wiley, 1983, pp. 37–52, 615–618. Rase, H. F., *Chemical Reactor Design for Process Plants,* vol. 1, Wiley, 1977, pp. 715–733.

GAS/LIQUID/SOLID REACTIONS

In many important cases of reactions involving gas, liquid, and solid phases, the solid phase is a porous catalyst. It may be in a fixed bed or it may be suspended in the fluid mixture. In general, the reaction occurs either in the liquid phase or at the liquid/solid interface. In fixed-bed reactors the particles have diameters of about 3 mm (0.12 in) and occupy about 50 percent of the vessel volume. Diameters of suspended particles are limited to 0.1 to 0.2 mm (0.004 to 0.008 in) minimum by requirements of filterability and occupy 1 to 10 percent of the volume in stirred vessels.

A list of 74 GLS reactions with literature references has been compiled by Shah (*Gas-Liquid-Solid Reactions,* McGraw-Hill, 1979), classified into groups where the solid is a reactant, or a catalyst, or inert. A list of 75 reactions made by Ramachandran and Chaudhari (*Three-Phase Chemical Reactors,* Gordon and Breach, 1983) identifies reactor types, catalysts, temperature, and pressure. They classify the processes according to hydrogenation of fatty oils, hydrodesulfurization, Fischer-Tropsch reactions, and miscellaneous hydrogenations and oxidations.

Some contrasting characteristics of the main kinds of three-phase reactors are summarized in Table 23-15. In *trickle bed reactors* both phases usually flow down, the liquid as a film over the packing. In *flooded reactors,* the gas and liquid flow upward through a fixed bed. *Slurry reactors* keep the solids in suspension mechanically; the overflow may be a clear liquid or a slurry, and the gas disengages from the vessel. The fluidized three-phase mixture is pumped through an *entrained solids reactor* and the effluent is separated into its phases in downstream equipment. In petroleum cracking technology this kind of equipment is called a *transfer line reactor.* In *fluidized bed reactors,* a stable bed of solids is maintained in the vessel and only the fluid phases flow through, except for entrained very fine particles. Most of the concern in this section is with trickle bed reactors, but some superior features of the other types are cited.

OVERALL RATE EQUATIONS WITH DIFFUSIONAL RESISTANCES

Say the concentration of dissolved gas A is A^*. The series rates involved are from the gas to the interface where the concentration is A_i and from the interface to the surface of catalyst where the concentration is A_s and where the reaction rate is $\eta w k_m A_s^m$. At steady state,

$$r_A = k_L a_B (A^* - A_i) = k_s a_p (A_i - A_s) = \eta w k_m A_s^m \qquad (23\text{-}107)$$

For a first-order reaction, $m = 1$, the catalyst effectiveness η is independent of A_s, so that after elimination of A_i and A_s the explicit solution for the rate is

$$r_A = A^* \left[\frac{1}{k_L a_B} + \frac{1}{k_s a_p} + \frac{1}{\eta w k_1} \right]^{-1} \qquad (23\text{-}108)$$

TABLE 23-15 Characteristics of Gas/Liquid/Solid Reactors

Property	Trickle bed	Flooded	Stirred tank	Entrained solids	Fluidized bed
Gas holdup	0.25–0.45	Small	0.2–0.3		
Liquid holdup	0.05–0.25	High	0.7–0.8		
Solid holdup	0.5–0.7		0.01–0.10		0.5–0.7
Liquid distribution	Good only at high liquid rate		Good	Good	Good
RTD, liquid phase	Narrow	Narrower than for entrained solids reactor	Wide	Wide	Narrow
RTD, gas phase	Nearly plug flow		Backmixed	Backmixed	Narrow
Interfacial area	20–50% of geometrical	Like trickle bed reactor	100–1,500 m^2/m^3	100–400 m^2/m^3	Less than for entrained solids reactor
MTC, gas/liquid	High		Intermediate		
MTC, liquid/solid	High		High		
Radial heat transfer	Slow		Fast	Fast	Fast
Pressure drop	High with small d_p		Hydrostatic head		

Analytical solutions also are possible when η is constant and $m = 0$, ½, or 2. More complex chemical rate equations will require numerical solutions. Such rate equations are applied to the sizing of plug flow, CSTR, and dispersion reactor models by Ramachandran and Chaudhari (*Three-Phase Chemical Reactors,* Gordon and Breach, 1983).

TRICKLE BEDS

The catalyst is a fixed bed. Flows of gas and liquid are cocurrent downwards. Liquid feed is at such a low rate that it is distributed over the packing as a thin film and flows by gravity, helped along by the drag of the gas. This mode is suited to reactions that need only short reaction times, measured in seconds, short enough to forestall undesirable side reactions such as carbon formation. In the simplest arrangement the liquid distributor is a perforated plate with about 10 openings/dm^2 (10 openings/15.5 in^2) and the gas enters through several risers about 15 cm (5.9 in) high. More elaborate distributor caps also are used. Thicknesses of liquid films have been estimated to vary between 0.01 and 0.2 mm (0.004–0.008 in).

Liquid holdup is made up of a dynamic fraction, 0.03 to 0.25, and a stagnant fraction, 0.01 to 0.05. The high end of the stagnant fraction includes the liquid that partially fills the pores of the catalyst. The effective gas/liquid interface is 20 to 50 percent of the geometric surface of the particles, but it can approach 100 percent at high liquid loads with a consequent increase of reaction rate as the amount of wetted surface changes.

Both phases are substantially in plug flow. Dispersion measurements of the liquid phase usually report Peclet numbers, $u_L d_p/D$, less than 0.2. With the usual small particles, the wall effect is negligible in commercial vessels of a meter or so in diameter, but may be appreciable in lab units of 50 mm (1.97 in) diameter. Laboratory and commercial units usually are operated at the same space velocity, LHSV, but for practical reasons the lengths of lab units may be only 0.1 those of commercial units.

Countercurrent gas flow is preferred in pollution control when removal of gaseous impurities is desired.

Trickle Bed Hydrodesulfurization The first large-scale application of trickle bed reactors was to the hydrodesulfurization of petroleum oils in 1955. The temperature is elevated to enhance the specific rate and the pressure is elevated to improve the solubility of the hydrogen. A large commercial reactor may have 20 to 25 m (66 to 82 ft) total depth of catalyst, and may be up to 3 m (9.8 ft) diameter in several beds of 3 to 6 m (9.8 to 19.7 ft), limited by the crushing strength of the catalyst and the need for cold shots. Each bed is adiabatic, but the rise in temperature usually is limited to 30°C (86°F) by injection of cold hydrogen between beds. Conditions depend on the boiling range of the oil. Pressures are 34 to 102 atm (500 to 1,500 psi), temperatures 345 to 425°C (653 to 797°F). Catalyst granules are 1.5 to 3.0 mm (0.06 to 0.12 in), sometimes a little more. Catalysts are 10 to 20 percent Co and Mo on alumina.

Limiting flow rates are listed in Table 23-16. The residence times of the combined fluids are figured for 50 atm (735 psi), 400°C (752°F), and a fraction free volume between particles of 0.4. In a 20-m (66-ft) depth, accordingly, the contact times range from 6.9 to 960 s in commercial units. In pilot units the packing depth is reduced to make the contact times about the same.

An apparent first-order specific rate increases with liquid rate as the fraction of wetted surface improves. Catalyst effectiveness of particles 3 to 5 mm (0.12 to 0.20 in) diameter has been found to be about 40 to 60 percent.

A case study has been made (Rase, *Chemical Reactor Design for Process Plants,* vol. 2, Wiley, 1977, pp. 179–182) for removing 50 percent of the 1.9 percent sulfur from a 0.92 SG oil at the rate of 24,000 bbl/d with 2,300 SCF H_2/bbl at 375°C (707°F) and 50 atm (735 psi). For a particular catalyst, the bed height was 8.75 m (29 ft) and the diameter 2.77 m (9.09 ft).

Figure 23-39 is a sketch of a unit to handle 20,000 bbl/d of a light cracker oil with a gas stream containing 75% H_2. Liquid rate was 115,000 kg/h (253,000 lbm/h), gas rate 12,700 kg/hr (28,000 lbm/h), catalyst charge 40,000 kg (88,000 lbm) or 45 m^3 (1600 ft^3), LHSV ≅ 3. Operating conditions were 370°C (698°F) and 27 atm (397 psi). Vessel dimensions were not revealed, but with an $H/D = 5$, the catalyst bed will have the dimensions 2.25 × 11.25 m (7.38 × 36.9 ft).

FLOODED FIXED BED REACTORS

When the gas and liquid flows are cocurrent upward, a screen is needed at the top to retain the catalyst particles. Such a unit has been used for the hydrogenation of nitro and double bond compounds and

TABLE 23-16 Hydrodesulfurization Feed Rates of Gas and Liquid and Residence Times of the Mixture

	Superficial liquid velocity		Superficial gas velocity				Residence time s/m	
			ft/h (STP)		kg/m^2·s			
	ft/h	kg/m^2·s	A*	B*	A*	B*	A	B
Pilot plant†	1–30	0.08–2.5	180–5,400	890–27,000	0.0013–0.040	0.0066–0.20	480–16	97–3.5
Commercial reactor	10–300	0.8–25	1,800–54,000	8900–270,000	0.013–0.40	0.066–2.0	48–1.6	9.7–0.35

*The values of gas velocity are shown for (A) 1,000 and (B) 5,000 std ft^3 of H_2 per barrel, assuming that all the oil is in the liquid phase. To convert ft^3/bbl to m^3/m^3, multiply by 0.178.

†The length of the pilot-plant reactor was assumed to be one-tenth the length of the commercial reactor.

SOURCE: Partly after Satterfield, *AIChE Journal,* **21,** 209–228 (1975).

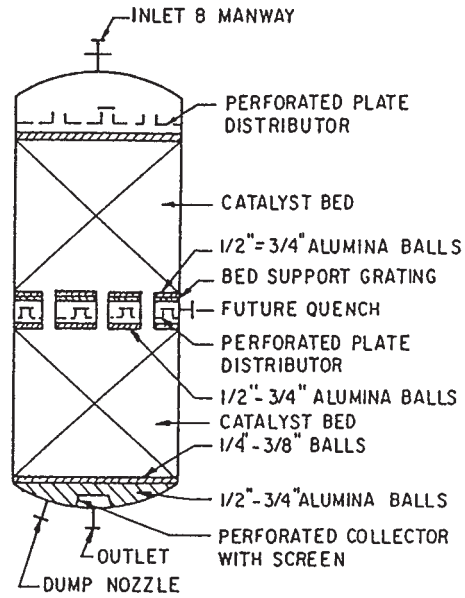

FIG. 23-39 Trickle bed reactor for hydrotreating 20,000 bbl/d of light catalytic cracker oil at 370°C and 27 atm. To convert atm to kPa, multiply by 101.3. (*Gianetto and Silveston,* Multiphase Chemical Reactors, *Hemisphere, 1986, pp. 533–563.*)

nitriles (Ovcinnikov et al., *Brit. Chem. Eng.,* **13,** 1,367 [1968]). High gas rates can cause movement and attrition of the particles. Accordingly, such equipment is restricted to low gas flow rates; for instance, where a hydrogen atmosphere is necessary but the consumption of hydrogen is slight. Backmixing is substantial in commercial-size columns, but less than in bubble columns. Liquid distribution is not a problem, and heat transfer is much better than in the trickle vessel. Liquid holdup and residence times are greater under flooding conditions, which may encourage side reactions.

Downward flow of both fluids imposes no restriction on the gas rate, except that the pressure drop will be high. On the whole, the trickle bed is preferred to the flooded bed.

SUSPENDED CATALYST BEDS

There are three main types of three-phase (GLS) reactors in which the catalyst particles move about in the fluid, as follows.

Slurry Reactors with Mechanical Agitation The catalyst may be retained in the vessel or it may flow out with the fluid and be separated from the fluid downstream. In comparison with trickle beds, high heat transfer is feasible, and the residence time can be made very great. Pressure drop is due to sparger friction and hydrostatic head. Filtering cost is a major item.

Entrained Solids Bubble Columns with the Solid Fluidized by Bubble Action The three-phase mixture flows through the vessel and is separated downstream. Used in preference to fluidized beds when catalyst particles are very fine or subject to disintegration in process.

GLS Fluidized with a Stable Level of Catalyst Only the fluid mixture leaves the vessel. Gas and liquid enter at the bottom. Liquid is continuous, gas is dispersed. Particles are larger than in bubble columns, 0.2 to 1.0 mm (0.008 to 0.04 in). Bed expansion is small. Bed temperatures are uniform within 2°C (3.6°F) in medium-size beds, and heat transfer to embedded surfaces is excellent. Catalyst may be bled off and replenished continuously, or reactivated continuously. Figure 23-40 shows such a unit.

In the reactor shown in Fig. 23-41, a stable fluidized bed is maintained by recirculation of the mixed fluid through the bed and a draft tube. An external pump sometimes is used instead of the built-in impeller shown. Such units were developed for the liquefaction of coal and are called *ebullating beds.*

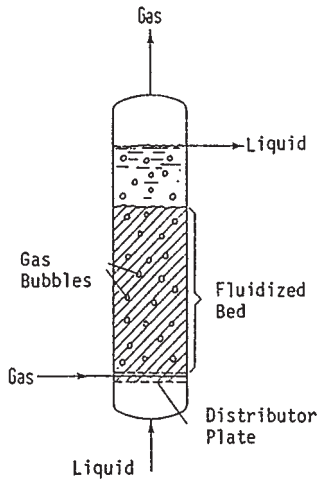

FIG. 23-40 Three-phase fluidized bed reactor.

Three-phase fluidized bed reactors are used for the treatment of heavy petroleum fractions at 350 to 600°C (662 to 1,112°F) and 200 atm (2,940 psi). A biological treatment process (Dorr-Oliver Hy-Flo) employs a vertical column filled with sand on which bacterial growth takes place while waste liquid and air are charged. A large interfacial area for reaction is provided, about 33 cm^2/cm^3 (84 in^2/in^3), so that an 85 to 90 percent BOD removal in 15 min is claimed compared with 6 to 8 h in conventional units.

TRICKLE BED PARAMETERS

Numerous studies have been made of the hydrodynamics and other aspects of the behavior of gas/liquid/solid systems, in particular of trickle beds, and including absorption and extraction in packed beds. Some of the literature is reviewed in the references at the end of this subsection.

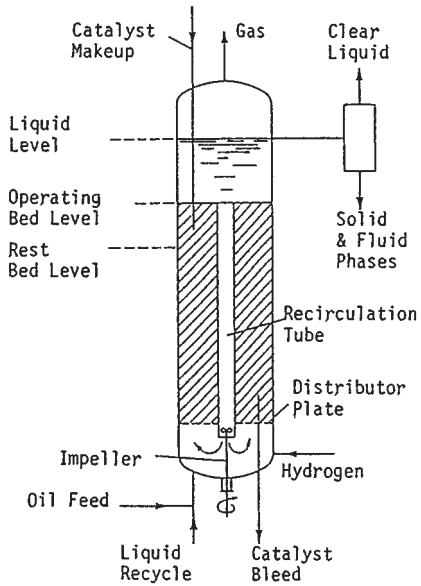

FIG. 23-41 Gas/liquid fluidized (ebullating) bed reactor for hydroliquefaction of coal. (*Kampiner, in Winnacker-Keuchler,* Chemische Technologie, *vol. 3, Hanser, 1972, p. 252.*)

Although many processes have progressed satisfactorily through the laboratory, pilot plant, and commercial scales, design from first principles and scale-up procedures have proved elusive. The various pieces of this puzzle that will be cited in this section, however, do tell us some of what is going on and should aid in the appraisal of the effects of changes in capacity and operating conditions of existing units.

Pressure Drop Some models regard trickle bed flow as analogous to gas/liquid flow in pipe lines. Various flow regimes may exist like those typified in Fig. 23-25*l* but in a vertical direction. The two-phase ΔP_{GL} is related to the pressure drops of the individual phases on the assumptions that they are flowing alone. The relation proposed by Larkin et al. (*AIChE Journal,* **7,** 231 [1961]) is

$$\ln \frac{\Delta P_{GL}}{\Delta P_L + \Delta P_G} = \frac{5.0784}{3.531 + (\ln X)^2}$$

$$X = \sqrt{\frac{\Delta P_L}{\Delta P_G}}, \qquad 0.05 \le X \le 30 \qquad (23\text{-}109)$$

Several other correlations are cited in the literature, some of which agree with the one quoted here. Pressure drop usually is not a major factor in the design of a trickle bed.

Example 6: Conditions of a Trickle Bed A system has the properties of air/water at room conditions. Liquid is at 0.5 cm/s, gas at 10 cm/s, free volume fraction $\varepsilon_B = 0.4$, particle diameter $d_p = 0.5$ cm. The pressure drops by one of the many correlations for packed bed flow are $\Delta P_L = 217$, $\Delta P_G = 100$, so that $X = 1.47$ and $\Delta P_{GL} = 1{,}270$ N/m^3, Newtons/m^3 or 0.0124 atm/(m^2·m).

Liquid Holdup The major factor influencing this property is the liquid flow rate, but the shape, size, and wetting characteristics of the particles and the gas rate and the initial distribution of liquid also enter in. One of the simpler correlations is that of Midoux et al. (*J. Chem. Eng. Japan,* **9,** 350 [1976]).

$$\frac{\varepsilon_L}{\varepsilon_B} = \frac{0.66X^{0.81}}{1 + 0.66X^{0.81}}, \qquad 0.1 \le X \le 80 \qquad (23\text{-}110)$$

where ε_B is the bed porosity. For Example 6 with $X = 1.47$ and $\varepsilon_B = 0.4$,

$$\varepsilon_L = 0.4(0.474) = 0.190$$

A correlation due to Sato (*J. Chem. Eng. Japan,* **6,** 147 [1973]) is

$$\frac{\varepsilon_L}{\varepsilon_B} = 0.185\left[\frac{6(1-\varepsilon_B)}{d_p}\right]^{1/3} X^{0.22} = 0.3659 \qquad (23\text{-}111)$$

for the same example. There are also correlations for the static holdup; that is, when the flow rate is zero after wetting. For nonporous catalysts, usually $\varepsilon_{static} < 0.05$.

Gas/Liquid Mass Transfer This topic has been widely investigated for gas absorption in packed beds, usually countercurrent. One correlation for cocurrent flow in catalyst beds is by Sato et al. (*First Pacific Chemical Engineering Congress,* Pergamon, 1972, p. 187):

$$k_L a_B = 6.185(10^{-3}) d_p^{-0.5} u_L^{0.8} u_G^{0.8}, \qquad 1/\text{s}$$

For Example 6, this gives $k_L a_B = 8.8(10^{-3})$/s.

Gas/Liquid Interfacial Area This has been evaluated by measuring absorption rates like those of CO_2 in NaOH. A correlation by Charpentier (*Chem. Eng. Journal,* **11,** 161 [1976]) is

$$\frac{a_B}{a_p(1-\varepsilon_B)} = 0.05\left[\frac{\Delta P_{GL}\varepsilon_B}{a_p(1-\varepsilon_B)}\right]^{1.2} \qquad (23\text{-}112)$$

With $a_p = 6/d_p = 1{,}200$/m, $\varepsilon_B = 0.4$, and $\Delta P_{GL} = 1{,}260$ N/m^3,

$$a_B = 0.05(1{,}200)(0.6)\left[\frac{1{,}260(2/3)}{1{,}200}\right]^{1.2} = 23.5 \text{ m}^2/\text{m}^3$$

For comparison, the geometrical area of the particles is

$$a_{geom} = \frac{6(1-\varepsilon_B)}{d_p} = \frac{6(0.6)}{0.005} = 72 \text{ m}^2/\text{m}^3$$

Liquid/Solid Mass Transfer The dissolved gas and the solvent react in contact with the surface of the catalyst. For studying the rate of transfer to the surface, an often-used system was benzoic acid or naphthalene in contact with water. A correlation of Dharwadkar and Sylvester (*AIChE Journal,* **23,** 376 [1977]) that agrees well with some others is

$$k_s = 1.637 u_L \text{Re}_L^{-0.331} \left(\frac{\rho_L D}{\mu_L}\right)^{2/3} \qquad (23\text{-}113)$$

For the example with diffusivity of oxygen $D = 2.1(10^{-5})$ cm^2/s,

$$k_s = 1.637(0.1)\left[\frac{0.5(0.1)(1)}{0.01}\right]^{-0.331}\left[\frac{1(2.1)(10^{-5})}{0.01}\right]^{2/3}$$

$$= 1.7(10^{-3}) \text{ cm/s}$$

Axial Dispersion and the Peclet Number Peclet numbers are measures of deviation from plug flow. They may be calculated from residence time distributions found by tracer tests. Their values in trickle beds are ⅓ to ⅙ those of flow of liquid alone at the same Reynolds numbers. A correlation by Michell and Furzer (*Chem. Eng. J.,* **4,** 53 [1972]) is

$$\text{Pe}_L = \frac{u_L d_p}{D_{EL}} = \left(\frac{\text{Re}_L}{\varepsilon_L}\right)^{0.7}\left(\frac{\mu_L^2}{d_p^3 g \rho_L^2}\right)^{0.32} \qquad (23\text{-}114)$$

where D_{EL} is the axial dispersion coefficient of the liquid, cm^2/s. In the range of Re = 10 to 100, the Peclet number is in the range 0.2 to 0.6 cm^2/s (0.03 to 0.09 in^2/s). It is insensitive to the kind of packing and to the gas flow. Gas-phase dispersions also have been measured and found to be one or two orders of magnitude less than in single-phase gas flows.

Plug flow is approached at low values of the dispersion coefficient or high values of Peclet number. A criterion developed by Mears (*Chem. Eng. Sci.,* **26,** 1361 [1971]) is that conversion will be within 5 percent of that predicted by plug flow when

$$\text{Pe} = \frac{u_L L}{D} > 20\, n \ln \frac{1}{1 - x_B} \qquad (23\text{-}115)$$

where n is the order of the reaction with respect to B and x_B is the fractional conversion of B. For instance, when $L = 100$ cm, $n = 1$, $u_L = 0.8$ cm/s, and $x_B = 0.96$, then $D = 1.25$ cm^2/s. Note that the Pe numbers of the last two equations do not have the same linear term.

References for Gas/Liquid/Solid Reactions

de Lasa, H. I., *Chemical Reactor Design and Technology,* Martinus Nijhoff, 1986. Gianetto, A., and P. L. Silveston, eds., *Multiphase Chemical Reactors,* Hemisphere, 1986. Ramachandran, P. A., and R. V. Chaudhari, *Three-Phase Chemical Reactors,* Gordon & Breach, 1983. Rodrigues, A. E. et al., eds., *Multiphase Chemical Reactors,* vol. 2, Sijthoff & Noordhoff, 1981. Satterfield, C. N., "Trickle Bed Reactors," *AIChE Journal,* **21,** 209–228 (1975). Shah, Y. T., *Gas-Liquid-Solid Reactor Design,* McGraw-Hill, 1979.

REACTIONS OF SOLIDS

Many reactions of solids are industrially feasible only at elevated temperatures which are often obtained by contact with combustion gases, particularly when the reaction is done on a large scale. A product of reaction also is often a gas that must diffuse away from a remaining solid, sometimes through a solid product. Thus, thermal and mass-transfer resistances are major factors in the performance of solid reactions.

There are a number of commercial operations where the object is to make useful products with solid reactions. Design and practice, however, do not appear to rely generally on sophisticated kinetics, and they are rarely divulged completely. The desirable information is about temperatures, configuration, quality of mixing, and residence times or space velocities. Most of the information about current practice of reactions of solids is proprietary. Some of the sparse published data can

be cited. Scientific data for solid reactions are abundant but not very coherent. The same data can be fitted, equally badly, by several models. Nevertheless, quotation of some of those kinetic and mechanistic conclusions from the literature may throw some light on these processes. Some data for reactions of solids are shown in Fig. 23-42.

THERMAL DECOMPOSITIONS

All substances are unstable above certain temperatures. The main theory of the rates of decomposition of solids is that they begin at positions of strain on the surface, called *nuclei* or *active sites;* as the reaction progresses, the number of nuclei and their sizes grow. In accordance with this theory the conversion varies as some power of the time, that is, as t^n, where n commonly assumes a value of 3 to 6 but the range is from about 1 to 8. Other rate expressions also have been fitted to certain results. Activation energies represented by the Arrhenius equation sometimes change during the course of a reaction, indicating a change of mechanism.

Decompositions may be exothermic or endothermic. Solids that decompose without melting upon heating are mostly such that can give rise to gaseous products. When a gas is made, the rate can be affected by the diffusional resistance of the product zone. Particle size is a factor. Aging of a solid can result in crystallization of the surface that has been found to affect the rate of reaction. Annealing reduces strains and slows any decomposition rates. The decompositions of some fine powders follow a first-order law. In other cases, the decomposed fraction x is in accordance with the Avrami-Erofeyev equation (cited by Galwey, *Chemistry of Solids,* Chapman Hall, 1967)

$$-\ln (1 - x) = kt^n \tag{23-116}$$

with n = 3.5 to 4. Another rule of simple form also cited by Galwey that sometimes applies is

$$x = k(t - t_1)^n \tag{23-117}$$

with n as great as 6. The equation of Prout and Tompkins is of autocatalytic form,

$$\frac{dx}{dt} = kx(1 - x), \qquad \ln \frac{x}{1 - x} = kt + C \tag{23-118}$$

It states that the rate is proportional to the fraction x that has decomposed (which is dominant early in the reaction) and to the fraction not decomposed (which is dominant in latter stages of reaction). The decomposition of potassium permanganate and some other solids is in accordance with this equation. The shape of the plot of x against t is sigmoid in many cases, with slow reactions at the beginning and end, but no theory has been proposed that explains everything.

Organic Solids A few organic compounds decompose before melting, mostly nitrogen compounds: azides, diazo compounds, and nitramines. The processes are exothermic, classed as explosions, and may follow an autocatalytic law. Temperature ranges of decomposition are mostly 100 to 200°C (212 to 392°F). Only spotty results have been obtained, with no coherent pattern. The decomposition of malonic acid has been measured for both the solid and the supercooled liquid. The first-order specific rates at 126.3°C (259.3°F) were 0.00025/min for solid and 0.00207 for liquid, a ratio of 8; at 110.8°C (231.4°F), the values were 0.000021 and 0.00047, a ratio of 39. The decomposition of oxalic acid (m.p. 189°C) obeyed a zero-order law at 130 to 170°C (266 to 338°F).

Exothermic Decompositions These decompositions are nearly always irreversible. Solids with such behavior include oxygen-containing salts and such nitrogen compounds as azides and metal styphnates. When several gaseous products are formed, reversal would require an unlikely complex of reactions. Commercial interest in such materials is more in their storage properties than as a source of desirable products, although ammonium nitrate is an important explosive. A few typical examples will be cited to indicate the ranges of reaction conditions. They are taken from the review by Brown et al. ("Reactions in the Solid State," in Bamford and Tipper, *Comprehensive Chemical Kinetics,* vol. 22, Elsevier, 1980).

Silver oxalate decomposes smoothly and completely in the range 100 to 160°C (212 to 320°F). One investigation showed $x = k(t - t_1)^n$ with n = 3.5 to 4, and an activation energy of 27 kcal/g mol (48,600 Btu/lb mol).

Ammonium chromates and some other solids exhibit aging effects. Material that has been stored for months or years follows a cubic law with respect to time, but fresh materials are about fifth-order. At 199°C (390°F), the Prout-Tompkins law was followed.

Ammonium nitrate decomposes into nitrous oxide and water. In the solid phase, decomposition begins at about 150°C (302°F) but becomes extensive only above the melting point (170°C) (338°F). The reaction is first-order, with activation energy about 40 kcal/g mol (72,000 Btu/lb mol). Traces of moisture and Cl^- lower the decomposition temperature; thoroughly dried material has been kept at 300°C (572°F). All oxides of nitrogen, as well as oxygen and nitrogen, have been detected in decompositions of nitrates.

Styphnic acid is a nitrogen compound. Lead styphnate monohydrate was found to detonate at 229°C (444°F), but the course of decomposition could be followed at 228°C and below.

Many investigations are reported on azides of barium, calcium, strontium, lead, copper, and silver in the range 100 to 200°C (212 to 392°F). Time exponents were 6 to 8 and activation energies of 30 to 50 kcal/g mol (54,000 to 90,000 Btu/lb mol) or so. Some difficulties with reproducibility were encountered with these hazardous materials.

Endothermic Decompositions These decompositions are mostly reversible. The most investigated substances have been hydrates and hydroxides, which give off water, and carbonates, which give off CO_2. Dehydration is analogous to evaporation, and its rate depends on the moisture content of the gas. Activation energies are nearly the same as reaction enthalpies. As the reaction proceeds in the particle, the rate of reaction is impeded by resistance to diffusion of the water through the already formed product. A particular substance may have several hydrates. Which one is present will depend on the partial pressure of water vapor in contact. $FeCl_2$, for instance, combines with 4, 5, 7, or 12 molecules of water with melting points ranging from about 75 to 40°C (167 to 104°F).

Dehydration of $CuSO_4$ pentahydrate at 53 to 63°C (127 to 145°F) and of the trihydrate at 70 to 86°C (158 to 187°F) obey the Avrami-Erofeyev equation. The rate of water loss from $Mg(OH)_2$ at lower temperatures is sensitive to partial pressure of water. Its decomposition above 297°C (567°F) yields appreciable amounts of hydrogen and is not reversible.

Carbonates decompose at relatively high temperatures, 660 to 740°C (1,220 to 1,364°F) for $CaCO_3$. When large samples are used the rate of decomposition can be controlled by the rate of heat transfer or the rate of CO_2 removal.

Some ammonium salts decompose reversibly with release of ammonia, for example,

$$(NH_4)_2SO_4 \Leftrightarrow NH_4HSO_4 + NH_3$$

at 250°C (482°F). Further heating can release SO_3 irreversibly.

The decomposition of silver oxide was one of the earliest solid reactions studied. It is smoothly reversible below 200°C (392°F) with equation for partial pressure of oxygen,

$$\frac{dp}{dt} = k\left(\frac{1 - p}{p_{\text{equilib}}}\right)$$

The reaction is sensitive to the presence of metallic silver at the start, indicating autocatalysis, and to the presence of silver carbonate, which was accidentally present in some investigations.

SOLID REACTION EXAMPLES

Diffusion of ions or molecules in solids is preliminary to reaction. It takes place through the normal crystal lattices of reactants and products as well as in channels and fissures of imperfect crystals. It is slow in comparison with that in fluids even at the elevated temperatures at which such reactions have to be conducted. In cement manufacture, for instance, reaction times are 2 to 3 h at 1,200 to 1,500°C (2,192 to 2,732°F) even with 200-mesh particles.

Large contact areas between solid phases are essential. For experimental purposes they are enhanced by forming and mixing fine powders and compressing them. The practices of powder metallurgy are

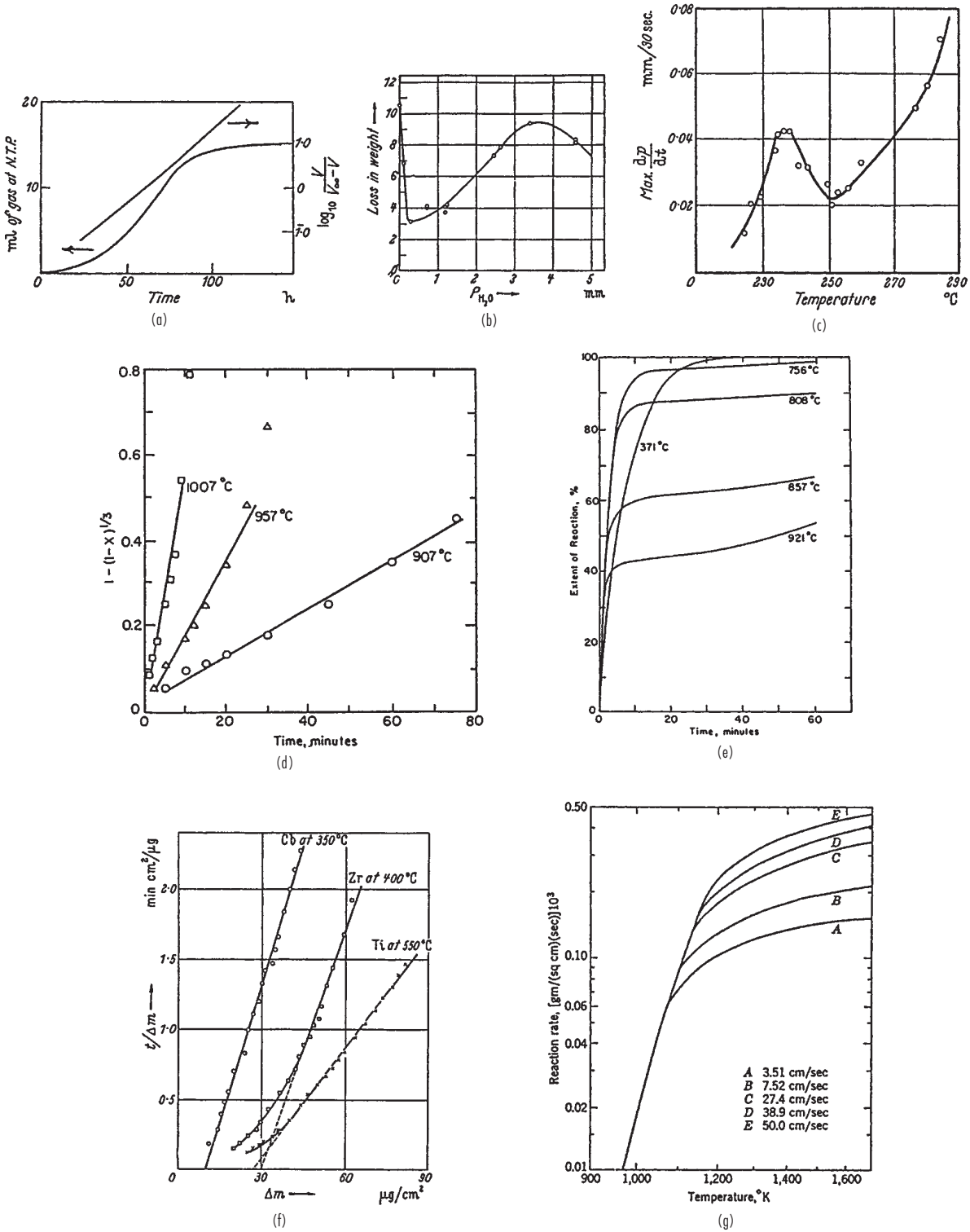

FIG. 23-42 Data for reactions of solids. (*a*) Thermal decomposition of 2-nitrobenzene-4-diazo-1 oxide at 99.1°C (*Vaughan and Williams,* J. Chem. Soc., *p. 1,560* [*1946*]). (*b*) Decomposition of $CuSO_4 \cdot 5H_2O$; the first four molecules are removed easily, the last with difficulty (*Kohlschutter and Nitschmann, 1931*). (*c*) Decomposition of ammonium perchlorate (*Bircumshaw and Newman,* Proc. Roy. Soc., ***A227,*** *228* [*1955*]). (*d*) Reduction of hematite by graphite in the presence of lithium oxide catalyst (*Rao,* Met. Trans., **2,** *1439* [*1971*]). (*e*) Reduction of nickel oxide by hydrogen; sintering begins just above 750°C (*Hashimoto and Silveston,* AIChE Journal, ***19,*** *268* [*1973*]). (*f*) Oxidation of metals, examples of parabolic law, with rate inversely proportional to the weight gain (*Gulbransen and Andrew,* Trans. Electrochem. Soc., ***96,*** *364* [*1949*]). (*g*) Effect of air velocity on combustion of carbon (*Tu et al.,* Ind. Eng. Chem., ***26,*** *749* [*1934*]).

examples, where particles are 0.1 to 1,000 μm and pressures are 138 to 827 MPa (20,000 to 60,000 psi). Apart from research laboratories, reactions of solids occur in ceramic, metallurgical, and other technologies. Commercial processes of this category include:

- Cement manufacturing
- Boron carbide from boron oxide and carbon
- Calcium silicate from lime and silica
- Calcium carbide by reaction of lime and carbon
- Leblanc soda ash

A limited number of laboratory results of varied nature will be cited for perspective. The mechanism of formation of zinc ferrite,

$$ZnO + Fe_2O_3 \Rightarrow ZnFe_2O_4$$

has been extensively studied at up to 1,200°C (2,192°F). At some lower temperatures the ZnO is the mobile phase and migrates to coat the Fe_2O_3 particles. In the reaction $MgO + Fe_2O_3 \Rightarrow MgFe_2O_4$, the MgO likewise is the mobile phase. There, smaller particles (<1 μm) obeyed the power law $x = k \ln t$, but larger ones had a more complex behavior. In the reaction

$$2AgI + HgI_2 \Rightarrow Ag_2HgI_4$$

nearly equivalent amounts of the ions Ag^+ and Hg^{2+} migrating in opposite directions arrived at their respective interfaces after 66 days at 65°C (149°F).

For the reaction $KClO_4 + 2C \Rightarrow KCl + CO_2$, fine powders were compressed to 69 MPa (10,000 psi) and reacted at 350°C (662°F), well below the 500°C (932°F) melting point. The kinetic data were fitted by the equation

$$\frac{dx}{dt} = k(a-x)^{2/3}x^{-1/3}$$

The term $(a-x)^{2/3}$ was included as a measure of the surface area of the oxidizing salt and the $x^{-1/3}$ term is associated with the reduction of contact area from product formation.

Several other reactions that yield gaseous products have attracted investigators because their progress is easily followed, for instance,

$$MnO_3 + 2MoO_3 \Rightarrow 2MnMoO_4 + 0.5O_2$$

where MoO_3 was identified as the mobile phase, and

$$Ca_3(PO_4)_2 + 5C \Rightarrow 3CaO + P_2 + 5CO$$

which obeyed the equation

$$-\ln(1-x) = kt$$

The reaction

$$CuCr_2O_4 + CuO \Rightarrow Cu_2Cr_2O_4 + 0.5O_2$$

eventually becomes diffusion-controlled and becomes described by

$$[1-(1-x)^{1/3}]^2 = k \ln t$$

In the case where two solid products are formed,

$$CsCl + NaI \Rightarrow CsI + NaCl$$

the rate-controlling step is the diffusion of iodide ion in CsCl.

The kinetic equation can vary with a number of factors. For the reaction between tricalcium phosphate and urea, relatively coarse material (–180+200 mesh) obeyed the law $x^2 = kt$ with E = 18 kcal/g mol (32,400 Btu/lb mol) and finer material (–300+320 mesh) obeyed a first-order equation with E = 28 kcal/g mol.

Carbothermic Reactions Some apparently solid/solid reactions with carbon apparently take place through intermediate CO and CO_2. The reduction of iron oxides has the mechanism

$$Fe_xO_y + yCO \Rightarrow xFe + yCO_2, \qquad CO_2 + C \Rightarrow 2CO$$

Some results of the reduction of hematite by graphite at 907 to 1,007°C in the presence of lithium oxide catalyst were correlated by the equation $1-(1-x)^{1/3} = kt$. The reaction of solids ilmenite and carbon has the mechanism

$$FeTiO_3 + CO \Rightarrow Fe + TiO_2 + CO_2, \qquad CO_2 + C \Rightarrow 2CO$$

and that between chromium oxide and chromium carbide,

$$\frac{1}{6}Cr_{23}O_6 + CO_2 \Rightarrow \frac{23}{6}Cr + 2CO, \qquad \frac{1}{3}Cr_2O_3 + CO \Rightarrow \frac{2}{3}Cr + CO_2$$

A similar case is the preparation of metal carbides from metal and carbon,

$$C + 2H_2 \Rightarrow CH_4, \qquad Me + CH_4 \Rightarrow MeC + 2H_2$$

SOLIDS AND GASES

Commercial processes of solid/gas reactions include:

- Oxidation with air of sulfides in ores to oxides or sulfates that are more easily processed for metal recovery.
- Conversion of Fe_2O_3 to magnetic Fe_3O_4 in contact with reducing atmosphere of CO in combustion gases.
- Chlorination of ores of uranium, titanium, zirconium and aluminum. For titanium, carbon also is needed:

$$TiO_2 + C + 2Cl_2 \Rightarrow TiCl_4 + CO_2$$

- Manufacture of hydrogen by action of steam on iron.
- Manufacture of blue gas by action of steam on carbon.
- Calcium cyanamide by action of atmospheric nitrogen on calcium carbide.
- Nitriding of steel.
- Atmospheric corrosion.
- Combustion of solid fuels.

A classification of processes can be made with respect to the nature of the reaction product, as follows:

1. The product is a gas, as in the reaction between finely divided nickel and CO which makes nickel carbonyl, boiling point 42°C.
2. The product is a loose solid that offers no appreciable diffusional resistance to the gas reactant.
3. The product is an adherent solid that may or may not be permeable to the gas reactant.
4. The reacting solid is in granular form. Decrease in the area of the reaction interface occurs as the reaction proceeds. The mathematical modeling is distinguished from that with flat surfaces, which are most often used in experimentation.

Literature A number of informative researches can be cited, but again the difficulties of experimentation and complicating factors have made the kinetic patterns difficult to generalize. The most investigated gas reactants have been oxygen and hydrogen and some chlorine systems.

When the product of reaction does not prove a barrier to further chemical change, the rate is constant, zero-order, and the weight of product is proportional to time,

$$w = kt$$

Such behavior is observed with alkali and alkaline earth oxidations where the oxide volume is less than the metal volume and cracks develop in the product coat, permitting ready access for further reaction.

Oxide films of Al and Cr, for instance, are protective beyond a small amount of reaction, since they are nonporous and adherent.

When the product layer is porous the reaction will continue but at decreasing rate as the diffusional resistance increases with increasing conversion. Then,

$$\frac{dw}{dt} = \frac{k}{w}$$

This rate expression is known as the *parabolic law.* It is obeyed by oxidation of Ni, Ti, Cu, and Cr and by halogenation of silver. The product coat retards both diffusion and heat transfer.

The behavior type may change with temperature range. For instance, oxidation of zinc above 350°C (662°F) obeys the parabolic law, but at lower temperature the product coat seems to develop cracks and the *logarithmic law,* $\ln w = kt$, is observed.

One mathematical model of the oxidation of nickel spheres was confirmed when it took into account the decrease in the reaction surface as the reaction proceeded.

EQUIPMENT AND PROCESSES

Reactions of solids of commercial interest almost always involve a gas as a reagent and/or a heat source. Some of the equipment in use is represented in Fig. 23-43. Temperatures are usually high so the

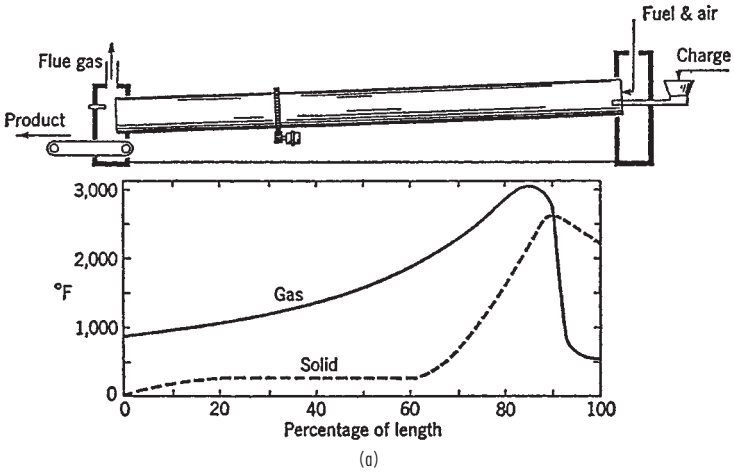

(a)

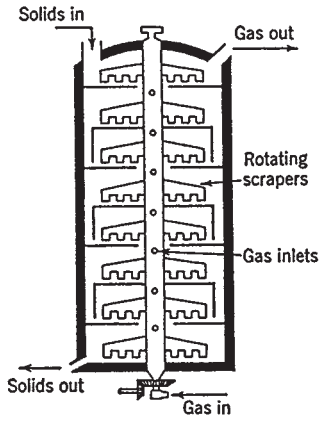

(b)

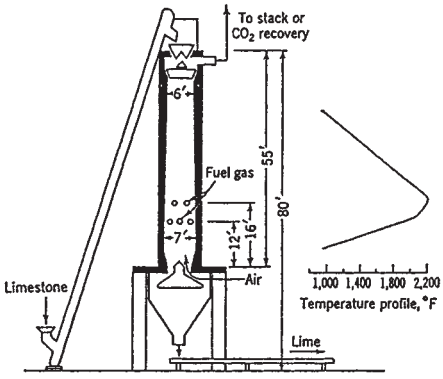

(c)

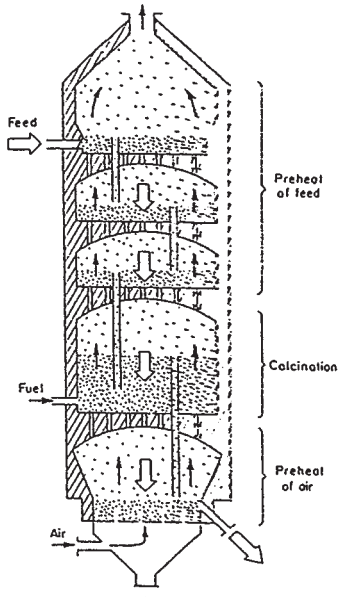

(d)

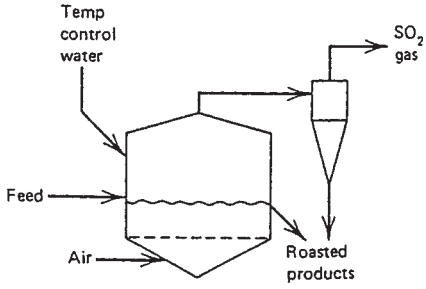

(e)

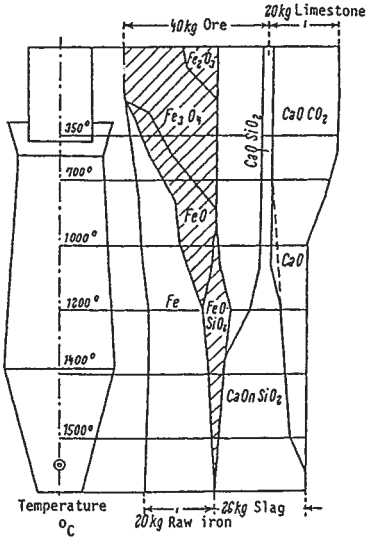

(f)

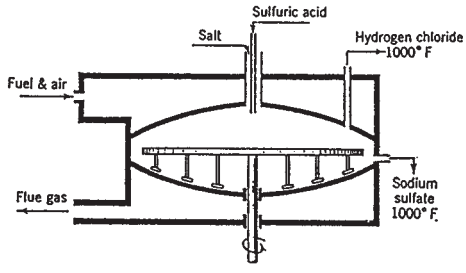

(g)

FIG. 23-43 Reactors for solids. (*a*) Temperature profiles in a rotary cement kiln. (*b*) A multiple hearth reactor. (*c*) Vertical kiln for lime burning, 55 ton/d. (*d*) Five-stage fluidized bed lime burner, 4 by 14 m, 100 ton/d. (*e*) A fluidized bed for roasting iron sulfides. (*f*) Conditions in a vertical moving bed (blast furnace) for reduction of iron oxides. (*g*) A mechanical salt cake furnace. To convert ton/d to kg/h, multiply by 907.

equipment is mostly refractory-lined. The solid is in granular form, at most a few mm or cm in diameter. Historically, much of the equipment was developed for the treatment of ores and the recovery of metals. More than 50 processes for reduction of iron ores, for instance, have been developed, although the clear winner is the blast furnace. This is a vertical moving-bed device; iron oxides and coal are charged at the top and flow countercurrently to combustion and reducing gases. Units of 1,080 to 4,500 m^3 (38,000 to 159,000 ft^3) may produce up to 9×10^6 kg (20×10^6 lbm) of molten iron per day. Figure 23-43*f* identifies the temperature and composition profiles (Blom, Stahl, and Eisen, **47,** 955 [1927]). Reduction is with CO and H_2 that are made from coal, air, and water within the reactor.

Pyrometallurgical Processes Such high temperature processes convert certain minerals into others for easier separation from gangue or for easier recovery of metal. They are accomplished in kilns, hearth furnaces or fluidized bed reactors.

Oxidation Proceeds according to the stoichiometry $MeS + 1.5O_2 \Rightarrow MeO + CO_2$. Applied to Fe, Pb, Cu, and Ni.

Calcining Proceeds according to $MeCO_3 \Rightarrow MeO + CO_2$. Applied to Ca, Mg, and Ba.

Sulfating $MeS + 2O_2 \Rightarrow MeSO_4$. Applied to Cu, of which the sulfate is water-soluble.

Chlorination $MeO + Cl_2 + C \Rightarrow MeCl_2 + CO$. Applied to Mg, Be, Ti, and Zr, whose chlorides are water-soluble. The chlorine can be supplied indirectly, as in $Cu_2S + 2NaCl + O_2 \Rightarrow 2CuCl + Na_2SO_4$.

Reduction $MeO + H_2 \Rightarrow Me + H_2O$, $MeO + CO \Rightarrow Me + CO_2$. Applied to Fe, W, Mo, Ge, and Zn.

Magnetic Roasting $Fe_2O_3 + CO \Rightarrow Fe_3O_4$. Recovered magnetically.

Rotary Kiln Equipment A rotary kiln is a long, narrow cylinder inclined 2 to 5 degrees to the horizontal and rotated at 0.25 to 5 rpm. It is used for the decomposition of individual solids, for reactions between finely divided solids, and for reactions of solids with gases or even with liquids. The length/diameter ratio ranges from 10 to 35, depending on the reaction time needed. The solid is in granular form and may have solid fuel mixed in. The granules are scooped into the vapor space and are heated as they cascade downwards. Holdup of solids is 8 to 15 percent of the cross section. For most free-falling materials, the solids pattern approaches plug flow axially and complete mixing laterally. Rotary kilns can tolerate some softening and partial fusion of the stock.

Approximate ranges of space velocities in rotary kilns, metric tons/(m^3·d), of selected processes are as follows:

Cement, dry process	0.4–1.1
Cement, wet process	0.4–0.8
Cement, with heat exchange	0.6–1.8
Lime burning	0.5–0.9
Dolomite burning	0.4–0.6
Pyrite roasting	0.2–0.35
Clay calcination	0.5–0.8
Magnetic roasting	1.5–2.0
Ignition of inorganic pigments	0.15–2.0
Barium sulfide preparation	0.35–0.8

Formulas for capacity and residence time in terms of operating conditions are due to Heiligenstaedt:

$$W = 148n\phi D^3 \tan \vartheta, \qquad \text{t/(m}^3\text{·d)} \qquad (23\text{-}119)$$

$$\tau = \frac{L}{60\pi nD \tan \vartheta}, \qquad \text{h} \qquad (23\text{-}120)$$

where n = rpm
ϕ = fraction of cross section occupied
D = diameter, m
L = length, m
ϑ = degrees inclination to the horizontal

High-temperature heat transfer from the gas is by radiation and convection.

Vertical Kilns These kilns are used primarily where no fusion or softening occurs, as in the burning of limestone or dolomite, although rotary kilns also are used for these operations. The blast furnace, Fig. 23-43*f,* is a vertical kiln in which fusion takes place in the lower section. A cross section of a continuous lime kiln is shown in Fig. 23-43*c* which is for 50,000 kg/day (110,000 lbm/d). The diameter range of these kilns is 2.4 to 4.5 m (7.9 to 14.8 ft) and height 15 to 24 m (49 to 79 ft). Peak temperatures in lime calcination are 1,200°C (2,192°F), although decomposition proceeds freely at 1,000°C (1,832°F). Fuel supply may be coke mixed and fed with the limestone or other fuel. Space velocity of the kiln is 14 to 25 kg CaO/(m^3·h) (0.87 to 1.56 lbm/[ft^2·h]) or 215 to 485 kg CaO/(m^2·h) (44 to 99 lbm/[ft^2·h]), depending on the size and modernity of the kiln, the method of firing, and the lump size, which is in the range of 10 to 25 cm (3.9 to 9.8 in). A five-stage fluidized bed calciner is sketched in Fig. 23-43*d.* Such a unit 4 m (13 ft) in diameter and 14 m (46 ft) high has a production of 91,000 kg CaO/d (200,000 lbm/d).

Cement Manufacture Kilns These kilns are up to 6 m (17 ft) in diameter and 200 m (656 ft) long. Inclination is 3 to 4 degrees, and rotation is 1.2 to 2.0 rpm. Typical temperature profiles are shown in Fig. 23-43*a.* Near the flame the temperature is 1,800 to 2,000°C (3272 to 3632°F). The temperature of the solid reaches 1,350 to 1,500°C (2,462 to 2,732°F) which is necessary for clinker formation. In one smaller kiln, a length of 23 m (75 ft) was allowed for drying, 34 m (112 ft) for preheating, 19 m (62 ft) for calcining, and 15 m (49 ft) for clinkering. Total residence time is 40 min to 5 h, depending on the type of kiln. The time near the clinkering temperature of 1,500°C (2,732°F) is 10 to 20 min. Subsequent cooling is as rapid as possible.

A kiln 6 m (20 ft) in diameter by 200 m (656 ft) can produce 2.7×10^6 kg/d (6×10^6 lbm/d) of cement. For production rates less than 270,000 kg/d (600,000 lbm/d), shaft kilns are used. These are vertical cylinders 2 to 3 m (6.5–10 ft) by 8 to 10 m (26–33 ft) high, fed with raw meal pellets and finely ground coal.

Roasting of Sulfide Ores In this process iron sulfide (pyrite) is burned with air for recovery of sulfur and to make the iron oxide from which the metal is more easily recovered. Sulfides of other metals also are roasted. The original kind of equipment was a multiple hearth furnace, as shown in Fig. 23-43*b.* In some designs the plates rotate, in others the scraper arms rotate, and in still others the arms oscillate and discharge the material to lower plates at each stroke. Material is charged at the top, moves along as the rotation proceeds, and drops onto successively lower plates while combustion gases or gaseous reactants flow upward. A reactor with 9 trays 5 m (16 ft) in diameter and 12 m (39 ft) high can roast about 600 kg/h (1,300 lbm/h) of pyrite. Another unit with 11 trays 2 m (7 ft) in diameter is said to have a capacity of 114,000 kg/d (250,000 lbm/d).

A major portion of the reaction is found to occur in the vapor space between trays. A unit in which most of the trays are replaced by empty space is called a *flash roaster;* its mode of operation is like that of a spray dryer.

Molybdenum sulfide is roasted at the rate of 5500 kg/d (12,000 lbm/d) in a unit with 9 stages, 5 m (16 ft) diameter, at 630 ± 15°C (1,166 ± 27°F), sulfur going from 35.7 percent to 0.04 to 0.006 percent.

A Dorr-Oliver fluidized bed roaster 5.5 m (18 ft) in diameter, 7.6 m (25 ft) high, with a bed height of 1.2 to 1.5 m (3.9 to 4.9 ft) has a capacity of 154,000 to 200,000 kg/d (340,000–440,000 lbm/d) at 650 to 700°C (1,200 to 1,300°F) (Kunii and Levenspiel, *Fluidization Engineering,* Butterworth, 1991). Two modes of operation can be used for a fluidized bed unit like that shown in Fig. 23-43*e.* In one operation, a stable bed level is maintained at a superficial gas velocity of 0.48 m/s (1.6 ft/s); a unit 4.8 m (16 ft) in diameter, 1.5 m (4.9 ft) bed depth, 3 m (9.8 ft) freeboard, has a capacity of 82,000 kg/d (180,000 lbm/d) pyrrhotite, 200 mesh, 53 percent entrained solids, 875°C (1,600°F). In the other mode, the superficial gas velocity is 1.1 m/s (3.6 ft/s) and 100 percent entrainment occurs. This is called *transfer line* or *pneumatic transport reaction;* a unit 6.6 m (22 ft) diameter by 1.8 m (5.9 ft) handles 545,000 kg/d (1.2×10^6 lbm/d), 200 mesh, 780°C (1,436°F).

Magnetic Roasting In this process ores containing Fe_2O_3 are reduced with CO to Fe_3O_4, which is magnetically separable from gangue. Rotary kilns are used, temperatures 700 to 800°C (1,292 to 1,472°F). Higher temperatures form FeO. A reducing-gas atmosphere is created by firing a deficiency of air with carbonaceous fuels. Data for two installations are as follows.

Measurements	Charge, t/d	Product, t/d
3.6 by 44 m	900–960, 21% Fe	350–368, 41–42% Fe
3.6 by 50 m	1,300	—

A unit for 2.3×10^6 kg/d (5×10^6 lbm/d) has a power consumption of 0.0033 to 0.0044 kwh/kg (3 to 4 kwh/ton) and a heat requirement of 180,000 to 250,000 kcal/ton (714,000 to 991,000 Btu/ton). The magnetic concentrate can be agglomerated for further treatment by pelletizing or sintering.

Sodium Sulfate A single-hearth furnace is used, like that shown in Fig. 23-40*g.* Sodium chloride and sulfuric acid are charged continuously to the center of the pan and the rotating scrapers gradually work the reacting mass to the periphery, where the sodium sulfate is discharged at 540°C (1,000°F). Pans are 3.3 to 5.5 m (11 to 18 ft) in diameter and can handle 5,500 to 9,000 kg/d (12,000 to 20,000 lbm/d) of salt. Rotary kilns also are used for this purpose. Such a unit 1.5 m (4.9 ft) in diameter by 6.7 m (22 ft) has a capacity of 22,000 kg/d (48,000 lbm/d) of salt cake. A pan furnace also is used, for instance, in the Leblanc soda ash process and for making sodium sulfide from sodium sulfate and coal.

Desulfurization with Dry Lime Limestone or lime or dolomite ($CaCO_3 \cdot MgCO_3$) in a fluidized bed coal combustor reacts with SO_2 in the gas to make $CaSO_4$. The most favorable conditions with lime are 1 atm (14.7 psi) and 800 to 850°C (1,472 to 1,562°F). At higher temperatures the sulfate tends to decomposition, according to $CaSO_4 + CO \Rightarrow CaO + CO_2 + SO_2$. Dolomite works better at 950°C (1,742°F) and 3 to 10 atm (44 to 147 psi). Although $MgSO_4$ is not formed, the pore structure with dolomite is more open to diffusion of SO_2. The pores of the CaO tend to be clogged by $CaSO_4$, but the attrition in a fluidized bed helps the extent of utilization of the lime which, at best, is only partial. A mol ratio Ca/S of 3 to 5 is needed to get as much as 70 to 80 percent removal of the sulfur. Reactivities of limestones are variable, depending on the content of impurities. Ground particle sizes are 1.5 to 5 mm (0.059 to 0.20 in), bed depths 1.2 to 3 m (3.9 to 9.8 ft), residence times of lime 0.5 to 2.5 s. The reaction seems to be first-order in SO_2. The solid $CaSO_4$ is a waste product. It is technically, although not economically, feasible to use it for making sulfuric acid.

REFERENCES FOR REACTIONS OF SOLIDS: Brown, W. E., D. Dollimore, and A. K. Galwey, "Reactions in the Solid State," in Bamford and Tipper, eds., *Comprehensive Chemical Kinetics,* vol. 22, Elsevier, 1980. Galwey, A. K., *Chemistry of Solids,* Chapman and Hall, 1967. Sohn, H. Y., and W. E. Wadsworth, eds., *Rate Processes of Extractive Metallurgy,* Plenum Press, 1979. Szekely, J., J. W. Evans, and H. Y. Sohn, *Gas-Solid Reactions,* Academic Press, 1976. Ullmann, ed., *Enzyklopaedie der technischen Chemie,* "Uncatalyzed Reactions with Solids," vol. 3, 4th ed., Verlag Chemie, 1973, pp. 395–464.